sciendo

ISSN 1820-8665

Vol. 23. No1. MARCH 2022

# Serbian Journal of Experimental and Clinical Research

2000

Vol. 23 (1) 2022

Serbian Journal of Experimental and Clinical Research

2000



**Print**

Faculty of Medical Sciences, University of Kragujevac

**Indexed in**

EMBASE/Excerpta Medica, Index Copernicus, BioMedWorld, KoBSON, SCIndeks, Chemical Abstracts Service, Cabell's Directory, Celdes, CNKI Scholar (China National Knowledge Infrastructure), CNPIEC, EBSCO Discovery Service, Elsevier - SCOPUS, Google Scholar, J-Gate, Naviga (Softweco), Primo Central (ExLibris), ReadCube, SCImago (SJR), Summon (Serials Solutions/ProQuest), TDOne (TDNet), WorldCat (OCLC)

**Address:**

Serbian Journal of Experimental and Clinical Research, Faculty of Medical Sciences, University of Kragujevac 69 Svetozara Markovica Street, 34000 Kragujevac, PO Box 124, Serbia

https:/medf.kg.ac.rs/sjecr
https://sciendo.com/journal/SJECR

SJECR is published four times annually

Serbian Journal of Experimental and Clinical Research is categorized as a scientific journal of M51 category by the Ministry of Education, Science and Technological Development of the Republic of Serbia

**ISSN 1820 – 8665**

**TABLE OF CONTENTS**

REVIEW PAPER

# OVERVIEW OF DEEP LEARNING MODELS IN BIOMEDICAL DOMAIN WITH THE HELP OF R STATISTICAL SOFTWARE

Vinaitheerthan Renganathan

*Skyline University College Sharjah, Sharjah United Arab Emirates*

Received: 18.07.2018.
Accepted: 12.10.2018.

**Corresponding author:**

**Vinaitheerthan Renganathan**

Head of Institutional Research, Skyline University College, P.O. Box 1797, University City, Sharjah, United Arab Emirates

Phone: 971-6-5441155, Fax: 971-6-5441166
E-mail: vinairesearch@yahoo.com

sciendo

UDK: 61:004.8
Ser J Exp Clin Res 2022; 23(1): 3-11
DOI: 10.2478/sjecr-2018-0063

## ABSTRACT

*With the increase in volume of data and presence of structured and unstructured data in the biomedical fi led, there is a need for building models which can handle complex & non-linear relations in the data and also predict and classify outcomes with higher accuracy. Deep learning models are one of such models which can handle complex and nonlinear data and are being increasingly used in the biomedical fi led in the recent years. Deep learning methodology evolved from artifi cial neural networks which process the input data through multiple hidden layers with higher level of abstraction. Deep Learning networks are used in various fi elds such as image processing, speech recognition, fraud deduction, classifi cation and prediction. Objectives of this paper is to provide an overview of Deep Learning Models and its application in the biomedical domain using R Statistical software Deep Learning concepts are illustrated by using the R statistical software package. X-ray Images from NIH datasets used to explain the prediction accuracy of the deep learning models. Deep Learning models helped to classify the outcomes under study with 91% accuracy. The paper provided an overview of Deep Learning Models, its types, its application in biomedical domain. - is paper has shown the effect of deep learning network in classifying images into normal and disease with 91% accuracy with help of the R statistical package.*

***Keywords:*** *Deep learning network, Convolution network, Classifi cation, image processing, Artifi cial Neural Network.*

## INTRODUCTION

With the increase in volume of data and presence of structured and unstructured data in the biomedical filed, there is a need for building models which can handle complex & non-linear relations in the data and also predict and classify outcomes with higher accuracy. Deep learning models are one of such models which can handle complex and nonlinear data and are being increasingly used in the biomedical filed in the recent years.

Deep learning (1, 2) networks or models evolved from the artificial neural networks which works on the basis of biological nervous system. Neuron is a centre point of nervous system which processes the information. It contains cell body, axon and dendrites. Neurons are connected to other neurons through synapses which include axon and dendrites structure at the two ends. Neuron receives the information from other neurons through its dendrites and sends the processed information through its axon. Neurons will be active only if the impulse they receive is above the threshold.

Artificial Neural Networks, like the biological nervous system, consists of input, hidden layer and output layer. Each layer consists of nodes which is equivalent to neurons in biological network. Hidden layer receives inputs from the input layer as weighted information and process the information through activation functions and sends it to the output layer. The weights are initially assigned randomly and updated based on the data and the network is trained several times before processing the final information.

Deep Learning networks contains more hidden layers which are capable of handling vast amount data such as pixels in images at higher level abstraction. Deep Learning Models are used in various fields such as image processing, speech recognition, fraud deduction, classification, segmentation and prediction.

## DEEP LEARNING MODELS IN BIOMEDICAL DOMAIN

Deep Learning models are particularly useful in biomedical field (3) due to the nature, type and volume of data present in the field. It helps to create predictive and classification models from the heterogeneous datasets. The Deep Learning models fits well for nonlinear data which is not possible with the help of traditional statistical models and it is capable of handling both structured and non-structured data. Deep learning models are especially useful for image processing (4-12), predicting the disease from the given patient characteristics (13-16), analyse the complex structure genomics datasets(17,18,19) and as a natural language processing tool to process clini-cal notes (20). Deep Learning models are becoming a one of the important tools in the field of Precision (20, 21) or personalized medicine which focuses on the providing treatment at the individual patient level.

## TYPES OF DEEP LEARNING NETWORKS

Deep learning models use the following types of networks: Convolution Neural Network (CNN), Recurrent Neural Network (RNN), Long Short Term Memory (LSTM) and Deep Belief Network layers.

### Convolution Neural Networks (CNN)

Convolution Neural Networks (CNN) is especially useful in image processing (7, 23, 24). The convolution networks are widely used due to the availability of Graphical Processing Units (GPU). GPUs are capable of processing high volume of information at the same time compared to the normal Central Processing Units (CPU). The architecture of the CNN network is given in the figure-1 below and also explained in the sections below:

Input Layer and Receptive Fields

In CNN, unlike the fully connected networks, each neuron is not connected to the other as it involves too many weights & complexities and it is connected to only 'receptive field'. Receptive fields are two dimension regions in the input image which is used to connect the neurons from image to the convolution layer.

Convolution Layer - Filtering and Feature maps

The convolution process is carried out by the convolution layer (25) which consists of filters or kernel and feature map. If Input layer is an image with dimension x*y*z where x is the height, y is the width and z is the color channels of the image then a filter for the image can be defined with dimension r*s*t where r is the length (< x) and s is the width (<y) and t is the color channel (<=z). When the filter slides through the full size of the image, it produces

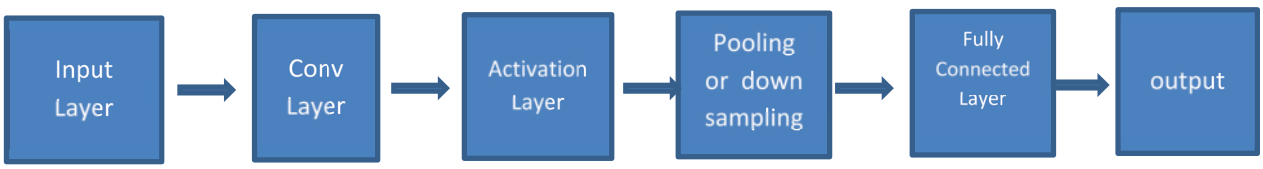


**Figure-1:** Convolution Neural Network Architecture

feature map of size x-r+1. The feature map with respect to an image can be edges and curves etc. If the CNN has 3 filters, then the filterx slides through the image and CNN convolve to produce 3 feature maps. The convolution process is also called activation. The feature maps are sampled using mean or maximum functions.

Let us take an example of 4*4*3 image with pixel values and show how a 4*4*3 image is filtered and feature map is produced through the CNN network.

a. Original image (4*4*3) (length-4, width-4, colour channel -3)

| | | | |
|---|---|---|---|
| 1 | 1 | 0 | 0 |
| 0 | 1 | 0 | 1 |
| 1 | 0 | 0 | 0 |
| 0 | 1 | 0 | 1 |

b. Filter (2*2*3) – (length-2, width-2, colour channel -3)

| | |
|---|---|
| 1 | 0 |
| 0 | 1 |

`

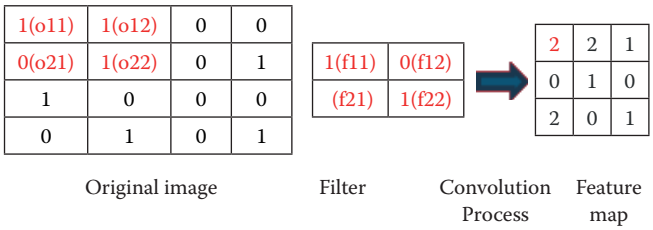


**Figure-2:** Convolution process – Creation of Feature map for an image by sliding image filters of a given size

**Convolution process:** The figure-2 shows how the filter of a given size will slide through the first four cells of the original image o11, o12, o21, o22 and each element in the original image will be multiplied by the corresponding cell elements in the filter f11, f12, f21, f22. For example in the first cell of feature map is derived from multiplying 1*1+1*0+0*0+1*1 = 2. Similarly all the other cells of the feature map which is of size 4-2+1= 3 (3*3) is obtained.

Activation Layer

After the convolution layer in the CNN network, a nonlinear functions such as tanh or sigmoid or ReLu function (26, 27) is used to introduce non linearity in the process as convolution layer uses linear functions during its operations. The process is carried out through the activation layer.

Pooling Layer

When the image sizes are large, it is desirable to introduce pooling layer or 'downsampling' layer which reduces the special size of the image through max pooling or average or L2 norm (mean square norm) pooling (28, 29). The same values are considered from each dimension of the image during the pooling process which helps to maintain the dimension of the image with reduced size.

Fully Connected Layer

Fully connected layer (30, 31) is the final layer in the CNN which takes the input from the previous layer as vector with one dimension and outputs the data**.**

Drop out layer

Drop out layer (32) is used to reduce the overfitting problem in the network as the network will be normally tuned to the training data and when new data comes in, it might over fit. To avoid over fitting problem, some of the activation will be dropped from the layer. It helps the network function work properly even some of the activation is dropped and also reduces the over fitting problem.

## Recurrent Neural Networks (RNN)

Recurrent Neural Networks (33, 34) takes into account the present input and as well as the previous input processed before it. RNN are capable of learning the dependencies between spatially correlated data such as image pixels. It adds memory into the network and creates a sequential process. The sequential information is processed by the hidden layers of RNN and correlation between the two periods of time are calculated and stored. The hidden layer in the network maintains a hidden state and updates it based on the input layer and previous hidden state. One of the problems with the RNN is it difficult to find the long-term dependencies due to vanishing gradients during back propagation process.

## Long Short Term Memory Networks (LSTM)

Long Short Term Memory (LSTM) networks (35, 36) overcome the problem of vanishing gradient by preserving the errors developed during the past. LSTM networks are used in Natural Language Processing, Speech recognition and pattern recognition. LSTM networks contain memory cell, input, output gate (to input and output information), forget gate (to drop information) which allows the network to maintain its state during the information flow. The LSTM models learn the current state and predict the future state of the parameters under study.

## Deep Belief Network

Deep Belief Network (DBN) (1) is multi-layer network which includes hidden layers which are connected to Restricted Boltzmann Machine (RBM). Restricted Boltzmann

Machines does not have connection between visible nodes but only among hidden nodes and enables us to get an unbiased sample from the posterior distribution. DBN captures higher level representation of input fed from the input layer and assigns weights initially and fine tunes through back-propagation. Deep Belief Network is used in image processing tasks.

## DEEP LEARNING MODEL FOR IMAGE CLASSIFICATION & SEGMENTATION, CLINICAL DATA MINING

Deep Learning models are used in classifying and segmenting the images such as X-rays, Mammograms, Histopathological images, predicting diseases from the given patient characteristics and processing the text in the clinical documents such as clinical notes. The process of each model is explained in the following sections 4.1-4.3:

### Deep learning models for image classification and segmentation

Deep Learning models are widely used for image classification and segmentation, as it has the advantage overthe other traditional models due to its processing speed, us-age of less resources, higher accuracy of the classification and segmentation(37,38). The images are processed through the convolution layer to derive the feature maps for the image. The nonlinearity is introduced through activation layer and the image sizes are optimized through the pooling layer. In next stage the fully connected layers coverts one dimension vector into output. The model uses training and test data set to classify or segment the image. The accuracy of classification is measured by Accuracy rate (Number classified correctly out of the total images) and through the Receive Operating Characteristics Curve (True Positive rate vs False Positive rate)

### Deep Learning models for clinical prediction

Deep Learning model uses the patient data from the sources such as Electronic Health Records (39, 40) and derive the patient characteristics using learning network for predicting the probability of having a disease condition(14,15,16). Each layer in the network encompasses a higher level of observed patient characteristics which are obtained from previous layers. The model uses training and test data set to predict the probability of a patient having a particular disease condition or not given the patient characteristics. The Receiver Operating Characteristic curve and the accuracy of prediction are calculated to decide the predictive accuracy of the model.

### Deep Learning Models for Natural Language Processing

Deep Learning Models are helpful in analysing vast amount of data present in the clinical field in the form of clinical notes (20, 41); Deep learning models are preferred over the other traditional models as data can trained with a single end-to-end model (42-44). Deep Learning models learn the features from the language data set and there is no need to manually specify and extract the features from the language dataset. Deep learning models are useful in carrying out tasks such Named Entity Recognition (patient name, drug name, city, etc.) or Part of Speech Tagging (marking of words according to the category).

## METHODS

### Compliance with Ethical Standards:

* **Disclosure of potential conflicts of interest**
  Conflict of Interest: Author declares that there is no conflict of interest.
* **Research involving human participants and/or animals:**
  Ethical approval: This article does not contain any studies with human participants performed by the author
* **Informed consent**
  Not Applicable. The study did not involve any human participants.
* **Funding:**
  This study was not funded by any organization.

## SAMPLE DEEP LEARNING NETWORK USING R STATISTICAL PACKAGE

The following example uses R open source statistical computing software (45) which is useful for carrying out various statistical tests and methods, graphics, text and data mining procedures (29). The R software can be down- loaded from the software website (45). The R software can be used in various integrated development environment (IDE) such R-Studio, Eclipse and StatET. The R software works with the concepts called packages which is a com- pilation of user created codes and can be used to perform specific functions.

The paper uses mxnet (46) package. The data set used chest x-ray images from NIH website (47) which is classified as normal (no finding) or with some disease for the study purpose. Users can also try mammograms images database such as DDSM (48), mini-MIAS (49), B-Screen (50) and histopathological images from MITOSIS-ATYPIA challenge (51) database. Results are shown for illustrative purpose only and are not meant to represent the true performance of the deep learning model.

The creation of sample deep learning model starts with the creation of working directory **(Table-1: Step-1) .** The X ray images needs to be stored in the respective directories for further processing. The images need to be reduced in size before converting and stored as Comma Separated

**Table-1:** Conversion of x-ray images into CSV files and creation of Train and Test Data sets

| Steps | Description and R code | R Code |
|---|---|---|
| Step-1 | Set working Directory | wd = "C:// Normal"<br>setwd(wd) |
| Step-2 | Call EBImage r –package | library("EBImage") |
| Step-3 | Define Label and Data frame for normal x-ray images | label <- 1<br>dataframe <- data.frame() |
| Step-4 | Convert the normal x-rays images into CSV files after reducing the image size into 36*36 dimension | for(i in 1:length(images))<br>{<br>normalimg <- readImage(images(i))<br>normalimg <- resize(normalimg, 36, 36)<br>normalimg1 <- normalimg@.Data<br>normalimg2 <- as.vector(t(normalimg1))<br>nomralvector <- c(label, nomarlimg2)<br>dataframe <- rbind(dataframe,normalvector)<br>}<br>wd = "C://datafiles"<br>setwd(wd)<br>names(dataframe) <- c("label", paste("pixel", c(1:1296)))<br>write.csv(dataframe, "normal..csv", row.names = FALSE) |
| Step-5 | Set working directory, define label and data frame for disease x-ray images | wd = "C://disease"<br>setwd(wd)<br><br>label <- 2<br>df <- data.frame()<br>images <- list.files() |
| Step-6 | Convert the disease x-rays images into CSV files after reducing the image size into 36*36 dimension | for(i in 1:length(images))<br>{<br>normalimg <- readImage(images(i))<br>normalimg <- resize(normalimg, 36, 36)<br>normalimg1 <- normalimg@.Data<br>normalimg2 <- as.vector(t(normalimg1))<br>nomralvector <- c(label, nomarlimg2)<br>dataframe <- rbind(dataframe,normalvector)<br><br>}<br>ke = "C://datafiles"<br>setwd(ke)<br>names(dataframe) <- c("label", paste("pixel", c(1:1296)))<br>write.csv(dataframe, "disease.csv", row.names = FALSE) |
| Step-7 | Calling the dataset | normal <- read.csv("normal.csv")<br>disease <- read.csv("disease.csv")<br>overall<- rbind(normal, disease)<br>reorded<-sample(overall(1:80),0) |
| Step-8 | Create the Train and test data sets | train <- reorded(1:240,)<br>test <- reorded(241:400,) |

Value (CSV) file. The EBimage r package (52) is used to convert the normal and disease x ray images into respective CSV file after reducing the size of the x images which are stored in the respective working directories **(Table-1 :Step2 to Step6).**

Once the data is converted into disease and normal CSV file, a combined overall dataset is created and in order to create a sample test and train dataset **(Table-1: Step 7 to Step8).**

During the next step the mxnet r package is called to start the modelling process by creating the dependent and independent variables x and y for both test and train dataset **(Table-2: Step9 to Step10).** After creating the dependent and independent variables, convolution layer, activation layer and pooling layers are created **(Table-2: Step-11).** The final layer in the model i.e fully connected layers is created before starting the model creation **(Table-2: Step12**) which provides the output to the model.

The model uses the output provided by the previous layers and independent and dependent variables to classify the images into disease or normal images **(Table-3: Step-13).** The final step in the whole process is to test and evaluate the accuracy of the model by using prediction function **(Table-3: Step-14)** which uses the test data which was created as a sample from the combined dataset **(Table-1:Step8).**

**Table-2:** Creation of independent and dependent Variables and layers

| Steps | Description and R code | R Code |
|---|---|---|
| Step-9 | Calling MXnet package | require(mxnet) |
| Step-10 | Define Dependent and independent variable from the train and test dataset | train <- data.matrix(train)<br>train.x <- t(train(,-1))<br>train.y <- train(,1)<br><br>train_x1 <- train.x<br>dim(train_x1) <- c(36, 36, 1, ncol(train.x))<br><br>test <- data.matrix(test)<br>test.x <- t(test(,-1))<br>test.y <- test(,1)<br>test.x1 <- test_x<br>dim(test.x1) <- c(36, 36, 1, ncol(test_x)) |
| Step-11 | Building 3 convolution, 3 activation and 3 pooling layers | data <- mx.symbol.Variable('data')<br>convolution1<- mx.symbol.Convolution(data= data, kernel = c(5,5), num_filter = 25)<br>activation1 <- mx.symbol.Activation(data= convolution1, act_type = "relu")<br>pooling1 <- mx.symbol.Pooling(data = activation1, pool_type = "max", kernel = c(2,2), stride = c(2,2))<br>convolution2<- mx.symbol.Convolution(data= data, kernel = c(5,5), num_filter = 30)<br>activation2 <- mx.symbol.Activation(data= convolution1, act_type = " relu")<br>pooling2 <- mx.symbol.Pooling(data = activation1, pool_type = "max", kernel = c(2,2), stride = c(2,2))<br>convolution2<- mx.symbol.Convolution(data= data, kernel = c(5,5), num_filter = 30)<br>activation3 <- mx.symbol.Activation(data= convolution1, act_type = " relu")<br>pooling3 <- mx.symbol.Pooling(data = activation1, pool_type = "max", kernel = c(2,2), stride = c(2,2)) |
| Step-12 | Building 3 Fully Connected layers | flattendata <- mx.symbol.Flatten(data = pool_2)<br>fully1 <- mx.symbol.FullyConnected(data = flattendata, num_hidden = 600)<br>activaton4 <- mx.symbol.Activation(data = fully1, act_type = "relu")<br>fully2 <- mx.symbol.FullyConnected(data = activation4, num_hidden =300)<br>activaton5 <- mx.symbol.Activation(data = fully2, act_type = "relu")<br>fully3<- mx.symbol.FullyConnected(data = activation5, num_hidden = 2)<br>DL <- mx.symbol.SoftmaxOutput(data = fully3)<br>mx.set.seed(200)<br>device <- mx.cpu() |

| Steps | Description and R code | R Code |
|---|---|---|
| Step-13 | Building Deep Convolution network model | model <- mx.model.FeedForward.create(DL, X = train.x1, y = train.y,<br>ctx = device,<br>num.round = 30,<br>array.batch.size = 100,<br>learning.rate = 0.05,<br>momentum = 0.9,<br>wd = 0.00001,<br>eval.metric = mx.metric.accuracy,<br>epoch.end.callback = mx.callback.log.train.metric(100)) |
| Step-14 | Building Deep Convolution network model predictions | prediction <- predict(model, test.x1)<br>predlabels <- max.col(t(prediction))-1<br>table(test(,1), predlabels) |

**Table-3:** Building Deep Learning Convolution model and prediction model

## RESULTS AND DISCUSSION

The initial output of the deep learning model is the conversion of the images into CSV file and stores them as train and test data set. The table-4 shows the sample test and train dataset content which are processed by EBimage package which are stored in the CSV file.

In Table 4a and Table4b above, the label indicates the type of image label 1-normal image and another is label2-disease image.

The training models iteration set for 200 in this example and after each iteration the training accuracy recorded and is shown in the below Table-5

To evaluate the accuracy and performance of the deep learning model, 60% dataset is used for training and 40% dataset is used for testing the model. The following Table-6 provides predicted values in comparison with the actual classification diseased vs. normal patient x-ray classification

From the above table-6, the classification accuracy is calculated as 91%.

**Table 4a**. Sample Train dataset - Conversion of images into CSV file and stored as pixels values

| Label | pixel.1 | pixel.2 | pixel.3 | pixel.4 | pixel.5 | ..... | pixel.1296 |
|---|---|---|---|---|---|---|---|
| 1 | 0.121917 | 0 | 0 | 0 | 0.003922 | | 0 |
| 2 | 0.036765 | 0.047059 | 0.043137 | 0.035294 | 0.027451 | | 0.156327 |
| 2 | 0.03927 | 0.054902 | 0.039216 | 0.035294 | 0.031373 | | 0.178422 |
| 1 | 0.024837 | 0.031373 | 0.031373 | 0.031373 | 0.189052 | | 0.003922 |

**Table 4b**. Sample Test dataset - Conversion of images into CSV file and stored as pixels values

| Label | pixel.1 | pixel.2 | pixel.3 | pixel.4 | pixel.5 | ..... | pixel.1296 |
|---|---|---|---|---|---|---|---|
| 2 | 0.195016 | 0.055882 | 0.047059 | 0.03893 | 0.03223 | | 0.152982 |
| 2 | 0.039049 | 0.058824 | 0.048584 | 0.039216 | 0.039216 | | 0.198641 |
| 1 | 0.121917 | 0 | 0 | 0 | 0.003922 | | 0 |
| 1 | 0.400605 | 0.003922 | 0.002397 | 0.43435 | 0.456645 | | 0 |

## CONCLUSION

This paper has shown the effect of deep learning network in classifying images into normal and disease with 91% accuracy with help of the R statistical package. Deep learning models showed considerable improvement in classifying images over the other models in terms of accuracy and speed due to the availability of powerful GPU systems. Deep learning models will play an important role in classifying the images in the future which will be of significant help to radiologist in reducing the time and prepare the reports. More number of free and large databases is required to train the model and increase the accuracy in the biomedical domain.

**Table 5**. Training Accuracy

| Iteration number | Train-accuracy |
|---|---|
| [1] | 0.6705694 |
| [2] | 0.6507439 |
| [3] | 0.6633542 |
| [4] | 0.6866255 |
| ... | ---- |
| [21] | 0.8738582 |
| [22] | 0.8920106 |
| [23] | 0.8885165 |
| [24] | 0.8518872 |
| .... | |
| [199] | 0.9034987 |
| [200] | 0.9414315 |

**Table-6:** Actual vs Predicted values for 160 test images

| | Normal | Disease |
|---|---|---|
| Normal | 70 | 10 |
| Disease | 5 | 75 |

## REFERENCES


1. Goodfellow I, Bengio Y, Courville A, Bengio Y. 2016. Deep learning (Vol. 1). Cambridge: MA, USA, MIT press.
2. LeCun Y, Bengio Y, Hinton G. Deep learning. Nature. 2015; 521(7553): 436.
3. Miotto R, Wang F, Wang S, Jiang X, Dudley JT. Deep learning for healthcare: review, opportunities and challenges. Briefings in bioinformatics. 2018; 19(6): 1236-46.
4. Urban G, Bache KM, Phan D, et al. Deep Learning for Drug Discovery and Cancer Research: Automated Analysis of Vascularization Images. IEEE/ ACM Transactions on Computational Biology and Bioinformatics. 2018; 16(3): 1029-35.
5. Lakhani P. Deep convolutional neural networks for endotracheal tube position and X-ray image classification: challenges and opportunities. Journal of digital imaging. 2017; 30(4): 460-8.
6. LeCun Y, Bengio Y. Convolutional networks for images, speech, and time series. The handbook of brain theory and neural networks. 1995; 3361(10).
7. Gao M, Bagci U, Lu L, et al. Holistic classification of CT attenuation patterns for interstitial lung diseases via deep convolutional neural networks. Computer Methods in Biomechanics and Biomedical Engineering: Imaging & Visualization. 2018; 6(1): 1-6.
8. Mohamed AA, Berg WA, Peng H, Luo Y, Jankowitz RC, Wu S. A deep learning method for classifying mammographic breast density categories. Medical physics. 2018; 45(1); 314-21.
9. Esteva A, Kuprel B, Novoa RA, et al. Dermatologistlevel classification of skin cancer with deep neural networks. Nature. 2017; 542(7639), 115.
10. Saltz J, Gupta R, Hou L, et al. Spatial organization and molecular correlation of tumor-infiltrating lymphocytes using deep learning on pathology images. Cell reports. 2018; 23(1): 181-93.

11. Kermany DS, Goldbaum M, Cai W, et al. Identifying medical diagnoses and treatable diseases by image-based deep learning. Cell. 2018; 172(5): 1122-31.
12. Gerard SE, Patton TJ, Christensen GE, Bayouth JE, Reinhardt JM. FissureNet: A deep learning approach for pulmonary fissure detection in CT images. IEEE transactions on medical imaging. 2018; 38(1): 156-66.
13. Hinton, G. Deep learning—a technology with the potential to transform health care. JAMA. 2018; 320(11): 1101-2.
14. Chen M, Hao Y, Hwang K, Wang L, Wang L. Disease prediction by machine learning over big data from healthcare communities. IEEE Access. 2017; 5: 8869-79.
15. Miotto R, Li L, Kidd BA, Dudley JT. Deep patient: an unsupervised representation to predict the future of patients from the electronic healthy records. Scientific reports. 2016; 6: 26094.
16. Liu S, Liu S, Cai W, Pujol S, Kikinis R, Feng D. Early diagnosis of Alzheimer's disease with deep learning. In Biomedical Imaging (ISBI). IEEE 11th International Symposium. 2014, p. 1015-1018.
17. Alipanahi B, Delong A, Weirauch MT, Frey BJ. Predicting the sequence specificities of DNAand RNA-binding proteins by deep learning. Nature biotechnology. 2015; 33(8): 831.
18. Park Y, Kellis M. Deep learning for regulatory genomics. Nature biotechnology. 2015; 33(8): 825.
19. Chen Y, Li Y, Narayan R, Subramanian A, Xie X. Gene expression inference with deep learning. Bioinformatics. 2016; 32(12): 1832-9.
20. Weng WH, Wagholikar KB, McCray AT, Szolovits P, Chueh HC. Medical subdomain classification of clinical notes using a machine learning- based natural language processing approach. BMC medical informatics and decision making. 2017; 17(1): 155.
21. Collins FS, Varmus H. A new initiative on precision medicine. New England Journal of Medicine. 2015; 372(9): 793-5.
22. Nezhad MZ, Zhu D, Li X, Yang K, Levy P. Safs: A deep feature selection approach for precision medicine. In Bioinformatics and Biomedicine (BIBM), IEEE International Conference, 15-18, Dec 2016, p. 501-06. Shenzhen, China, IEEE.
23. Lu L, Zheng Y, Carneiro G, Yang L. 2017. Deep Learning and Convolutional Neural Networks for Medical Image Computing. (1st Ed) MA, USA. Springer.
24. Lo, SCB, Chan HP, Lin JS, Li H, Freedman MT, Mun SK. Artificial convolution neural network for medical image pattern recognition. Neural networks. 1995; 8(7-8): 1201-14.
25. Ciresan DC, Meier U, Gambardella LM, Schmidhuber J. Convolutional neural network committees for handwritten character classifica-tion. In: Document Analysis and Recognition (ICDAR), International Conference, 2011, p. 1135-9. Beijing, China, IEEE.
26. Mou L, Ghamisi P, Zhu XX. Deep recurrent neural networks for hyperspectral image classification. IEEE Transactions on Geoscience and Remote Sensing. 2017; 55(7): 3639-55.
27. Tran SD, Manmatha R. U.S. Patent No. 9, 892,344. Washington, DC: U.S. Patent and Trademark.
28. Zhang Y, Shi B. Improving pooling method for regularization of convolutional networks based on the failure probability density. Optik-International Journal for Light and Electron Optics. 2017; 145, 258-65.
29. Del Fiol G, Michelson M, Iorio A, Cotoi C, Haynes RB. A Deep Learning Method to Automatically Identify Reports of Scientifically Rigorous Clinical Research from the Biomedical Literature: Comparative Analytic Study. Journal of medical Internet research. 2018; 20(6): e10281.
30. Choi K, Fazekas G, Sandler M, Cho K. (2017, March). Convolutional recurrent neural networks for music classification. In Acoustics, Speech and Signal Processing (ICASSP). IEEE International Conference. 2017, p. 2392-6. New Orleans, USA, IEEE.
31. Chen LC, Papandreou G, Kokkinos I, Murphy K, Yuille AL. Deeplab: Semantic image segmentation with deep convolutional nets, atrous convolution, and fully connected crfs. IEEE transactions on pattern analysis and machine intelligence. 2018; 40(4): 834-48.
32. Kimmel J, Brack A, Marshall WF. Deep convolution neural networks allow analysis of cell motility during stem cell differentiation and neoplastic transformation. bioRxiv. 2017; 159202.
33. Graves A, Mohamed AR, Hinton G. Speech recognition with deep recurrent neural networks. In Acoustics, speech and signal processing (icassp), IEEE international conference, 2013 p. 6645-9. Vancouver, Canada, IEEE.
34. Sun X, Li T, Li Y, Li Q, Huang Y, Liu J. Recurrent neural system with minimum complexity: A deep learning perspective. Neurocomputing. 2018; 275: 1333-49.
35. Tan JH, Hagiwara Y, Pang W, et al. Application of stacked convolutional and long short-term memory network for accurate identification of CAD ECG signals. Computers in Biology and Medicine. 2018; 94:19–26.
36. Lipton ZC, Kale DC, Elkan C, Wetzel R. Learning to diagnose with LSTM recurrent neural networks. arXiv preprint arXiv. 2015; 1511.03677.
37. Jnawali K, Arbabshirani MR, Rao N, Patel AA. (2018, February). Deep 3D convolution neural network for CT brain hemorrhage classification. In Medical Imaging

2018: Computer-Aided Diagnosis (Vol. 10575, p. 105751C).
38. Acharya UR, Oh SL, Hagiwara Y, Tan JH, Adeli H. Deep convolutional neural network for the automated detection and diagnosis of seizure using EEG signals. Computers in biology and medicine, 2018; 100: 270-8.
39. Li W, Shi S, Gao Z, et l. Improved deep belief network model and its application in named entity recognition of Chinese electronic medical records. In Big Data Analysis (ICBDA), IEEE 3rd International Conference, 2018 p. 356-60. Shanghai, China, IEEE.
40. Shickel B, Tighe PJ, Bihorac A, Rashidi P. Deep EHR: A survey of recent advances in deep learning techniques for electronic health record (EHR) analysis. IEEE journal of biomedical and health informatics. 2018; 22(5): 1589-1604.
41. Zech J, Pain M, Titano J, et l. Natural Language–based Machine Learning Models for the Annotation of Clinical Radiology Reports. Radiology. 2018; 287(2), 570-80.
42. Del Fiol G, Michelson M, Iorio A, et al. A Deep Learning Method to Automatically Identify Reports of Scientifically Rigorous Clinical Research from the Biomedical Literature: Comparative Analytic Study. Journal of medical Internet research, 2018; 20(6).
43. Young T, Hazarika D, Poria S, Cambria E. Recent trends in deep learning based natural language processing. ieee Computational intelligenCe magazine, 2018; 13(3), 55-75.
44. Deng L, Liu Y. A joint introduction to natural language processing and to deep learning. In: Deep learning in natural language processing. 2018, p. 1-22. Springer, Singapore.
45. R Core Team R: A language and environment for statistical computing. R Foundation for Statistical Computing, Vienna, Austria. Retrieved September 21, 2018 from http://www.R-project.org/.
46. Chen T, Kou Q, He T. mxnet. MXNet [2015]. Retrieved September 21, 2018 from https://github. com/dmlc/ mxnet/R-package.
47. Wang X, Peng Y, Lu L, Lu Z, Bagheri M, Summers RM. ChestX-ray8: Hospital-scale Chest X-ray Database and Benchmarks on Weakly-Supervised Classification and Localization of Common Thorax Diseases. IEEE CVPR, 21-26 July 21-26 2017( 2097-2106). Honolulu, Hawaii,IEEE.
48. Heath M, Bowyer K, Kopans D, et al. Current status of the digital database for screening mammography. In Digital mammography (pp. 457-460). Springer, Dordrecht.
49. J Suckling et al. The Mammographic Image Analysis Society Digital Mammogram Database Exerpta Medica. International Congress Series. 1994; 1069: 375-8.
50. Diagnostic image Analysis Group [2009] Retrieved September 21, 2018 from http://www.diagnijmegen.nl/index.php/NWO__Bayesian_Decision_Support_in_ Medical_Screening_%28B-SCREEN%29
51. MITOS-ATYPIA [2014] Retrieved September 21, 2018 from https://mitos-atypia-14.grand-challenge .org/
52. Pau G, Fuchs F, Sklyar O, Boutros M, Huber W. EBImage—an R package for image processing with applications to cellular phenotypes. Bioinformatics. 2010; 26(7): 979-81.

ORIGINAL SCIENTIFIC ARTICLE

# COMPARISON OF DIFFERENT DOSES BOTULINUM TOXIN TYPE A EFFICACY IN CHRONIC ANAL FISSURE TREATMENT

Nikolaj Aleksandrovich Goloktionov[1], Vladimir Nikolaevich Kashnikov[1], Olga Vladimirovna Tkalich[1], Aleksej Alekseevich Ponomarenko[1], Roman Yurevich Khryukin[1], Ivan Vasilevich Kostarev[1], Predrag Krstic[2], Sergej Valerevich Slozhenikin[3], Evgenij Alekseevich Zagryadskiy[4], Vladimir Yurevich Medvedev[3], Oksana Yurevna Fomenko[3], Svetlana Viktorovna Nekhrikova[1], Karina Ibakovna Arslanbekova[1], Viktor Kazbekovich Misikov[5], Mikhail Albertovich Akulov[6], Aleksandra Sergeevna Orlova[7] and Evgenij Evgenevich Zharkov[1]

[1] FSBI A.N. Ryzhykh Scientific Medical Research Center for Coloproctology of the Ministry of Healthcare of Russia, Moscow
[2] Military Medical Academy, Department of Hematology, Belgrade, Serbia
[3] SBHI MR L`vov Regional Hospital, Moscow
[4] International Medical Center ON CLINIC, Moscow, Russia
[5] SBHI MR M.F. Vladimirskiy Moscow Regional Research Clinical Institute, Moscow
[6] N.N. Burdenko National Scientific and Practical Centre for Neurosurgery, Moscow
[7] I.M. Sechenov First Moscow State Medical University (Sechenov University), Moscow

Received: 26.01.2022
Accepted: 03.02.2022.

**Corresponding author:**

**Aleksandra Sergeevna Orlova, PhD**

Department of Human Pathology, I.M. Sechenov First Moscow State Medical University (Sechenov University), Moscow, Russian Federation

Phone: +79260499811
E-mail: orlovaas@yandex.ru

sciendo

UDK: 616.352-002.44-085:615.917
615.917:579.852.13
Ser J Exp Clin Res 2022; 23(1): 13-28
DOI: 10.2478/sjecr-2222-0006

## ABSTRACT

***Objective**: To compare the results of chronic anal fissure treatment with 10 IU and 40 IU botulinum toxin type A.*
***Patients and methods**: 56 patients were enrolled in case-control study divided into 2 groups consistent by the main clinical criteria. 28 patients in the study group had fissure excision in combination with 10 IU botulinum toxin type A (Xeomin) injection into internal anal sphincter, while 28 patients in control group received 40 IU product injections.*
***Results**: No statistically significant results in the pain assessment during the day and after bowel movement were obtained (p=0.41 and p=0.93, respectively). The groups were comparable by the frequency of complications such as transient anal incontinence, perianal skin hematoma, acute urinary retention (p>0.05). Complications such as thrombosis of external hemorrhoids and chronic non-healing wounds were most common in the study group (p=0.43 and p=0.0005, respectively). The product dose increase to 40 IU has a more significant effect on the functional treatment results (p=0.0053 and p=0.0002, respectively) and increases the odds for postoperative wound epithelialization 15-fold (p=0.01). Conclusion: 40 IU Botulinum toxin type A shows improvement in the treatment of chronic anal fissure without any increased risk of postoperative complications.*

***Keywords**: anal fissure, internal sphincter spasm, botulinum toxin type A.*

## INTRODUCTION

Chronic anal fissure (CAF) is a defect of anoderm with cicatricial-inflammatory changes indicating a long-lasting abnormality (1). The course of disease is characterized by intense pain syndrome usually occurring after the bowel movement. It is caused by internal anal sphincter (IAS) spasm, which underlies the pathogenesis of this condition impeding the defect healing (2-5). The IAS spasm elimination is therefore a pathogenetically justified method for treating patients with CAF (6). Various methods for drug relaxation of IAS (organic nitrates, calcium channel blockers, etc.) are currently available (7-9), however, the lateral subcutaneous sphincterotomy still remains the "gold" standard for CAF treatment (10,11). Persistent anal incontinence developing in some patients is a significant limitation of this method (12). Various authors have reported the development of this complication in 8-30% of patients (13-17). The attempts to replace the IAS excision with its dosed stretching have not improved the treatment results with the frequency of anal incontinence reported in the studies in the early and long-term postoperative period reaching 41% (18-20). Drug relaxation of IAS that does not result in persistent damage of anal sphincter is an alternative approach (7-9, 21).

Organic nitrates and calcium channel blockers are most commonly used for IAS spasm elimination. Both groups of drugs have a comparable efficacy and are not associated with IAS damage, however they induce side effects such as headache, orthostatic hypotension and require frequent and long-term use, which reduces the treatment compliance of the patients. Eventually, this results in a decreased efficacy and increased recurrence (7-9). Botulinum toxin type A (BTA) products are devoid of the above disadvantages; however the established recommendations for its use in CAF treatment are not available at the moment. In certain studies the authors suggest that there are no clinically significant differences between the BTA doses administered, and the product administration technique (22), while there are some authors stating the opposite (23). In this regard, it was decided to conduct a comparative study on the use of different doses of BTA in the treatment of chronic anal fissure with sphincter spasm.

## MATERIALS AND METHODS

A case-control study enrolling 56 patients with CAF with IAS spams was conducted from 2018 to 2021 at A.N. Ryzhykh SMRC for Coloproctology. The study group included 28 patients who had fissure excision in combination with 5 IU BTA (Xeomin) injection into the internal anal sphincter at 3 and 9 hours (in total 10 IU); control group included 28 patients consistent with the study group by the common clinical characteristics: gender, age, disease duration, number of fissures, pain syndrome after bowel movement and during the day, fibrous polyps of the anal canal and sentinel piles, external and internal hemorrhoids, and the nature of bowel movements. 10 IU of the product into 4 points at 1.5, 7 and 11 hours (in total 40 IU) were injected in controls after fissure excision.

**Figure 1.** Study Design.

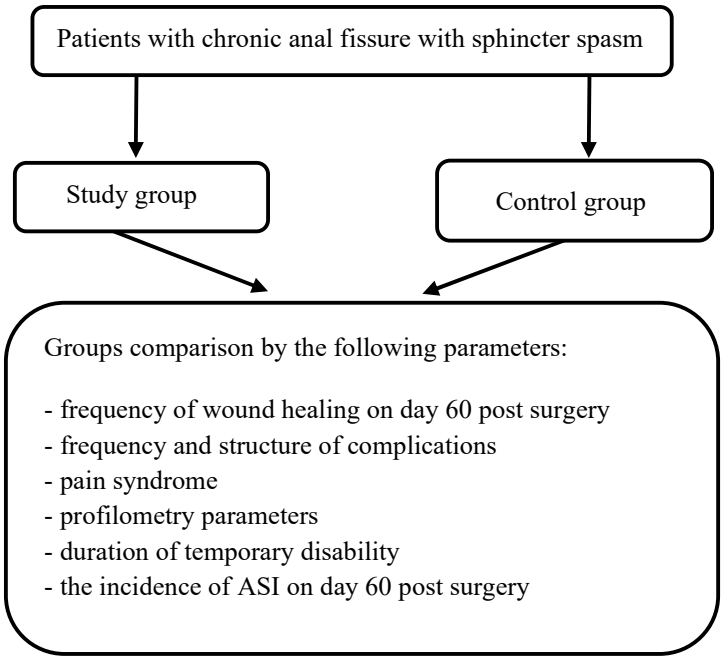

All patients enrolled in the study had profilometry prior to and on day 60 post surgery. Patients assessed their pain syndrome using visual analogue scale, and also the severity of anal incontinence using Wexner scale on a daily basis. On day 60 were performed: digital rectal examination, and anoscopy. The number and duration of pain medications use were recorded throughout the observation period.

**Table 1.** Clinical and Functional Characteristics of Patients with Chronic Anal Fissure.

| **Parameter** | **Spasm elimination method** | | **p** |
|---|---|---|---|
| | **10 IU Botulotoxin n=28** | **40 IU Botulotoxin n=28** | |
| Median age | 36 (32; 43.5) | 34 (31; 43) | 0.1 |
| Gender:<br>males<br>females | <br>10 (35.71%)<br>18 (64.29%) | <br>11 (39. 29%)<br>17 (60. 71%) | 0.5 |
| Duration of disease (months) | 21 (7; 36) | 12 (6;28) | 0.5 |
| Number of fissures:<br>One<br>Two<br>Three | <br>23 (82%)<br>5 (18%)<br>0 (0%) | <br>24 (85.7%)<br>4 (14.3%)<br>0 (0%) | 0.5 |
| Median pain after bowel movement (quartiles) | 4.5 (1; 6) | 5.5(4;7) | 0.0702 |
| Median pain during the day (quartiles) | 1 (0; 3) | 3 (2; 6) | 0.063 |
| Fibrous polyp<br>One<br>Two | <br>10 (35. 71%)<br>1 (3.57%) | <br>8 (28.57%)<br>0 (0%) | 0.5 |
| Sentinel pile<br>One<br>Two | <br>10 (35.71%)<br>2 (7.14%) | <br>9(32.14%)<br>0(0%) | 0.3 |
| External hemorrhoids<br>One<br>Two<br>Three | <br>5 (17.86%)<br>2 (7.14%)<br>0 (0%) | <br>3 (10.71%)<br>1 (3.57%)<br>1 (3.57%) | 0.58 |
| Internal hemorrhoids | | | |
| One | 2 (7.14%) | 0 (0%) | 0.08 |
| Two | 0 (0%) | 0 (0%) | |
| Three | 0 (0%) | 3 (10.71%) | |
| Bowel movement:<br>Normal stool<br>Constipation | <br>20 (71.43%)<br>8 (28.57%) | <br>23 (82.14%)<br>5 (17.86%) | 0.12 |
| Anal sphincter incompetence by Wexner scale | 0 | 0 | - |

## RESULTS

The intensity of pain syndrome after bowel movement and during the day was analyzed in the study and control groups.

**Figure 2.** Pain Syndrome Intensity During the Day in Preoperative and Postoperative Period.

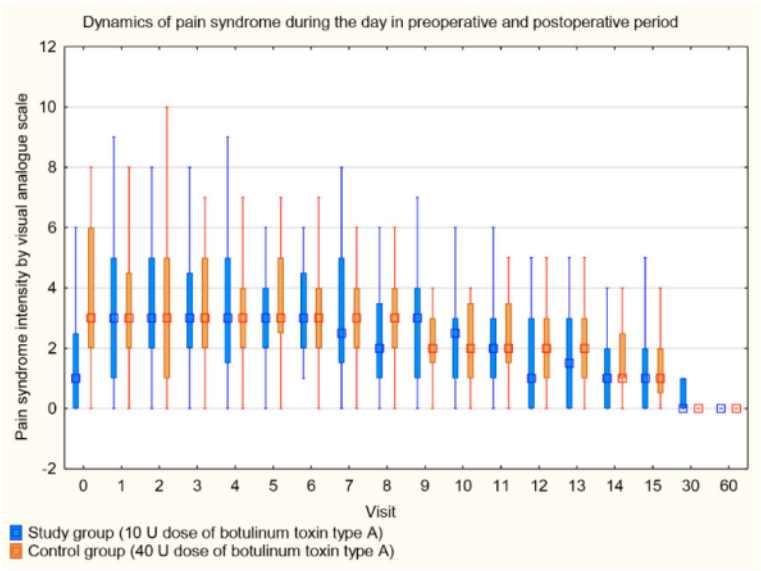


No clinically significant differences between the groups in the intensity of pain syndrome during the day were observed, p=0.41 (Fig. 2).

**Figure 3.** Pain Syndrome Intensity after Bowel Movement in Preoperative and Postoperative Period.

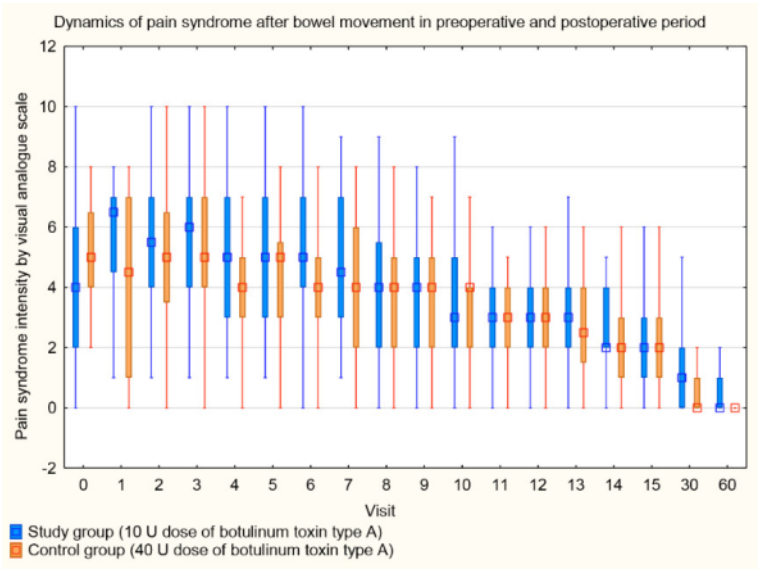


No significant differences between the groups in parameters and dynamics of pain syndrome after bowel movement were observed, p=0.93 (Fig. 3).

**Figure 4.** Need for Pain Medications Use in Preoperative and Postoperative Period.

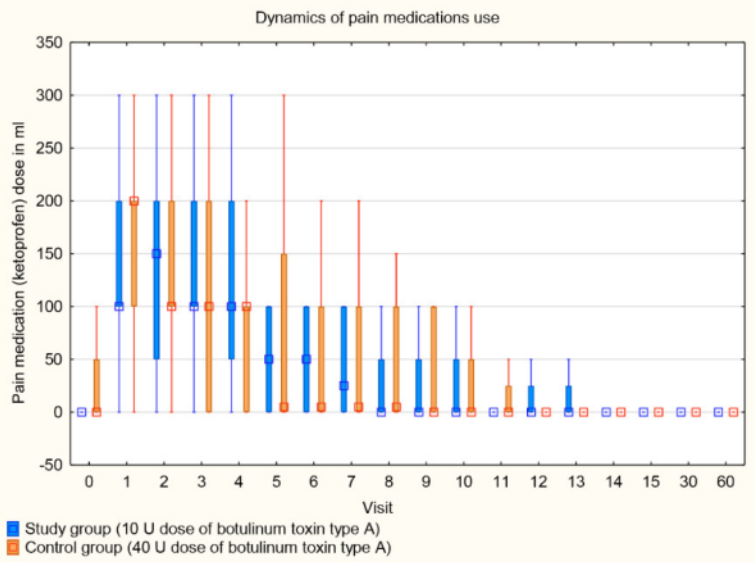


The duration of pain medications (ketoprofen) use and their dosage were assessed in postoperative period. No statistically significant differences in the assessment of these parameters were found, p=0.18 (Fig. 4).

**Figure 5.** Proportion of Patients (%) Taking Pain Medications in Preoperative and Postoperative Period.

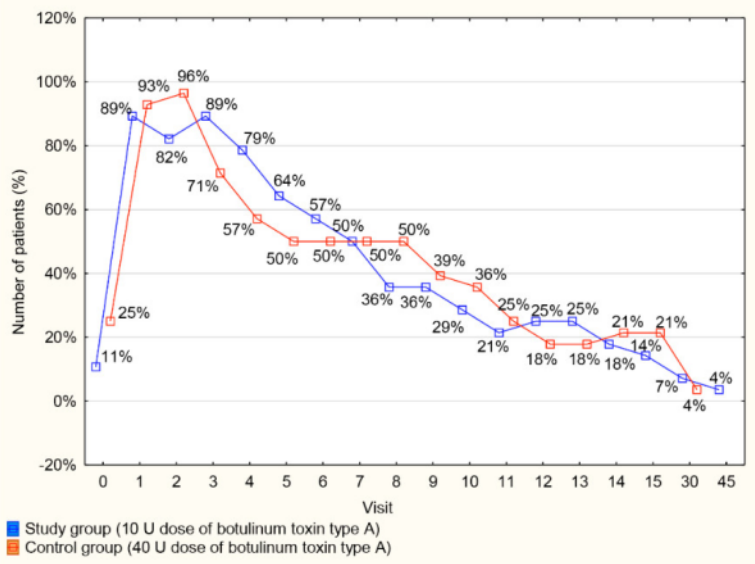


No differences in the number of patients taking pain medications for 60 days post surgery were found, p=0.71. (Fig. 5)

**Figure 6.** Maximum Pressure in the Anal Canal at Rest Preoperatively and on Day 60 Post Surgery.

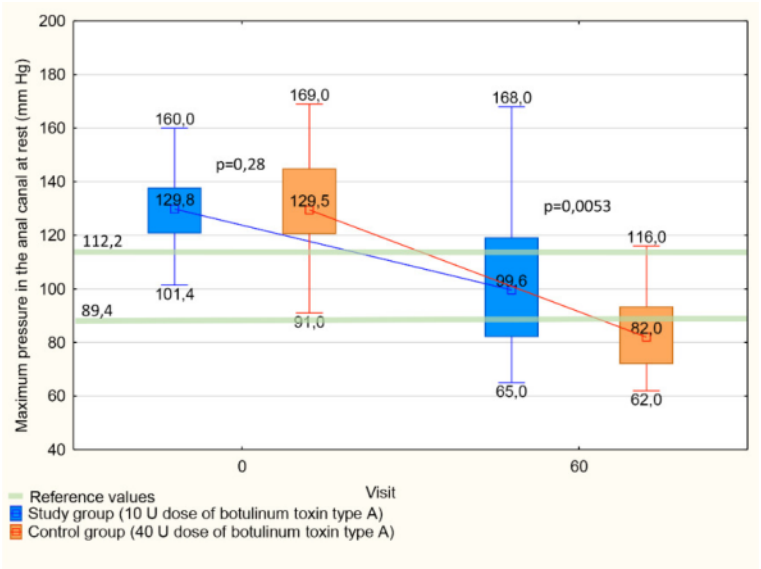


The maximum pressure in the anal canal at rest on day 60 post surgery was statistically significantly lower in control group, p=0.0053 (Fig. 6).

**Table 2.** Patients Distribution by Maximum Pressure Level in the Anal Canal at Rest 60 days Post Surgery.

| **Maximum pressure in the anal canal at rest** | **10 IU Botulinum toxin type A group n = 28** | **40 IU Botulinum toxin type A group n = 28** | **p** |
|---|---|---|---|
| Increased (>112.2 mm Hg) | 8 (29%) | 2 (7%) | 0.68 |
| Normal (89.4 – 112.2 mm Hg) | 9 (32%) | 8(29%) | |
| Decreased (<89.4 mm Hg) | 11 (39 %) | 18 (64%) | |

No statistically significant deviations of the studied parameter from the reference values on day 60 post surgery were found, p=0.68 (Table 2).

**Figure 7.** Medium Pressure in the Anal Canal at Rest Preoperatively and on Day 60 Post Surgery.

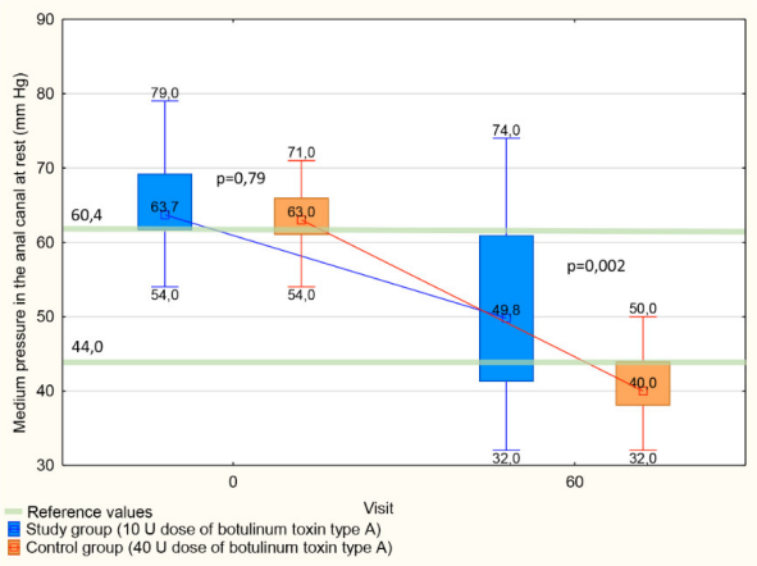


Medium pressure in the anal canal at rest on day 60 post surgery was statistically significantly lower in control group, p=0.002 (Fig. 7).

**Table 3.** Patients Distribution by the Medium Pressure Level in the Anal Canal at Rest 60 days Post Surgery.

| **Maximum pressure in the anal canal at rest** | **10 IU Botulinum toxin type A group, n = 28** | **40 IU Botulinum toxin type A group, n = 28** | **p** |
|---|---|---|---|
| Increased (>60.4 mm Hg) | 8 (29%) | 0 (0%) | 0.02 |
| Normal (44.0-60.4 mm Hg) | 9 (32%) | 6(21%) | |
| Decreased (<44.0 mm Hg) | 11 (39 %) | 22 (79%) | |

Statistically significant differences between the study and control groups in the medium pressure in the anal canal at rest on day 60 post surgery were observed, p=0.002 (Table 3).

**Figure 8.** Maximum Pressure in the Anal Canal at Voluntary Constriction Preoperatively and on day 60 Post Surgery.

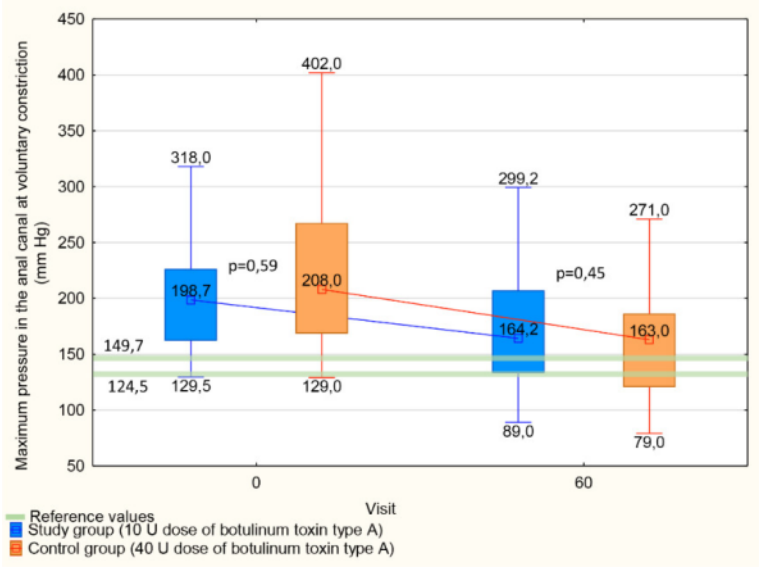


Whereas, the groups were comparable by the maximum pressure in the anal canal at voluntary constriction on day 60 post surgery, p=0.45 (Fig. 8).

**Table 4.** Patients Distribution by Maximum Pressure Level in the Anal Canal at Voluntary Constriction on day 60 Post Surgery.

| **Maximum pressure in the anal canal at rest** | **10 IU Botulinum toxin type A group, n = 28** | **40 IU Botulinum toxin type A group, n = 28** | **p** |
|---|---|---|---|
| Increased (>149.7 mm Hg) | 17 (61%) | 16 (57%) | 0.57 |
| Normal (124.5–149.7 mm Hg) | 6 (21%) | 4(14%) | |
| Decreased (<124.5 mm Hg) | 5 (18 %) | 8 (29%) | |

No statistically significant results for patients distribution by the level of maximum pressure in the anal canal were obtained, p=0.57 (Table 4).

**Figure 9.** Medium Pressure in the Anal Canal at Voluntary Constriction Preoperatively and on Day 60 Post Surgery.

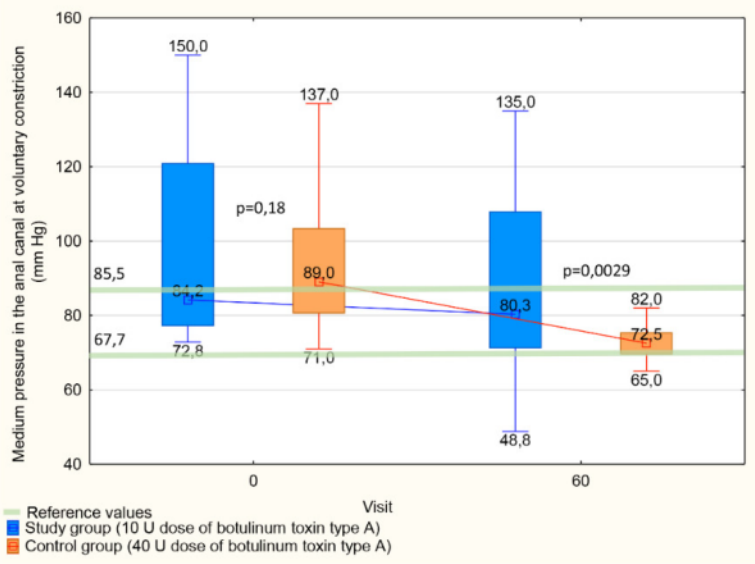


Whereas, the medium pressure in the anal canal at voluntary constriction on day 60 post surgery was statistically significantly lower in control group, p=0.0029 (Fig. 9).

**Table 5.** Patients Distribution by Medium Pressure Level in the Anal Canal at Voluntary Constriction 60 Days Post Surgery.

| Maximum pressure in the anal canal at rest | 10 IU Botulinum toxin type A group, n = 28 | 40 IU Botulinum toxin type A group, n = 28 | p |
|---|---|---|---|
| Increased (>85.5 mm Hg) | 10 (36%) | 3 (11%) | 0.49 |
| Normal (67.7–85.5 mm Hg) | 16 (57%) | 19(68%) | |
| Decreased (<67.7 mm Hg) | 2(7 %) | 6 (21%) | |

No statistically significant results for patients distribution by medium pressure level in the anal canal were obtained, p=0.49 (Table 5).

**Table 6.** Number of Patients with Preoperative and Postoperative Signs of Transient Anal Incontinence by Wexner scale (limit score = 0).

| Period | Number of patients with signs of transient anal sphincter incompetence | | p |
|---|---|---|---|
| | Study group, (n = 28) | Control group, (n = 28) | |
| Preoperative | 0 | 0 | - |
| Day 30 | 6 (21%) | 10 (36%) | 0.18 |
| Day 60 | 3 (11%) | 4 (14%) | 0.5 |

Groups were compared by anal incontinence occurrence according to Wexner scale on day 30 and day 60, whereas the analysis has shown no significant results, p=0.18 and p=0.5, respectively (Table 6).

**Figure 10.** Assessment of Continence Function in Groups by Wexner Scale Preoperatively and 30, 60 Days Post Surgery.

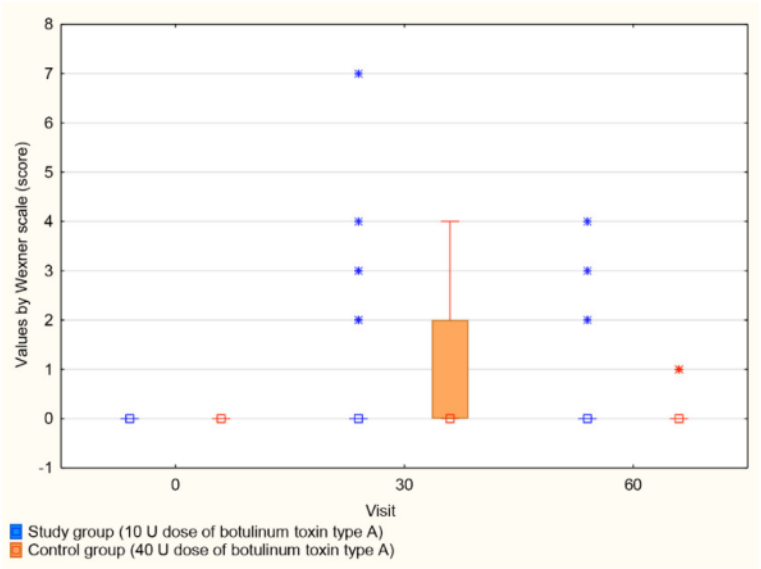


Assessment of transient anal incontinence severity by Wexner scale on day 30 and day 60 post surgery has shown no statistically significant results, p=0.93 and 0.37, respectively (Fig. 10).

**Table 7.** Frequency of Postoperative Complications.

| **Complications** | **Method for IAS spasm relaxation** | | **p** |
|---|---|---|---|
| | **Study group (n = 28)** | **Control group (n = 28)** | |
| Hematoma | 1 (4%) | 0(0%) | 0.31 |
| Thrombosis of external hemorrhoids | 6(21%) | 1(4%) | 0.043 |
| Urinary retention | 0(0%) | 0(0%) | 1 |
| Chronic non-healing wound | 10(36%) | 0(0%) | 0.0005 |

Groups were comparable in terms of complications such as hematoma, and acute urinary retention (p=0.31 and p=1.0, respectively). However, thrombosis of external hemorrhoids (6 (21%) vs 1 (4%), p=0.043) and non-healing wounds (10 (36%), p=0.0005) were statistically significantly more common in the study group (Table 7).

**Figure 11.** Duration of Temporary Disability Following Treatment

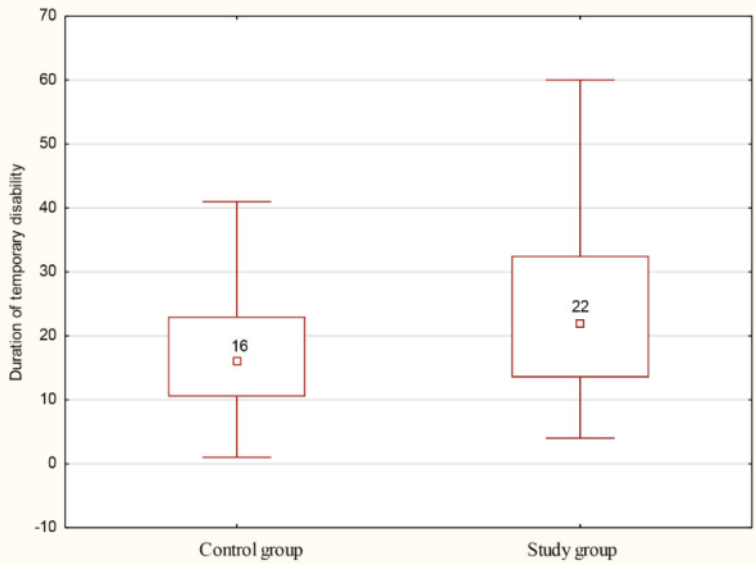


Groups were comparable by the duration of temporary disability, p=0.625 (Fig. 11).

**Table 8.** Risk Factors of Postoperative Chronic Non-Healing Wounds.

| Risk factors | OR (CI 95%) | p |
|---|---|---|
| Treatment method:<br>40 IU Botulotoxin type A<br>10 IU Botulotoxin type A | <br>15(1.8-127.6)<br>1 | 0.01 |
| Persistent sphincter spasm:<br>Yes<br>No | <br>5.6 (1.3-24.4)<br>1 | 0.02 |
| Specific infections:<br>Yes<br>No | <br>36.7 (3.6-369.5)<br>1 | 0.002 |

**Figure 12.** Factors Affecting the Period of Operative Wounds Healing.

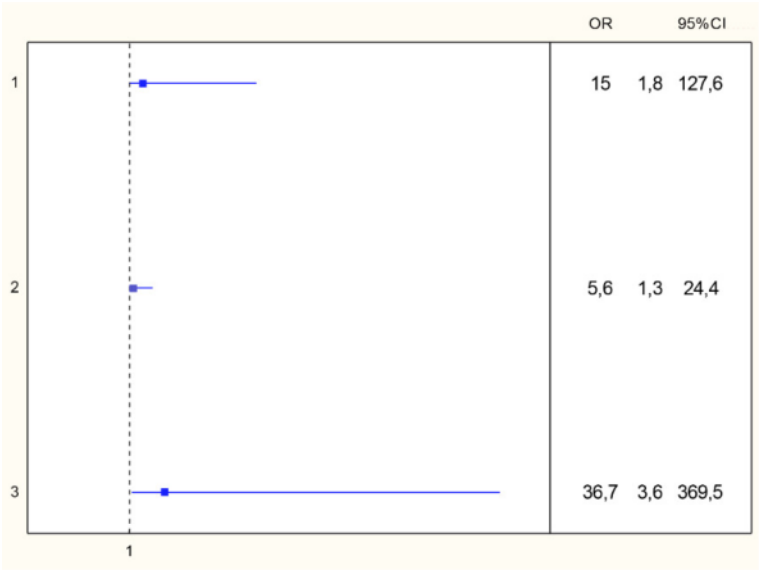


Treatment method (10 IU Botulinum toxin type A/40 IU Botulinum toxin type A)
IAS spasm (Yes/No)
Specific wound infections (Yes/No)

As shown in Table 8 and Figure 12, the odds for non-healing of postoperative wounds is 5.6-fold higher with IAS spasm persisting on day 60 post surgery (p = 0.02), 15-fold higher with 10 IU BTA (p=0.01), and 36.7-fold higher with specific wound infections (p=0.002).

**Figure 13.** Factors Affecting Transient Anal Incontinence Occurrence on Day 30 Postoperatively.

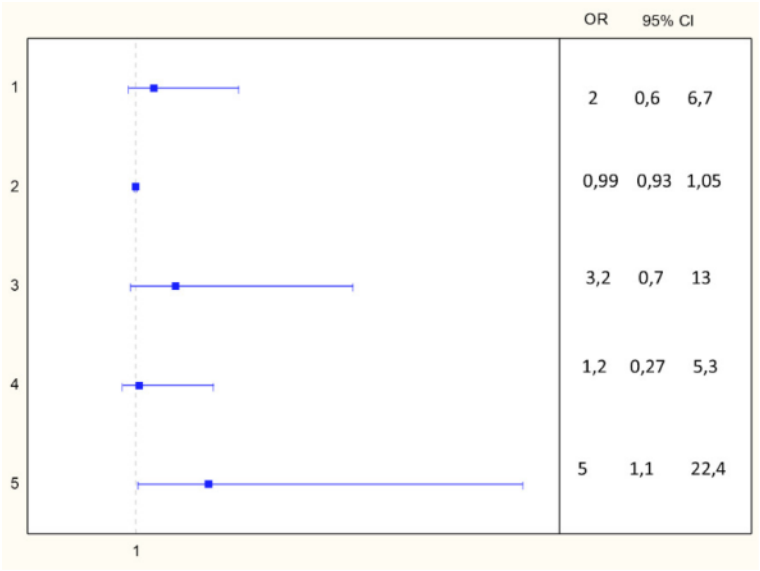


1. Treatment method (40 IU Botulinum toxin type A/10 IU Botulinum toxin type A)
2. Age
3. Gender (Females/Males)
4. Number of births (≥2/0-1)
5. Complicated labor (Yes/No)

**Table 9.** Factors Affecting Transient Anal Incontinence Occurrence on Day 30 Postoperatively.

| Risk factors | OR (CI 95%) | p |
|---|---|---|
| Botulotoxin dose:<br>40 IU<br>10 IU | <br>2 (0.6-6.7)<br>1 | 0.24 |
| Patients age | 0.99 (0.93-1.05) | 0.81 |
| Gender:<br>Females<br>Males | <br>3.2 (0.7-13.0)<br>1 | 0.1 |
| Number of births:<br>2 and more<br>0-1 | <br>1.2 (0.27-5.3)<br>1 | 0.81 |
| Complicated labor:<br>Yes<br>No | <br>5 (1.1-22.4)<br>1 | 0.035 |

Whereas, a history of complicated labor is the only factor that increases the odds for transient ASI occurrence on day 30 post surgery, p=0.035 (Table 9).

**Figure 14.** Factors Affecting Transient Anal Incontinence Persistence for 60 days in Postoperative Period.

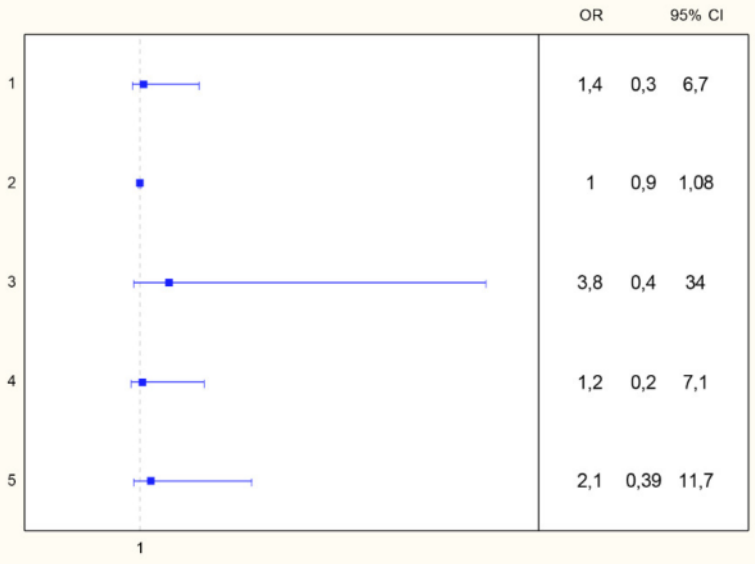


1. Treatment method (40 IU Botulinum toxin type A/10 IU Botulinum toxin type A)
2. Age
3. Gender (Females/Males)
4. Number of births (≥2/0-1)
5. Complicated labor (Yes/No)

**Table 10.** Risk Factors Affecting Postoperative Transient Sphincter Ani Externum Incompetence Persistence for 60 days Post Surgery.

| Risk factors | OR (CI 95%) | p |
|---|---|---|
| Botulotoxin dose:<br>40 IU<br>10 IU | <br>1.4 (0.3-6.7)<br>1 | 0.69 |
| Patients age | 1.0 (0.90-1.08) | 0.97 |
| Gender:<br>Females<br>Males | <br>3.8 (0.4-34.0)<br>1 | 0.23 |
| Number of births:<br>2 and more<br>0-1 | <br>1.2 (0.2-7.1)<br>1 | 0.88 |
| Complicated labor:<br>Yes<br>No | <br>2.1(0.39-11.7)<br>1 | 0.38 |

No factors increasing the risk of transient anal incontinence occurrence on day 60 post surgery were observed (Table 10, Fig. 14).

## DISCUSSION

A large number of publications on the use of BTA injection into the internal anal sphincter as a method for CAF treatment is currently available (7,22-24). However, the product doses and methods of administration are still unclear. According to Bobkiewicz et al., the increase in the doses and number of injection points has no effect on the treatment efficacy (22). On the other hand, according to O.V. Tkalich et al., administration of higher dose botulinum toxin and the increased number of injection points in recurrent patients helps to achieve stable IAS relaxation and CAF healing (19). This is supported by the results obtained by the authors in their study, where the increased doses of botulotoxin and changed administration technique helped to improve treatment efficacy. A 15-fold increase in BTA doses increases the odds for postoperative wounds epithelialization. To authors` opinion, this is due to a 5.6-fold increase in the odds for achieving stable IAS relaxation with 40 IU product injection, p=0.02.

An increase in the product doses and the number of injection points statistically significantly reduces the maximum and medium pressure in the anal canal at rest, thus considerably effecting the main pathogenetic mechanism of CAF – the IAS spasm (p=0.0053 and p=0.0002 , respectively). However, as profilometry data show, it is associated with more pronounced negative effects on the external sphincter function. Thus, the pressure in the anal canal at voluntary constriction is more significantly decreased in control patients.

Despite the fact that botulotoxin has no evident diffusion, the product is more likely to be delivered to the external rectal sphincter with the increased number of injection points. However, it should be noted that this negative effect does not affect the severity of clinical signs of transient anal incontinence, both on day 30 and day 60 postoperatively, p=0.18 and p=0.5, respectively (18). This again suggests that other factors play an essential role in anal incontinence development. Women, who had a history of complicated labor, are at 5-fold higher risk of anal incontinence, which indicates a hidden dysfunction of obturative rectum apparatus prior to surgery in this cohort of patients (12).

## CONCLUSION

This study demonstrates that an increase in the product doses and number of injection points helps to improve treatment efficacy without negative effects on the incidence of complications, and, in particular, on transient anal incontinence occurrence. Taking into account the small number of patients and the comparative nature of the study, further increase in the product doses and changes in administration technique are still outstanding issues requiring further studies with randomization design.

## CONTRIBUTION OF AUTHORS

**Study concept and design:** V.N. Kashnikov, A.A. Ponomarenko, I.V. Kostarev, E.E. Zharkov, O.V. Tkalich, S.V. Slozhenikin, E.A. Zagryadskiy, N.A. Goloktionov, R.Yu. Khryukin. **Materials collection and processing:** R.Yu. Khryukin, O.V. Tkalich, N.A. Goloktionov, S.V. Slozhenikin, E.A. Zagryadskiy, V.Yu. Medvedev, E.E. Zharkov , O.Yu. Fomenko, S.V. Nekhrikova, K.I. Arslanbekova, V.K. Misikov. **Statistical processing:** A.A. Ponomarenko, E.E. Zharkov , O.V. Tkalich N.A. Goloktionov, R.Yu. Khryukin, A.A. Akulov, A.S. Orlova. **Text writing:** N.A. Goloktionov, R.Yu. Khryukin, O.V. Tkalich, E.E. Zharkov, A.A. Akulov, A.S. Orlova. **Editing**: V.N. Kashnikov, A.A. Ponomarenko, I.V. Kostarev

## CONFLICT OF INTEREST

The authors declare that there is no conflict of interest.

## REFERENCE


1. Titov A.Y., Zharkov E.E., Vardanjan A.V. Differential diagnosis for anal fissure and ulcerative lesions of anal canal and perianal skin. Koloproktologia, 2012. C.3-10.
2. Renzi A, Izzo D, Di Sarno G et al. Clinical, manometric, and ultrasonographic results of pneumatic balloon dilatation vs. lateral internal sphincterotomy for chronic anal fissure: a prospective, randomized, controlled trial. Dis Colon Rectum. 2008; 51(1): c.121-127. DOI: 10.1007/s10350-007-9162-7
3. Nasr M, Ezzat H, Elsebae M. Botulinum toxin injection versus lateral internal sphincterotomy in the treatment of chronic anal fissure: a randomized controlled trial. World J Surg. 2010; 34(11): c.2730-2734.
4. Valizadeh N, Jalaly NY, Hassanzadeh M et al. Botulinum toxin injection versus lateral internal sphincterotomy for the treatment of chronic anal fissure: randomized prospective controlled trial. Langenbecks Arch Surg. 2012; 397(7): c.1093-1098. DOI: 10.1007/s00423-012-0948-2
5. Magdy A, Nakeeb A, Fouda Y et al. Comparative study of conventional lateral internal sphincterotomy, V-Y anoplasty, and tailored lateral internal sphincterotomy with V-Y anoplasty in the treatment of chronic anal fissure. J Gastrointest Surg. 2012; 16(10): c.1955-1962. DOI: 10.1007/s11605-012-1984-5
6. Blagodarnyy L.A., Poletov N.N., Zharkov E.E. Pathogenesis of anal fissures. Koloproktologia. 2007; no. 1(19): pp. 38-41. (in Russ.)
7. Tkalich O.V., Zharkov E.E., Ponomarenko A.A. Modern methods of drug relaxation of the internal sphincter in patients with anal fissure. Khirurg. 2019; no. 8: pp. 26-42. (in Russ.).
8. Stewart DB, Gaertner W, Glasgow S et al. Clinical Practice Guideline for the Management of Anal Fissures. Dis Colon Rectum. 2017. T. 60, № 1: c.7-14. DOI: 10.1097/DCR.0000000000000735
9. Richard CS, Gregoire R, Plewes EA et al. Internal sphincterotomy is superior to topical nitroglycerin in the treatment of chronic anal fissure: results of a randomized, controlled trial by the Canadian Colorectal Surgical Trials Group. Dis Colon Rectum. 2000. T. 43, № 8: c.1048-57. DOI: 10.1007/bf02236548
10. Nasr M, Ezzat H, Elsebae M. Botulinum toxin injection versus lateral internal sphincterotomy in the treatment of chronic anal fissure: a randomized controlled trial. World J Surg. 2010. T. 34, № 11: c.2730-4. DOI: 10.1186/1471-230x-4-7
11. Shelygin Yu.A. Clinical recommendations. Coloproctology. Ed. Corresponding Member RAS Yu.A. Shelygin. M.: GEOTAR-Media, 2015, pp. 12-29. (in Russ.)
12. Shelygin Yu.A., Zharkov E.E., Orlova L.P. Risk of anal incontinence after anal fissure excision in combination with lateral subcutaneous sphincterotomy. Koloproktologia. 2005; no.1 (11), pp.10-16. (in Russ.).
13. Renzi A, Izzo D, Di Sarno G et al. Clinical, manometric, and ultrasonographic results of pneumatic balloon dilatation vs. lateral internal sphincterotomy for chronic anal fissure: a prospective, randomized, controlled trial. Dis Colon Rectum. 2008. T. 51, № 1: c. 121-7. DOI: 10.1007/s10350-007-9162-7
14. Valizadeh N., Jalaly N. Y., Hassanzadeh M. et al. Botulinum toxin injection versus lateral internal sphincterotomy for the treatment of chronic anal fissure: randomized prospective controlled trial. Langenbecks Arch Surg. 2012. T. 397, № 7: c. 1093-8. DOI: 10.1007/s00423-012-0948-2
15. Sohn N, Eisenberg MM, Weinstein MA et al. Precise anorectal sphincter dilatation--its role in the therapy of anal fissures. Dis Colon Rectum. 1992. T. 35, № 4: c. 322-7.
16. Stewart DB, Gaertner W, Glasgow S et al. Clinical Practice Guideline for the Management of Anal Fissures. Dis Colon Rectum. 2017. T. 60, № 1: c. 7-14. DOI: 10.1097/DCR.0000000000000735
17. Richard CS, Gregoire R, Plewes EA et al. Internal sphincterotomy is superior to topical nitroglycerin in the treatment of chronic anal fissure: results of a randomized, controlled trial by the Canadian Colorectal Surgical Trials Group. Dis Colon Rectum. 2000. T. 43, № 8: c. 1048-57. DOI: 10.1007/bf02236548
18. Tkalich O.V., Ponomarenko A.A., Fomenko O.Yu. et al. The treatment of chronic anal fissures with fissure excision and botulinum toxin type A injection (ISRCTN97413456). Koloproktologia. 2020; 19(1):80-99. DOI: 10.33878/2073-7556-2020-19-1-80-99
19. Yu. A. Shelygin, O. V. Tkalich, A. A. Ponomarenko. Follow-Up results of combination treatment of chronic anal Fissure. International Journal of Pharmaceutical Research. Jul - Dec 2020. Vol 12. DOI: https://doi.org/10.31838/ijpr/2020.SP2.040
20. Arslanbekova K.I., Khryukin R.Yu., Zharkov E.E. Anoplasty and lateral internal sphincterotomy for chronic anal fissure (systematic review and meta-analysis). Koloproktologia. 2020; 19(4): pp. 115-130. DOI: 10.33878/2073-7556-2020-19-4-115-130

21. Nekhrikova S.V., Titov A.Yu., Kashnikov V.N. Outpatient treatment of patients with diseases of the anal canal and perianal region. Dokazatel'naya gastroenterologiya. 2019; v.8, no. 3: pp. 27-37. (in Russ.)
22. Bobkiewicz A, Francuzik W, Krokowicz L et al. Botulinum toxin injection for treatment of chronic anal fissure: Is there any dose-dependent efficiency? A MetaAnalysis. World J Surg. 2016. DOI: 10.1007/s00268-016-3693-9
23. 23 M Mfnguez, F Melo, Al Espf et al. Therapeutic effects of different doses of botulinum toxin in chronic anal fissure. Dis Colon Rectum. August 1999.Vol. 42. № 8: c. 1016-1021. DOI: 10.1007/bf02236694
24. Khryukin R.Yu., Kostarev I.V., Arslanbekova K.I. et al. Botulinum toxin type a and lateral subcutaneous sphincterotomy for chronic anal fissure with the sphincter spasm. What to choose? (systematic literature review and meta-analysis). Koloproktologia. 2020; v. 19, no. 2(72), pp. 113-128 (in Russ.). DOI: 10.33878/2073-7556-2020-192-113-128.

ORIGINAL SCIENTIFIC ARTICLE

# DOSIMETRIC COMPARISON: INTENSITY MODULATED RADIATION THERAPY VS. 3D CONFORMAL RADIOTHERAPY IN PROSTATE CANCER RADICAL TREATMENT

Slavica Maric[1], Snezana Lukic[2], Milan Mijailovic[2], Ljiljana Tadic Latinovic[3], Milan Zigic[4] and Pavle Banovic[1]

[1]*International Medical Center of Banja Luka, Center of Radiotherapy, Banja Luka, the Republic of Srpska*
[2] *University of Kragujevac Faculty of Medical Sciences, Department of Radiology, Kragujevac, Serbia*
[3]*University Clinical Center of the Republika of Srpska, Department of Pathology, Banja Luka, the Republic of Srpska*
[4] *University Clinical Center of the Republika of Srpska, Clinic of Urology, Banja Luka, the Republic of Srpska*

Received: 25.05.2019.
Accepted: 05.10.2019.

**Corresponding author:**

**Slavica Maric**

181b Bul. Stepe Stepanovica Street, Banja Luka

Phone: +387 66 906 773
E-mail: masa.maric3@gmail.com

UDK: 616.65-085:615.849
615.849.015.3
Ser J Exp Clin Res 2022; 23(1): 29-36
DOI: 10.2478/sjecr-2019-0046

## ABSTRACT

*3D - Conformal Radiotherapy (3DCRT) for decades was a standard technique in the prostate cancer radical radiotherapy treatment. Technological advances and implementation of an innovative radiotherapy technique-Intensity Modulated Radiation Therapy (IMRT), enable even more precise treatment of the prostate cancer patients. Intensity Modulated Radiation Therapy (IMRT) is a technological advancement in Conformal Radiotherapy which allows superior conformity and homogeneity of the absorbed dose in planning target volume with maximal sparing organs of risk. This technique gives us possibility to escalate the radiotherapy dose, prerequisite for the adequate local tumor control. Evaluation of dosimetric parameters 3DCRT vs. IMRT: the homogeneity index, the conformity index, parameters of absorbed dose in planning target volume, dose volume constraints for organs of risk shows that IMRT is an optimal technique in the prostate cancer radical treatment.*

**Keywords**: *3D-Conformal Radiotherapy, prostate cancer, planning target volume, Intensity Modulated Radiation Therapy.*

## INTRODUCTION

Prostate cancer is the second most common cause of death in male population, and the most common diagnosed cancer in men. Incidence is very high in developed countries-over three quarters of cases (1). According to the National Comprehensive Cancer Network NCCN recommendations for the treatment of prostate cancer, patients in any risk group can have radiotherapy as an indication in the primary setting as the radical treatment, or as one modality of the treatment (2). Radiation therapy for the prostate cancer has evolved dramatically over the past 2 decades. Treatment has evolved from X-ray fields based on bony anatomy to dose escalated radiation therapy with image-guidance and the IMRT. 3D conformal radiotherapy was introduced in 1980 and was the first form radiotherapy that can adjust shape of the beam to the shape of the tumor. The goal of conformal radiotherapy is to deliver a high radiation dose to the tumor, while minimizing radiation therapy dose in organs of risk (3). The Intensity Modulated Radiation Therapy (IMRT) is technological advancement in Conformal Radiotherapy and it is unique technique because it allows inverse planning. The essence of Intensity Modulated Radiotherapy is the use of the intensity modulated beams that allows two or more intensity levels for any direction of the beam and for any position of the source. Using this mechanism, plans developed by the Intensity Modulated Radiotherapy are able to generate a concave dose distribution and dose gradients with sharper margins than 3DCRT technique (4). The Intensity Modulated Radiation Therapy can provide clinical benefit in terms of the increased tumor control due to the escalation of a dose, which is extremely important in the prostate carcinoma radical treatment.

Several clinical studies show benefit of escalation of a dose in the radical treatment of the clinically localized prostate carcinoma (5, 6). Theoretically, the escalated dose with IMRT technique can increase an incidence of acute and late gastrointestinal and genitourinary toxicity. Published dose-volume constraints, that can reduce or prevent rectal injury, have been established and are achievable with IMRT (7). Previous studies demonstrate in most cases that the Intensity Modulated Radiation Therapy compared to the Three-Dimensional Conformal Radiotherapy is superior in the radical treatment of the clinically localized prostate carcinoma, particularly in terms of more conformal and homogenous delivered dose, produced by intensity modulated small fields(8,9).

## PATIENTS AND METHODS

A total of 70 patients with the verified clinically localized prostate cancer were included in this study (3DCRT technique: 35 patients, IMRT technique: 35 patients)

Inclusion parameters were: Adenocarcinoma prostate, a low risk and intermediate risk group, Gleason score (GS) 6-7, Prostate specific antigen PSA less than 10 or 10-20ng/ml, TNM classification T1-T2a, b, c N0 M0 (10). Patients were divided into two groups. Group A: N=35 radical treatment was planned with the Three-Dimensional Conformal Radiotherapy (3DCRT). Group B: N=35, radical treatment was planned with the Intensity Modulated Radiotherapy. Preparation for radiotherapy treatment in study group B planned with IMRT also contains a consultative exam of an Urologist, and the implantation of fiducially gold markers in prostate (11). After an adequate preparation of the patient, the Urologist implanted three fiducially gold markers in the prostate-two into the prostate base, one into the apex (Figure 1). Fiducially markers allow an adequate verification of the prostate position before delivery of treatment, and reduce the possibility of inter and intra-fraction movement of the prostate (12).

**Figure 1.** Implanted gold fiducially markers in prostate

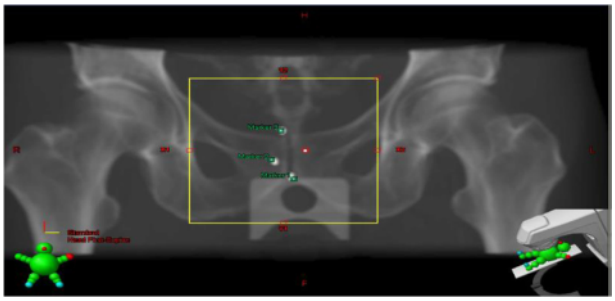

Patients in study group A were planned on the Eclipse Planning System -Varian Medical Systems version 10.0 and treated with the Three-Dimensional Conformal Radiotherapy technique (Figure 2 and Figure 3).

**Figure 2.** 3D Conformal plan prostate cancer

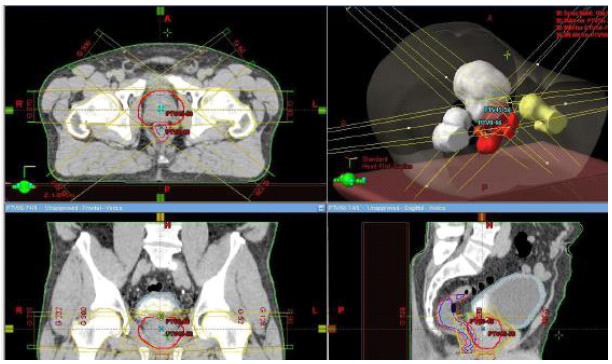

**Figure 3.**Radical 3DCRT technique

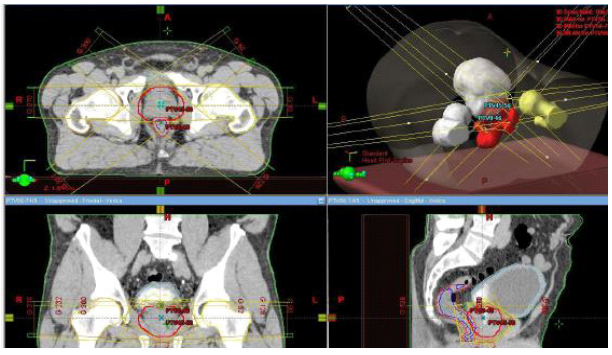

In 18 patients the prescribed dose was 70 Grey (Gy) in 35 fractions, while in 17 patients the prescribed dose was 74 Gy in 37 fractions.

Patients in study group B were planned by inverse planning on the Eclipse Planning System Varian Medical Systems, version 10.0 and treated with the Intensity Modulated Radiation Therapy. The prescribed dose was 78 Gy in 39 fractions in all patients (Figure 4 and Figure 5).

**Figure 4.** IMRT plan prostate cancer

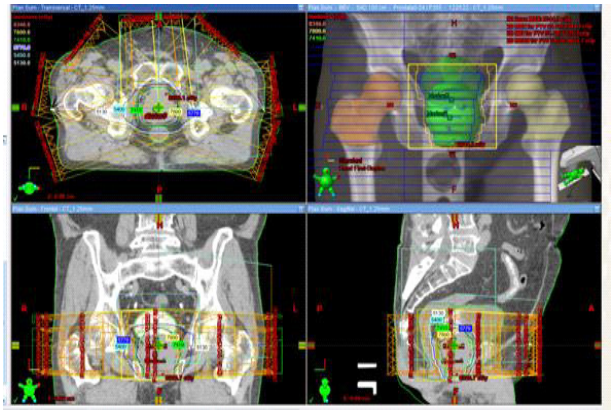

**Figure 5.** Radical IMRT treatment

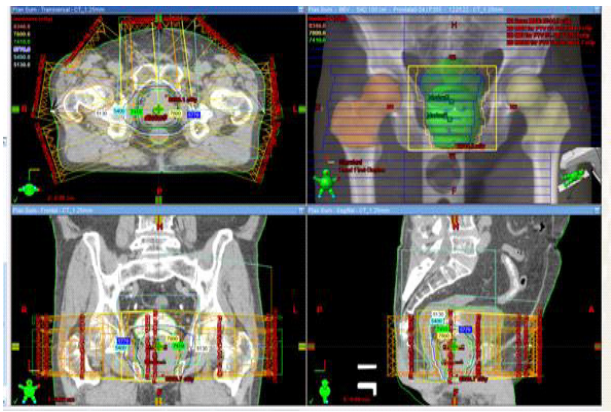

Evaluation of the dose received in planning target volume (prostate) and the dose received in organs of risk (bladder, rectum) was done with a dose-volume histogram DVH (13)

Analysis of the dose volume histogram is very important factor in radiotherapy planning. The DVH will be evaluated using the recommended dose volume constraints for the organs of the risk-bladder, rectum for both techniques (Figure 6).

In clinical practice, radiobiological effects of the radiotherapy treatment are extremely important, in particular the possibility of local tumor control (prostate) and the possibility of early or late toxicity in organs of risk (bladder, rectum).

According to the RTOG-Radiation Therapy Oncology Group recommendations, a dose volume constraint in radiation therapy for the organ of risk bladder is :V65 <50%. A dose of 65 Gray should receive less than 50 % volume of the bladder. Dose volume constraints for the organ of risk rectum are: V60 <50% A dose of 60 Gray should receive less than 50% volume of the rectum, V70% <25%. A dose of 70 Grey should receive less than 25% of the volume of the rectum (14).

**Figure 6.** Dose volume histogram- volume per fraction /dose per fraction ratio

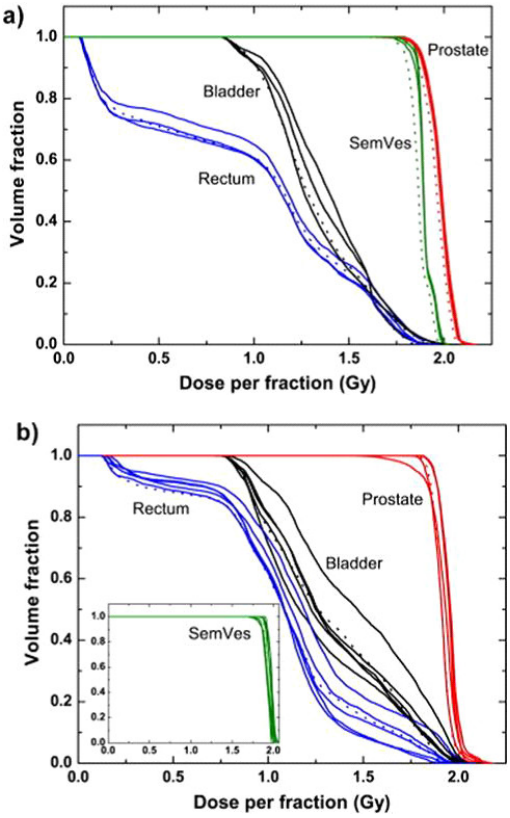


It is also recommended that the range of a high dose region and a low dose region in the planning target volume should be specified and evaluated with the DVH (15): D2%- the largest asbsorbed dose in minimal volume, D98% -the lowest absorbed dose in maximal volume, D50%- the absorbed dose which cover 50% planning target volume, D98%-A minimum absorbed dose which covers 95% planning target volume. The Conformity Index (CI) defines the quality of radiotherapy plan and the connection between isodose distribution and planning target volume (16). CI = TV/PTV TV-treated volume dose selected and prescribed by a radiation Oncologist PTV – planning target volumen. The Conformity Index values are in the range 0-1. Value closer to a value 1 inidicates better conformity and coverage of the planning target volume. The Homogeneity Index (HI) is another important parameter for analizing the uniformity and homogeneity of the dose distribution in the planning target volume (17). HI = D2%-D98%:D50. Value of the homogeneity index closer to value 0 indicates that the absorbed dose distribution in planning target volume is more homogenous.

The T-test was used to compare registered values. The statistical difference considered significant was $p < 0.05$.

**The aim** of this study is to confirm that the IMRT is an innovative precise technique in the radical treatment of prostate cancer, with the optimal dosimetric benefit which allows the escalation radiation therapy dose in planning target volume and adequate local control with acceptable toxicity profile.

## RESULTS

Results show a comparative analysis of the dosimetric parameters of the prostate cancer patients in study group A and the study group B.

Basic parameters of observation in this study were: age, clinical stage of the disease, the androgen deprivation therapy as additional treatment.

69% patients in study group A were older than 70 year, 60% patients in study group B were older than 70 years. Results obtained from study group A and study group B (Chart 1 and Chart 2) correspond with the reference data which indicate that the prostate cancer is a disease of the older age male population (18).

**Chart 1.** Study group A age range

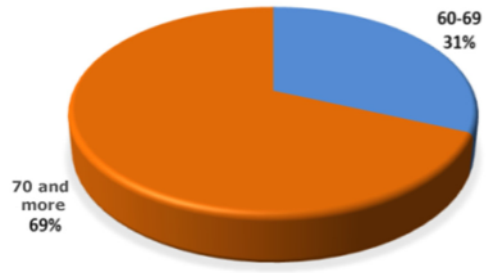


**Chart 2.** Study group B age range

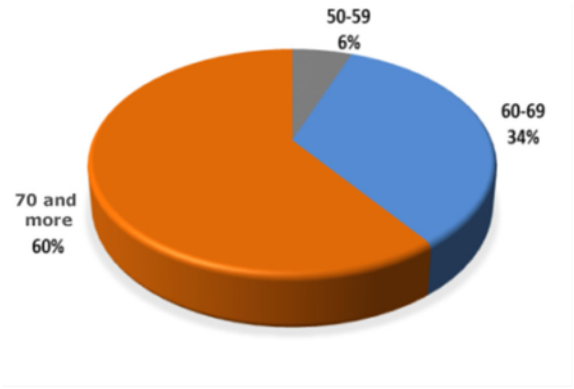


This study included patients with the clinically localized prostate cancer, the clinical stage of patients was T1a-T2c, and there was no statistically significant difference in TNM classification in study group A and study group B. Distribution of patients' study group A according to TNM classification and T status are shown in (Table 1).

**Table 1.** T status study group A

| TNM | Number of patients | |
|---|---|---|
| | N | % |
| T1a | 5 | 14,29 |
| T2a | 10 | 28,57 |
| T2b | 14 | 40,00 |
| T2c | 6 | 17,14 |
| Total | 35 | 100,00 |

Distribution of patients' study group B according to TNM classification and T status are shown in (Table 2).

**Table 2.** T status study group B

| TNM | Number of patients | |
|---|---|---|
| | N | % |
| **T1a** | 7 | 20,0 |
| **T2a** | 10 | 28,6 |
| **T2b** | 7 | 20,0 |
| **T2c** | 11 | 31,4 |
| **Total** | **35** | **100,00** |

There was no statistically significant difference between study group A and study group B when the androgen deprivation therapy as additional treatment was indicated. Distributions of patients' study group A with indication for the androgen deprivation therapy are shown in (Chart 3). Distributions of patients' study group B with indication for the androgen deprivation therapy are shown in (Chart 4).

Comparison of the Conformity Index (CI) values for the study group A and the study group B

Results of the comparison of conformity index values present a statistically significant difference ($p<0.05$) between the study group A and the study group B (Chart 5). In this case, the mean value of the study group A was dominant compared to the mean value of the study group B.

**Chart 3.** Study group A Hormonal Therapy

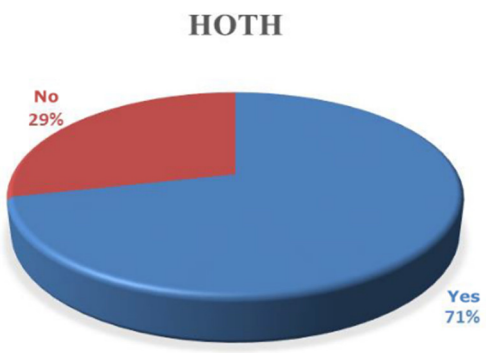

**Chart 4.** Study group B Hormonal Therapy


**Chart 5.** Comparison Study group A (marked with blue) and Study group B (red) mean value conformity index

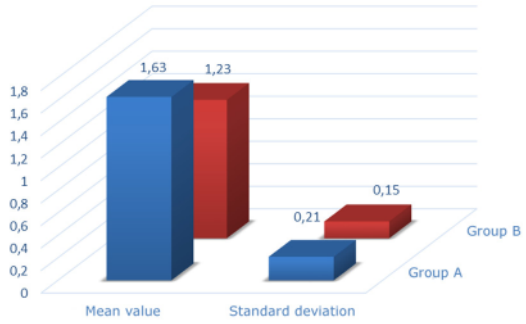


Comparison of the Homogeneity Index (HI) values for the study group A and the study group B

Results of the comparison of the Homogeneity Index values present a statistically significant difference ($p<0.05$) between study group A and study group B (Chart 6).

In this case, t -test ($t= 2.307$; $p = 0.$) showed that mean value of study group A was a statistically significantly higher compared to the mean value of study group B.

**Chart 6.** Comparison Study group A (marked with blue) and Study group B (red) mean value homogeneity index


Comparison of values D2% - the largest absorbed dose in minimal volume.

Based on results of the t-test ($t= 3.053$; $p = 0.000$) there was a statistically significant difference ($p<0.05$) between the mean value of the study group A and the study group B (Chart 7). The value D2% was a statistically significantly higher in the study group B planned with the IMRT.

**Chart 7.** Comparison Study group A (marked with blue) and Study group B (red) - mean value D2%

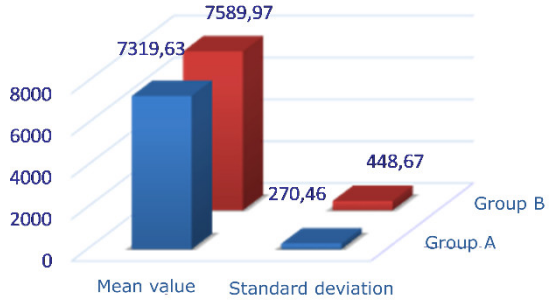


Comparison of values D98% - the lowest absorbed dose in maximal volume.

Based on results of the t -test ($t= -6.185$; $p = 0.000$) there was a statistically significant difference ($p<0.05$) between the mean value of the study group A and the study group B (Chart 8). The value D98% was a statistically significantly higher in the study group B planned with the IMRT.

Comparison of values D50% -the absorbed dose which covers 50% planning target volume

Based on results of the t -test ($t= -5.346$; $p = 0.000$) there was statistically significant difference ($p<0.05$) between the mean value of the study group A and the study group B (Chart 9). The value 50% was a statistically significantly higher in the study group B planned with the IMRT.

**Chart 8.** Comparison Study group A (marked with blue) and Study group B (red)- mean value D98%

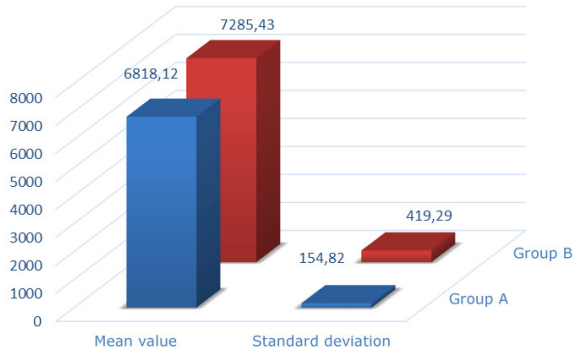

**Chart 9.** Comparison Study group A (marked with blue) and Study group B (red) - mean value D50%

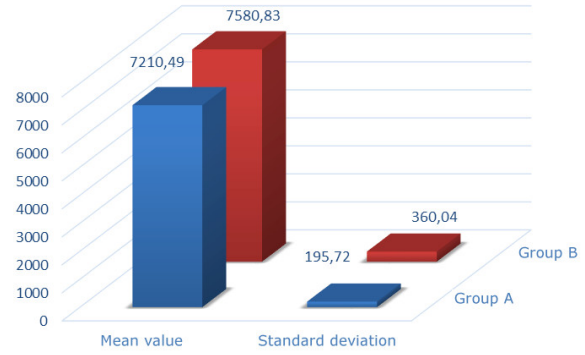


Comparison of values D95%- the absorbed dose which covers 95% planning target volume

Based on results of the t -test (t= -5.346; p = 0.000) there was statistically significant difference (p<0.05) between the mean value of the study group A and the study group B (Chart 10). The value 50% was a statistically significantly higher in the study group B planned with the IMRT.

**Chart 10.** Comparison Study group A (marked with blue) and Study group B (red) - mean value D95%

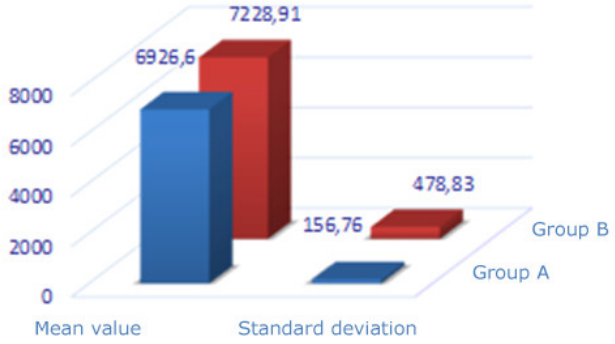


Comparison of a dose volume constraint for the organ of risk- bladder V65<50%

New standards in the radiotherapy practice are very often established in the treatment of prostate cancer.

Most of the new techniques proved their superiority in the radiotherapy of prostate cancer and later expanded their clinical application to other clinical localizations. Why is the prostate such a good model? The prostate has a relatively simple geometric shape and well-defined treatment plans can be generated for this planning volume.

This allows a Doctor to focus on the coverage of the target volume as well as the sparing of surrounding organs from the risk. Delivering a high radiation dose on the prostate with limitation of a dose to surrounding organs of risk in terms of minimizing acute and late gastrointestinal and

Results of the comparison of the value V65 study group A with the value V65 study group B with the t-test present statistically significant difference (p <0.05) in the mean value (Chart 11).

**Chart 11.** Comparison Study group A(marked with blue) and Study group B (red) mean value V65-bladder

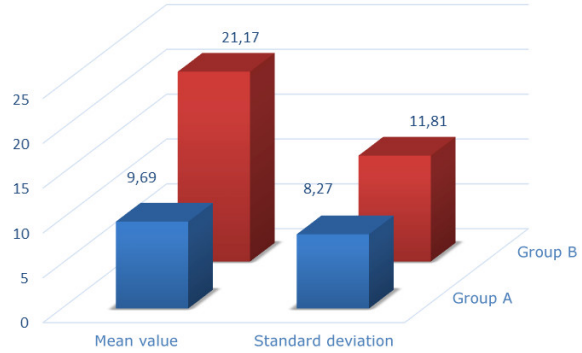


In this case, Levin test (F = 7.752; p = 0.007) showed that the mean value of V65 was approximately 2 times higher in the study group B.

Comparison of a dose volume constraint for the organ of risk- rectum: V60 <50%

Results of the comparison of the value V60 study group A with the value V60 study group B with the t-test for the organ of risk-rectum present that there was no statistically significant difference (p >0.05) when the mean value V60 was observed (Chart 6).

Comparison of a dose volume constraint for the organ of risk- rectum: V70 <25%

Results of the comparison of the value V70 study group A with the value V70 study group B with the t-test for the organ of risk-rectum, present that there was no statistically significant difference (p >0.05) when mean value V70 was observed (Chart 7).

## DISCUSSION

gastrointestinal effects is a significant challenge. With 3D CRT technique it is possible to deliver a radiation therapy dose up to 72-74 Gy in maximum. As it was previously mentioned, there are historical and prospective data that support the benefit of the escalated radiation therapy dose in the treatment of the clinically localized prostate cancer (19). The IMRT is a promising technique which gives us possibility of the escalation of radiation dose up to 78-80 Gy, and this technique today is preferable in every modern radiotherapy center. The implementation of the Intensity Modulated Radiation Therapy requires a significant investment both in the equipment and radiation therapy workflow.

Two important studies consistently demonstrate that higher radiation doses (78-79) Gy result in the reduced

recurrence of disease comparable to the lower radiation doses (20,21). Dose escalated IMRT treatment as demonstrated in previously mentioned studies has resulted with the increased local tumor control. Comparison in our study has shown that there was a statistically significant difference ($p<0.05$) between the study group A and the study group B when the mean values: D2% - the largest absorbed dose in minimal volume, D98% the lowest absorbed dose in maximal volume, D50%- the absorbed dose which cover 50% planning target volume, D95% -the absorbed dose which cover 95% planning target volume were compared. These are very important parameters that indicate the dosimetric quality of the radiotherapy plan and the quality of the absorbed dose distribution.

A statistically significant difference in values D2%, D50%, D95%, D98% indicates a better coverage of the planning target volume in the study group B planned with the Intensity Modulated Radiotherapy and consequently increased local tumor control.

The superiority of IMRT in relation to 3D CRT in the terms of more conformal delivered dose, especially in the case of concave tumor volumes was presented in different studies (22, 23).

The statistically significant difference ($p <0.05$) between mean values of the Homogeneity Index between the study group A and the study group B indicates a significantly more homogenous dose distribution in the study group B planned with the IMRT technique. The increased homogeneity and better conformity of a dose distribution in planning target volume result with precise radiotherapy treatment and adequate local tumor control.

There is a major concern that the delivery of high radiation doses can lead to the increased incidence of acute and late gastrointestinal and genitourinary toxicity. For this reason, evaluation of dosimetric parameters and dose volume recommendations and constraints for organs of risk-bladder and rectum is extremely important.

Comparison in our study has shown that there was a statistically significant difference ($p<0.05$) between the study group A and the study group B when mean values of delivered dose V65 for th eorgan of risk-bladder were compared. The mean value of delivered dose V65 for the organ of risk-bladder in the study group B was approximately 2 times higher than the mean value delivered dose V65 in the study group A.

Heaving in mind that the total delivered dose in the group A was 70-74Gy, it is expected that the mean dose of bladder in a certain number of patients in Group A will be significantly lower.

Results in this study showed that there was no statistically significant difference ($p>0.05$) between the study group A and the study group B when mean values of the delivered dose V70 and V60 for the organ of risk-rectum were evaluated.

These results are extremely important, because in the study group A patients were planned with 3DCRT technique and the total delivered dose was 70 Gy in 18 patients, and 74 Gy of total dose was delivered in 17 patients of this group, while in the study group B planed with the IMRT technique the total dose delivered was 78 Gy in all 35 patients.

Zelefsky et al. reported that the 10-year follow-up of gastrointestinal morbidity was lower for patients treated with the Intensity Modulated Radiotherapy 5% compared with patients treated with the Three-Dimensional Conformal Radiotherapy (13%), despite higher prescribed doses at the target volume in IMRT patients (24). Patients treated with the Intensity modulated radiation therapy compared with the 3DCRT are less common requiring additional cancer treatment. That is consistent with the use of the IMRT in dose escalated treatment, resulting in the increased local control as demonstrated by the above studies.

## CONCLUSION

Patients with the clinically localized prostate cancer have a disease that is likely to be cured, so the quality of radiation therapy treatment – (an escalated radiation dose) and the quality of life (gastrointestinal and genitourinary potential toxicity) after radical radiotherapy treatment is extremely important. Compared with the 3DCRT, the IMRT is superior technique in terms of a dosimetric benefit which permits the escalation of radiation therapy dose with acceptable genitourinary and gastrointestinal profile.

## REFERENCES


1. Jemal A, Center MM, De Santis C, Ward EM. Global patterns of cancer incidence and mortality rates and trends. Cancer Epidemiol Biomarker Prev 2010; 19(8):1893-907.
2. NCCN Guidelines Version 1.2018. Prostate cancer. January 2018.
3. Brundage M, Lukka H, Crook J, et al. The use of conformal radiotherapy ant the selection of radiation dose in T1 or T2 low or intermediate risk prostate cancer- a systematic review. Radiother Oncol 2002; 64(3):12.
4. Al-Mamgani A, Heemsbergen WD, Peeters ST, Lebesque JV. Role of intensity-modulated radiotherapy in reducing toxicity in dose escalation for localized prostate cancer. Int J Radiat Oncol Biol Phys 2009; 73(3):685-691.
5. Kuban DA, Tucker SL, Dong L et al. Long-term results of the MD Anderson randomized dose-escalation trial for prostate cancer. Int J Radiat Oncol Biol Phys 2008; 70:67 –74.

6. Beckendorf V, Guerif S, Le Prise E, Cosset JM, Bougnoux A, et al. 70 Gy Versus 80 Gy in Localized Prostate Cancer: 5-Year Results of GETUG 06 Randomized Trial. Int J Radiat Oncol Biol Phys 2011; 80: 1056–1063.
7. Sujenthiran A, Nossiter J, Charman SC, et al. National population-based study comparing treatment-related toxicity in men who received intensity modulated versus 3-dimensional conformal radical radiation therapy for prostate cancer. Int J Radiat Oncol Biol Phys 2017;99:1253-60.
8. Gary Luxton, Steven L. Hancock, Arthur L. Boyer. Dosimetry and radiobiological model comparison of IMRT and 3D conformal radiotherapy in treatment of carcinoma of the prostate. Int J Radiat Oncol Biol Phys 2004, 59 :( 1): 267–284.
9. H.V. James, C.D. Scrase, A.J. Poynter. Practical experience with intensity-modulated radiotherapy. Br J Radiol 2004; 77: 3–14.
10. Edges SB, Byrd DR, Compton CC.AJCC Cancer Staging Handbook. 7th edition. New York, NY: Springer 2010.
11. Litzenburg D, Dawson AD, Sandler H, et al. Daily prostate targeting using implanted radiopaque markers. Int J Radiat Oncol Biol Phys. 2002; 52(3):699–703.
12. Poggi MM, Gant DA, Sewchand W, Warlick WB. Marker seed migration in prostate localization. Int J Radiat Oncol Biol Phys. 2003; 56(5):1248–1251.
13. Drzamala RE,Mohan R, Brewster L, Chu J, Goitein M, Harms W, et al. Dose volume Histograms. Int J Radiat Oncol Biol Phys 1991; 21:71-78.
14. Cox JD et al.Toxicity criteria of Radiation Therapy Oncology Group (RTOG) and the European Organization for Research and Treatment of Cancer (EORTC). Int J Radiat Oncol Biol Phys 1995; 31(5):1341-1346.
15. International Commission on Radiation Units and Measurements. Prescribing, recording, and reporting photon beam intensity- modulated radiation therapy. ICRU Report 83. Bethesda, MD: ICRU; 2010.
16. Feuvret L, Noel G, Mazeron JJ, Bey P. Conformity index- a review. Int J Radiat Oncol Biol Phys 2006; 64:333–42.
17. Yoon M, Park SY, Shin D, Lee SB, Pyo HR, Kim DY et al:A new homogeneity index based on statistical analysis of the dose-volumehistogram.J Appl Clin Med Phys 2007;8:(2):9-17.
18. Stangerberger A, Waldert M, Djuvan B. Prostate Cancer in elderly men. Rev Urol 2008; 10(2):111-119.
19. Viani GA, Stefano EJ, Alfonso SL et al. Higher than conventional radiation doses in localized prostate treatment: A meta- analysis of randomized, controlled trials. Int J Radiat Oncol Biol Phys 2009; 74(5):1405-18.
20. Pollack A, Zagars GK, Starkschall G, et al. Prostate cancer radiation dose response: Results of the M.D.Anderson phase III randomized trial. Int J Radiat Oncol Biol Phys 2002; 53 (5):1097-1105.
21. Zietman AL, De Silvio MR, Slater JD et al. Comparison of conventional dose vs. high dose conformal radiation therapy in clinically localized adenocarcinoma of the prostate. JAMA 2005; 294: 1233-1239.
22. Vincent W.C. Wu, Dora L.W. Kwong, Jonathan S.T. Sham. Target dose conformity in 3-dimensional conformal radiotherapy and intensity modulated radiotherapy Radiat Oncol 2004; 71: 201–206.
23. Gert De Meerleer, Luc Vakaet, Werner R.T. De Gersem, et al. Radiotherapy of prostate cancer with or without intensity modulated beams: a planning comparison Int J Radiat Oncol Biol Phys 2000; 47: (3) :639–648.
24. Zelefsky MJ, Levin EJ, Hunt M, et al. Incidence of late rectal and urinary toxicities after three dimensional conformal radiotherapy and intensity modulated radiation therapy for localized prostate cancer. Int J Radiat Oncol Biol Phys 2008; 70(4): 1124-1129.

ORIGINAL SCIENTIFIC ARTICLE

# COMPLICATED ROOT CANAL MORPHOLOGY OF PERMANENT MANDIBULAR LATERAL INCISORS IS ASSOCIATED WITH THE PRESENCE OF A SECOND MESIOBUCCAL CANAL IN PERMANENT MAXILLARY FIRST MOLARS

Milos Papic[1], Mirjana Papic[1], Miona Vuletic[1], Dejan Zdravkovic[1], Aleksandra Misic[1] and Suzana Zivanovic[1]

[1]*University of Kragujevac, Faculty of Medical Sciences, Department of Dentistry, Kragujevac, Serbia*

Received: 11.05.2019.
Accepted: 07.07.2019.

**Corresponding author:**

**Milos Papic**

Faculty of Medical Sciences, University of Kragujevac
Svetozara Markovića Str. 69
34000 Kragujevac, Serbia

Phone: (+381) 66 96 00 6 18
E-mail: milos_papic@live.com

sciendo

UDK: 611.314
Ser J Exp Clin Res 2022; 23(1): 37-44
DOI: 10.2478/sjecr-2019-0048

## ABSTRACT

*Many studies have been conducted in order to define the root canal morphology based on age, gender, ethnic and racial characteristics of the population. However, relations within morphological variations of certain groups of teeth have rarely been investigated. The aim of this study was to evaluate the root canal morphology of mandibular lateral incisors and to determine the association between their morphologic characteristics and the presence of a second mesiobuccal canal of maxillary first molars. Cone-beam computed tomography images from a pre-existing base were analyzed for the bilateral presence of both permanent mandibular lateral incisors and permanent maxillary first molars. Root canal morphology was analyzed according to the Vertucci classification. Associations of root canal morphologies between incisors and molars were calculated as probabilities using binary logistic regression analysis. In total, 126 mandibular lateral incisors and 126 maxillary first molars were included. 46% of all mandibular lateral incisors showed complicated root canal morphology and Vertucci type III canal configuration as the most frequent. Second mesiobuccal root canal was present in 62.7%. Root canal morphologies showed high level of bilateral symmetry in both tooth groups. The probability of a subject having complicated root canal morphology in lateral incisors was significantly higher when the second mesiobuccal canal was present. Clinicians should consider all available information on patients' root canal morphology when planning new endodontic treatment. Root canal morphology of permanent mandibular lateral incisors showed high association with the root canal morphology of permanent maxillary first molars.*

**Keywords**: *cone-beam computed tomography, incisors, mesiobuccal root, molars, root canal morpholog.*

## INTRODUCTION

The success of endodontic therapy relies on thorough cleaning, shaping and filling of root canal system. And thus the understanding of root canal morphology and its possible complexities decrease the incidence of procedural errors at any stage of endodontic treatment (1, 2). The introduction of cone-beam computed tomography into everyday dental practice has increased the availability of information on the root canal morphology in clinical conditions, which is in contrast to the previously used destructive laboratory techniques (3).

Permanent mandibular lateral incisors (PMLIs) are typically described as a single-rooted teeth with a single root canal (4). However, PMLIs with complex root canal system have been previously described, with varying incidence of two root canals depending on the studied population. The highest incidence was reported in Turkish population (63%) (5), which is in contrast to Chinese population (10%) (3). The permanent maxillary first molar (PMFM) is described as the tooth with the most variations in root and root canal morphology. It typically presents 3 roots with 3 or 4 root canals (6). The mesiobuccal root shows the highest complexity in root canal system. The incidence of the second mesiobuccal canal (MB2) varies from 36% to 75% depending on the population (7-15). Overall, difference in the incidence of multiple root canal complexities between Asian and Caucasian population is eminent, suggesting that morphological variations of root canal systems have racial basing (8).

Many studies have been conducted in order to define the root canal morphology based on age, gender, ethnic and racial characteristics of the population (8-10, 12). There are only a few studies regarding the association of morphological variations between different groups of teeth (2, 16). Recently, Wu et al. (17) examined the association between the presence of distolingual root in permanent mandibular molars and complex root canal morphology (PMLIs). However, to the authors' knowledge, the relation between the morphological variations of PMLIs and the variations of PMFMs has not yet been investigated.

## THE AIM OF THE PAPER

The aim of this study was to evaluate the root canal configuration of PMLIs and to determine the association between root canal configuration of PMLIs and the presence of MB2 in PMFMs.

## PATIENTS AND METHODS

### Image Acquisition

All images analyzed in this study were retrieved from a pre-existing CBCT database. CBCT scans were made at the Department of Dentistry, Faculty of Medical Sciences, University of Kragujevac, Serbia from October 2014 to October 2018. Scans were stored in the Digital Imaging and Communications in Medicine (DICOM) format. The reasons for patient's imaging were different (prosthetic, surgical, orthodontic and endodontic), but not with the intention of using them in this study. The study protocol was approved by the Ethics Committee of the Faculty of Medical Sciences, University of Kragujevac, Serbia (protocol number: 01-15837), and it was conducted in accordance with the Helsinki Declaration and Guidelines for Good Clinical Practice.

The scans were obtained using Orthophos XG 3D device (Sirona Dental Systems GmbH, Bensheim, Germany) with a three-dimensional settings for recording, VOL1 HD (85kV/6mA, exposure time - 14.3 seconds) or VOL2 HD (85kV/10mA, exposure time - 5.0 seconds), and a voxel size of 160μm or 100μm, respectively.

Initially, 150 patient's CBCT scans were examined for the bilateral presence of PMLIs and PMFMs, and 63 images qualified for further analysis based on the previously described inclusion criteria (17):

1. PMLIs and PMFMs were fully visible
2. Completed root formation
3. Absence of root canal treatment or obturation material
4. Absence of crown, post and core restorations
5. Absence of visible external or internal root resorptions

### Configuration Analysis and Classification

CBCT images were analyzed using a software GALAXIS v1.9.4 (Sirona Dental Systems GmbH, Bensheim, Germany). Observations were conducted using a Philips LED monitor, sized 23-inch, with a resolution of 1920 x 1080 pixels, in a room with dim lighting. Brightness and contrast were adjusted using software.

Root canal configurations in PMLIs and in mesiobuccal roots of PMFMs were analyzed on axial cross-sections and classified according to the Vertucci classification (18). The presence of type I root canal configuration (i.e. single canal) was noted as non-complicated root canal, while the presence of other types (i.e. two canals) was noted as complicated root canal. The presence or absence of MB2 in mesiobuccal roots of PMFMs was noted for every individual CBCT image.

Based on the bilateral presence of the second root canal in PMLIs (complicated root canal morphology) and in PMFMs (MB2), all images were further classified in the following groups:

**Figure 1.** Examples of subjects with different presence of PMLIs with complicated root canal morphology on axial cross-sections. Subjects were dived into three following groups: Non-Comp, Uni-Comp, Bi-Comp.

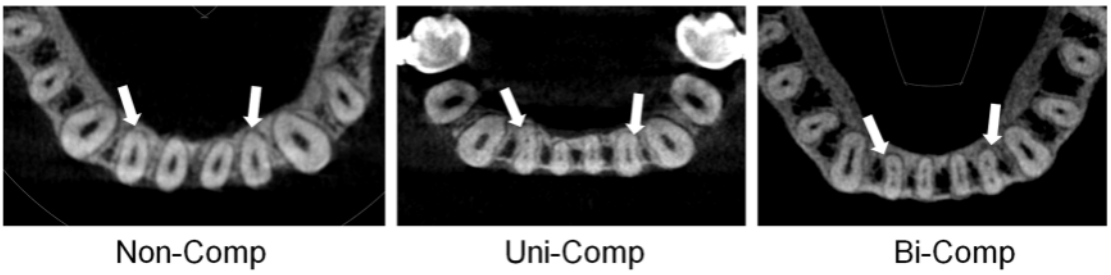


Non-Complicated (Non-Comp) - second root canals were absent in right or left PMLIs.

Unilateral Complicated (Uni-Comp) - second root canals were present in 1 PMLI (left or right); second root canal was absent in the other PMLI.

Bilateral Complicated (Bi-Comp) - second root canals were present in both left and right PMLIs.

**Figure 2.** Examples of subjects with different presence of PMFMs with MB2 on axial cross-sections. Subjects were dived into three following groups: Non-MB2, Uni-MB2, Bi-MB2.

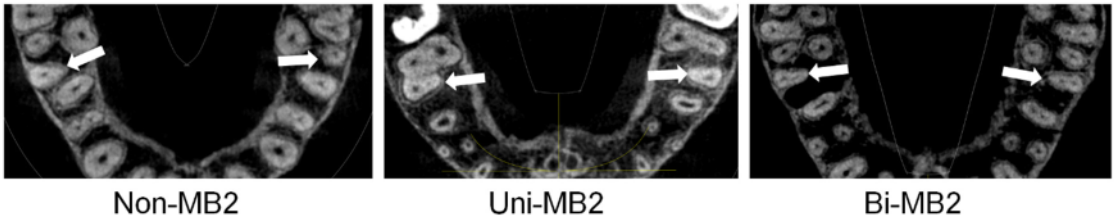


Non-MB2 (Non-MB2) - MB2 was absent in mesiobuccal roots of both left and right PMFMs.

Unilateral MB2 (Uni-MB2) - MB2 was present in mesiobuccal root of 1 PMFM (left or right); MB2 was absent in the other PMFM.

Bilateral MB2 (Bi-MB2) - MB2 was present in mesiobuccal roots of both left and right PMFMs.

**Statistical Analysis**

Descriptive statistics were expressed as mean values and standard deviations, frequencies and percentages. In order to examine the relation within categorical variables, such as the presence of complicated root canal configuration in PMLIs and PMFMs, age (<27 and ≥27), gender (female or male), side (left or right) and the presence of MB2 (Non-MB2, uni-MB2 and bi-MB2) the chi-square test was used. The binary logistic regression analysis was used to further evaluate the independent effect of the categorical variables in the presence of complicated PMLI root canal morphology. The confidence interval (CI) was set to 95%. For all statistical analysis, a P value of <.05 was considered significant. Statistical analysis was performed using SPSS for Windows v20.0 (SPSS Inc., Chicago, IL, USA).

## RESULTS

Out of 150 firstly examined patients' CBCT scans, 63 qualified for further analysis (126 PMLIs, and 126 PMFMs). Among these scans, 49.2% belonged to female, and 50.8% belonged to male patients. The patients' mean age was 26.29 ± 2.093, and 31.38 ± 2.015, respectively.

The frequency of PMLIs with complicated root canal morphology was 46% (58/126 teeth), present as type III configuration in 41.3%, and type II configuration in 4.8%. MB2 canal in PMFMs (i.e. complicated root canal morphology) was present in 62.7% (79/126 teeth). The most frequent root canal configuration in mesiobuccal roots of PMFMs was type II in 39.7%, followed by type I in 37.3% and type III in 12.7%. Less frequent were types V, VI, and IV present in 5.6%, 3.2%, and 1.6% respectively. There was no significant age difference in the presence of a complicated root canal (P = .699) and different types of a configuration in PMLIs

(P = .869). The gender difference was significant for complicated PMLIs (P = .001) and root canal configuration (P = .003). There was no significant side difference regarding above mentioned parameters (P = .284 and P = .543). The presence of the MB2 was significantly different depending on age (P = .013), but not significantly different depending on the gender (P = .490) or side (P = .357). The significant age, gender and side differences were found in the mesiobuccal root canal configuration (P=.021, .006, and .005 respectively) (Table 1).

The bilateral symmetry of the root canal morphology of PMLIs was 39.7% (25/63 scans) for non-Comp group, and 31.7% (20/63 scans) for bi-Comp group. Bilateral absence of MB2 in PMFMs (Non-MB2) was found in 23.8% (15/63 scans), while bi-MB2 was present in 49.2% (31/63 scans). Significant gender difference was found in the presence of bilateral root canal morphology for both PMLIs (P = .007) and PMFMs (P = .031). Also, bilateral symmetry showed significant age difference for the PMLIs (P = .038), but not for the PMFMs (P = .071). We also measured the bilateral presence of the same root canal configuration types in PMLIs and mesiobuccal roots of PMFMs. Same configuration types in PMLIs were found bilaterally in 69.9% (44/63 scans), while the mesiobuccal roots of PMFMs presented the bilateral configuration type symmetry in 30.2% (19/63 scans). The significant age difference was found only for PMLIs (P = .032) (Table 2).

The logistic regression analysis was adjusted for age, gender and side, and the frequency of complicated PMLIs was compared between the groups with absent or present MB2. The frequencies of complicated PMLIs in Uni-MB2 and Bi-MB2 groups, when compared to Non-MB2 group, were 7.733 (95%, 2.020 - 29.607, P = .003) and 11.662 (95%, 3.499 - 38.872, P < .001), respectively (Table 3).

**Table 1**. Frequency of PMLIs and PMFMs with complicated root canal morphology and differences in root canal system configurations related to age, gender and tooth side

| | | Root canal morphology, n (%) | | *P* | Root canal system configuration n (%) | | | | | | *P* |
|---|---|---|---|---|---|---|---|---|---|---|---|
| | | Non-complicated | Complicated | | Type I | Type II | Type III | Type IV | Type V | Type VI | |
| **PMLIs** | **Age** | | | | | | | | | | |
| | <27 | 41(55.4) | 33(44.6) | .699 | 41(55.4) | 3(4.1) | 30(40.5) | - | - | - | .869 |
| | ≥27 | 27(51.9) | 25(48.1) | | 27(51.9) | 3(5.8) | 22(42.3) | - | - | - | |
| | **Gender** | | | | | | | | | | |
| | Female | 43(69.4) | 19(30.6) | .001* | 43(69.4) | 2(3.2) | 17(27.4) | - | - | - | .003* |
| | Male | 25(39.1) | 39(60.9) | | 25(39.1) | 4(6.3) | 35(54.7) | - | - | - | |
| | **Side** | | | | | | | | | | |
| | Left | 31(49.2) | 32(50.8) | .284 | 31(49.2) | 3(4.8) | 29(46) | - | - | - | .543 |
| | Right | 37(58.7) | 26(41.3) | | 37(58.7) | 3(4.8) | 23(36.5) | - | - | - | |
| | **Total** | 68(54) | 58(46) | | 31(54) | 6(4.8) | 52(41.3) | - | - | - | |
| **PMFMs** | **Age** | | | | | | | | | | |
| | <27 | 21(28.4) | 53(71.6) | .013* | 21(28.4) | 33(44.6) | 10(13.5) | - | 7(9.5) | 3(4.1) | .021* |
| | ≥27 | 26(50) | 26(50) | | 26(50) | 17(32.7) | 6(11.5) | 2(3.8) | - | 1(1.9) | |
| | **Gender** | | | | | | | | | | |
| | Female | 25(40.3) | 37(59.7) | .490 | 25(40.3) | 17(27.4) | 10(16.1) | - | 7(11.3) | 3(4.8) | .006* |
| | Male | 22(34.4) | 42(65.6) | | 22(34.4) | 33(51.6) | 6(9.4) | 2(3.1) | - | 1(1.6) | |
| | **Side** | | | | | | | | | | |
| | Left | 26(41.3) | 37(58.7) | .357 | 26(41.3) | 26(41.3) | 2(3.2) | - | 5(7.9) | 4(6.3) | .005* |
| | Right | 21(33.3) | 42(66.7) | | 21(33.3) | 24(38.1) | 14(22.2) | 2(3.2) | 2(3.2) | - | |
| | **Total** | 47(37.3) | 79(62.7) | | 47(37.3) | 50(39.7) | 16(12.7) | 2(1.6) | 7(5.6) | 4(3.2) | |

PMLIs - permanent mandibular lateral incisors; PMFMs - permanent maxillary first molars; n - number of cases; * Statistically significant with the level of $P < .05$

**Table 2.** Bilateral symmetry in complicated root canal morphology and in root canal system configurations of PMLIs and PMFMs related to age and gender.

| PMLIs | Bilateral symmetry of complicated root canal morphology | | | *P* | Bilateral symmetry in root canal configuration types | | *P* |
|---|---|---|---|---|---|---|---|
| | Non-Comp, n(%) | Uni-Comp, n(%) | Bi-Comp, n(%) | | Same type, n(%) | Different type, n(%) | |
| **Age** | | | | | | | |
| <27 | 13(35.1) | 15(40.5) | 9(24.3) | .038* | 22(59.5) | 15(40.5) | .032* |
| ≥27 | 12(46.2) | 3(11.5) | 11(42.3) | | 22(84.6) | 4(15.4) | |
| **Gender** | | | | | | | |
| Female | 16(51.6) | 11(35.5) | 4(12.9) | .007* | 20(64.5) | 11(35.5) | .365 |
| Male | 9(28.1) | 7(21.9) | 16(50) | | 24(75) | 8(25) | |
| **Total** | 25(39.7) | 18(28.6) | 20(31.7) | | 44(69.8) | 19(30.2) | |
| **PMFMs** | Non-MB2, n(%) | Uni-MB2, n(%) | Bi-MB2, n(%) | | Same type, n(%) | Different type, n(%) | |
| **Age** | | | | | | | |
| <27 | 11(29.5) | 21(56.8) | 5(13.5) | .071 | 10(27) | 27(73) | .205 |
| ≥27 | 6(23.1) | 10(38.5) | 10(38.5) | | 11(42.3) | 15(57.7) | |
| **Gender** | | | | | | | |
| Female | 6(19.4) | 13(41.9) | 12(38.7) | .031* | 8(25.8) | 23(74.2) | .212 |
| Male | 9(28.1) | 4(12.5) | 19(59.4) | | 13(40.6) | 19(59.4) | |
| **Total** | 15(23.8) | 17(27) | 31(49.2) | | 21(33.3) | 42(66.7) | |

PMLIs - permanent mandibular lateral incisors; PMFMs - permanent maxillary first molars;
Non-Comp - Bilateral absence of the complicated root canal morphology; Uni-Comp-Unilateral presence of complicated root canal morphology; Bi-Comp - Bilateral presence of complicated root canal morphology;
Non-MB2 - Bilateral absence of a second mesiobuccal canal; Uni-MB2-Unilateral presence of second mesiobuccal canal; Bi-MB2-Bilateral presence of a second mesiobuccal canal; n - number of cases;
* Statistically significant with the level of $P < .05$

**Table 3.** The logistic regression analysis of the association between age, gender, tooth side, and the presence of second mesiobuccal canal in PMFMs with the presence of complicated root canal morphology in PMLIs.

| | PMLIs | | | |
|---|---|---|---|---|
| | | 95% CI | | |
| | Adjusted OR | Lower | Upper | *P* |
| **Age** | | | | |
| <27 | Ref | | | |
| ≥27 | 1.231 | .483 | 3.138 | .664 |
| **Gender** | | | | |
| Female | Ref | | | |
| Male | 4.511 | 1.757 | 11.581 | .002* |
| **Side** | | | | |
| Left | Ref | | | |
| Right | .602 | .267 | 1.357 | .221 |
| **MB2 Group** | | | | |
| Non-MB2 | Ref | | | |
| Uni-MB2 | 7.733 | 2.02 | 29.607 | < .001* |
| Bi-MB2 | 11.662 | 3.499 | 38.872 | < .001* |

* Statistically significant with the level of P < .05
PMLIs - permanent mandibular lateral incisors; CI - Confidence interval set at 95%;
OR - odds ratio; Ref - Referent category; Non-MB2 - Bilateral absence of second mesiobuccal canal;
Uni-MB2 - Unilateral presence of second mesiobuccal canal;
Bi-MB2 - Bilateral presence of second mesiobuccal canal;

## DISCUSSION

Inadequate cleaning and shaping of root canals with complicated morphology is a major cause of failure of endodontic treatment (19). PMLIs and PMFMs are one of the most challenging teeth to be treated thanks to the variations in their root canal morphology (20-22). The root canal morphology has been previously extensively studied in vitro with the use of method of clearing and staining (18), and more recently with the use of micro-CT (23, 24). In clinical setting the root canal morphology could be assessed with the use of retroalveolar radiology, dental operating microscope or CBCT. While the first two methods provide the vast information about root canals, CBCT is only which provides the clinician with the information about all aspects of root canal morphology throughout the whole canal working length (22). In our study, we used CBCT scans acquired by using two high definition settings for imaging with a voxel size of 0.16mm or 0.10mm. This voxel size with the use of high definition settings is reported to be adequate for proper root canal visualization (25).

Complicated root canal morphology of PMLIs has been previously described whit the varying incidence in different populations ranging from 11% to 40% (3, 4, 9, 24, 26, 27). Martins et al. (8) suggested that complicated root canal morphology is associated with the population's race or ethnicity, showing that Caucasians have higher incidence of complicated PMILs (30%) then Asians (5%). In line with this claim are the results of the study in Chinese population showing the frequency of complicated PMLIs in 10%. Our results (Table 1) correspond to results in Portuguese (30%) (9), Israeli (38%) (26), Brazilian (40%) (4), and Turkish population (48%) (28). In accordance to our results (Table 1), previous studies showed the highest frequency of type I root canal configuration, followed by type III as the next most frequent (3,4,9,26-28). Other than race and ethnicity, previous studies related the differences of root canal configurations to gender. Our study showed a significant gender difference (Table 1) where male subjects tend to have more complicated PMLIs, as shown in previous studies (26, 28, 29). We furtherly supported this claim analyzing the adjusted OR (Table 3), which showed that male subjects have over 4 times higher chance of presenting complicated PMLIs than female subjects.

The mesiobuccal root of PMFMs is reported having the highest incidence of variations in root canal configuration compared to distobuccal and palatal roots (30). The absence of MB2 could be rather called a variation than its presence, considering that the most previous studies show the incidence of MB2 to be higher than 50% (7, 10, 12, 14), and to be as high as 75% (13). Lower presence was shown in fewer studies, such as in the Malaysian (36%) (15) and in Taiwanese populations (46%) (11). The presence of MB2 was not found to be gender related in our study (Table 1), as shown by other authors (11, 12, 15). However, we found the significant gender difference in the root canal configurations (Table 1). Although both genders showed the highest frequency of type I and type II, male subjects presented type II configuration more frequent than female, while female subject presented more type III, and type V in their PMFMs compared to men. To analyze the influence of subject's age on root canal configurations, we selected to divide the subjects into two groups according to the median age value of studied sample. By analyzing those two groups, we found the age difference in presence of MB2, having shown that younger subject had more MB2 present in their PMFMs (Table 1). Previous studies also reported that the frequency of MB2 declines with the rise in subject's age (7, 31), but unlike in our study, their studies presented higher sample size with more heterogeneous age groups.

As we previously discussed, many studies have been conducted to define the root canal morphology based on the populations' race, ethnicity, gender, and age. Even though population studies could help clinician on what morphology should be expected in a patient, every case should be analyzed individually and treatment plan should be selected on the basis of the acquired information on that individual. In our study, we analyzed the bilateral symmetry of complicated and non-complicated root canal morphology and different types of root canal configurations in each subject (Table 2). Same root canal morphology of PMLIs and PMFMs was presented symmetrically in 71.4% (45/63 subjects) and 73% (46/63 subjects), respectively (Table 2). PMLIs showed a high bilateral symmetry in root canal configuration types (69.8%) wile in PMFMs configurations were found to be less symmetrical (33.3%) (Table 2). Bilateral symmetry of root canal morphology was found to be gender related previously (11,32), as it was in our study. Males showed higher symmetry in both PMLIs and PMFMs. Only recently, a few studies have been conducted in order to associate the root canal morphology of one group of teeth to another (2,16,17). Two of these studies found that the presence of distolingual root in permanent mandibular first molars was associated with the presence of complicated root canal morphology in permanent mandibular central incisors as well as in PMLIs (16, 17). In that manner, we tried to associate the presence of MB2 with the complicated root canal morphology in PMLIs by conducting binary logistic regression analysis. Our results (Table 3) showed that individuals presenting the MB2 in PMFMs unilaterally or bilaterally, have 7 and 11 times higher chance of having complicated PMLIs, respectively, compared to subjects with bilateral absence of MB2. The cause of this association is yet unknown, but could be found in the timing of their root formation, as the most of developmental stages in the formation of PMLIs and PMFMs appear at the similar time (33). Previously, it has been shown that if the factors that could compromise tooth development are introduced at a certain period of the dentition formation, it is most likely that developmental defects, such as molar-incisor hypomineralization, will appear on both permanent molars and incisors (34).

## CONCLUSION

Clinicians should be aware of possible root canal complexities and the differences in their presentations. Our study showed high frequency of complicated root canal morphology in PMLIs and PMFMs that fit in the range for Caucasian population. Female subjects are more prone to show non-complicated morphology when compared to male subject. Also, if the presence of MB2 is found in PMFMs, clinician should expect the presence of a complicated root morphology in PMLIs when planning the endodontic treatment of these teeth.

## REFERENCES


1. Vertucci FJ. Root canal morphology and its relationship to endodontic procedures. Endod Top. 2005;10(1):3-29.
2. Wu Y, Su C, Tsai YC, Cheng W, Chung M-P, Chiang H-S, et al. Complicated Root Canal Configuration of Mandibular First Premolars Is Correlated with the Presence of the Distolingual Root in Mandibular First Molars: A Cone-beam Computed Tomographic Study in Taiwanese Individuals. J Endod. 2017;43(7): 1064-71.
3. Zhengyan Y, Keke L, Fei W, Yueheng L, Zhi Z. Cone-beam computed tomography study of the root and canal morphology of mandibular permanent anterior teeth in a Chongqing population. Ther Clin Risk Manag. 2016; 12:19-25.
4. da Silva EJNL, de Castro RWQ, Nejaim Y, Silva AIV, Haiter-Neto F, Silberman A, et al. Evaluation of root canal configuration of maxillary and mandibular anterior teeth using cone beam computed tomography: An in-vivo study. Quintessence Int. 2016; 47(1): 19-24.
5. Sert S, Aslanalp V, Tanalp J. Investigation of the root canal configurations of mandibular permanent teeth in the Turkish population. Int Endod J. 2004; 37(7): 494-9.
6. Marceliano-Alves M, Alves FRF, Mendes D de M, Provenzano JC. Micro-Computed Tomography Analysis of the Root Canal Morphology of Palatal Roots of Maxillary First Molars. J Endod. 2016; 42(2): 280-3.
7. Martins JNR, Ordinola-Zapata R, Marques D, Francisco H, Caramês J. Differences in root canal system configuration in human permanent teeth within different age groups. Int Endod J. 2018; 51(8): 931-41.
8. Martins JNR, Gu Y, Marques D, Francisco H, Caramês J. Differences on the Root and Root Canal Morphologies between Asian and White Ethnic Groups Analyzed by Cone-beam Computed Tomography. J Endod. 2018; 44(7): 1096-104.
9. Martins JNR, Marques D, Francisco H, Caramês J. Gender influence on the number of roots and root canal system configuration in human permanent teeth of a Portuguese subpopulation. Quintessence Int. 2018; 49(2): 103-11.
10. Martins JNR, Marques D, Mata A, Caramês J. Root and root canal morphology of the permanent dentition in a Caucasian population: a cone-beam computed tomography study. Int Endod J. 2017; 50(11): 1013-26.
11. Su C, Huang R, Wu Y, Cheng W, Chiang H, Chung M-P, et al. Detection and location of second mesiobuccal canal in permanent maxillary teeth: A cone-beam computed tomography analysis in a Taiwanese population. Arch Oral Biol. 2019; 98(November 2018): 108-14.
12. Ratanajirasut R, Panichuttra A, Panmekiate S. A Cone-beam Computed Tomographic Study of Root and Canal Morphology of Maxillary First and Second Permanent Molars in a Thai Population. J Endod. 2018; 44(1): 56-61.
13. Ghobashy AM, Nagy MM, Bayoumi AA. Evaluation of Root and Canal Morphology of Maxillary Permanent Molars in an Egyptian Population by Cone-beam Computed Tomography. J Endod. 2017; 43(7): 1089-92.
14. Popovic M, Zivanovic S, Vucicevic T, Grujovic M, Papic M. Cone-beam computed tomography study of tooth root and canal morphology of permanent molars in a Serbian population. Vojnosanitetski pregl. 2020; 77(5): 470-8.
15. Pan JYY, Parolia A, Chuah SR, Bhatia S, Mutalik S, Pau A. Root canal morphology of permanent teeth in a Malaysian subpopulation using cone-beam computed tomography. BMC Oral Health. 2019; 19(1): 14.
16. Wu Y, Cheng W, Weng P, Chung M-P, Su C-C, Chiang H-S, et al. The Presence of Distolingual Root in Mandibular First Molars Is Correlated with Complicated Root Canal Morphology of Mandibular Central Incisors: A Cone-beam Computed Tomographic Study in a Taiwanese Population. J Endod. 2018; 44(5): 711-716.e1.
17. Wu Y, Cheng W, Chung M-P, Su C, Weng P-W, Cathy Tsai Y-W, et al. Complicated Root Canal Morphology of Mandibular Lateral Incisors Is Associated with the Presence of Distolingual Root in Mandibular First Molars: A Cone-beam Computed Tomographic Study in a Taiwanese Population. J Endod. 2018; 44(1): 73-79.e1.
18. Vertucci FJ. Root canal anatomy of the human permanent teeth. Oral Surg Oral Med Oral Pathol. 1984; 58(5): 589-99.
19. Tabassum S, Khan FR. Failure of endodontic treatment: The usual suspects. Eur J Dent. 2016; 10(1): 144-7.

20. Aggarwal K. Mandibular lateral incisor with Vertucci Type IV root canal morphological system: A rare case report. J Nat Sci Biol Med. 2016; (1): 101-4.
21. Yamaguchi M, Noiri Y, Itoh Y, Komichi S, Yagi K, Uemura R, et al. Factors that cause endodontic failures in general practices in Japan. BMC Oral Health. 2018; 18(1) :70.
22. Mirmohammadi H, Mahdi L, Partovi P, Khademi A, Shemesh H, Hassan B. Accuracy of Cone-beam Computed Tomography in the Detection of a Second Mesiobuccal Root Canal in Endodontically Treated Teeth: An Ex Vivo Study. J Endod. 2015; 41(10): 1678-81.
23. Briseño-Marroquín B, Paqué F, Maier K, Willershausen B, Wolf TG. Root Canal Morphology and Configuration of 179 Maxillary First Molars by Means of Micro-computed Tomography: An Ex Vivo Study. J Endod. 2015; 41(12) :2008-13.
24. Leoni GB, Versiani MA, Pécora JD, Damião de Sousa-Neto M. Micro-computed tomographic analysis of the root canal morphology of mandibular incisors. J Endod. 2014; 40(5): 710-6.
25. Aktan AM, Yildirim C, Karataşlıoğlu E, Çiftçi ME, Aksoy F. Effects of voxel size and resolution on the accuracy of endodontic length measurement using cone beam computed tomography. Ann Anat. 2016; 208: 96-102.
26. Shemesh A, Kavalerchik E, Levin A, Ben Itzhak J, Levinson O, Lvovsky A, et al. Root Canal Morphology Evaluation of Central and Lateral Mandibular Incisors Using Cone-beam Computed Tomography in an Israeli Population. J Endod. 2018; 44(1) :51-5.
27. Saati S, Shokri A, Foroozandeh M, Poorolajal J, Mosleh N. Root Morphology and Number of Canals in Mandibular Central and Lateral Incisors Using Cone Beam Computed Tomography. Braz Dent J. 2018; 29(3): 239-44.
28. Arslan H, Ertas H, Ertas ET, Kalabalık F, Saygılı G, Capar ID. Evaluating root canal configuration of mandibular incisors with cone-beam computed tomography in a Turkish population. J Dent Sci. 2015; 10(4): 359-64.
29. Lin Z, Hu Q, Wang T, Ge J, Liu S, Zhu M, et al. Use of CBCT to investigate the root canal morphology of mandibular incisors. Surg Radiol Anat. 2014; 36(9): 877-82.
30. Golmohammadi M, Jafarzadeh H. Root Canal Treatment of a Maxillary Second Premolar with Two Palatal Root Canals: A Case Report. Iran Endod J. 2016; 11(3): 234-6.
31. Naseri M, Safi Y, Akbarzadeh Baghban A, Khayat A, Eftekhar L. Survey of Anatomy and Root Canal Morphology of Maxillary First Molars Regarding Age and Gender in an Iranian Population Using Cone-Beam Computed Tomography. Iran Endod J. 2016; 11(4): 298-303.
32. Tu MG, Huang HL, Hsue SS, Hsu JT, Chen SY, Jou MJ, et al. Detection of permanent three-rooted mandibular first molars by cone-beam computed tomography imaging in Taiwanese individuals. J Endod. 2009; 35(4): 503-7.
33. Cavrić J, Vodanović M, Marušić A, Galić I. Time of mineralization of permanent teeth in children and adolescents in Gaborone, Botswana. Ann Anat. 2016; 203: 24-32.
34. Silva MJ, Scurrah KJ, Craig JM, Manton DJ, Kilpatrick N. Etiology of molar incisor hypomineralization - A systematic review. Community Dent Oral Epidemiol. 2016; 44(4): 342-53.

ORIGINAL SCIENTIFIC ARTICLE

# ASSESSMENT OF THE SYSTEMIC OXIDATIVE STRESS IN PREECLAMPSIA

Anca M. Bînă[1,2], Andreea I. Anechitei[1,2], Theia Lelcu[1,2], Adina V. Linţa[1,2], Daniela V. Chiriac[3], Adelina G. Mocanu[4], Elena Bernad[4], Zoran L. Popa[4], Marius L. Craina[4], Danina M. Muntean[1,2,*], Claudia Borza[1,2,*] and Octavian M. Creţu[5,6]

*[1]Department III Functional Sciences – Pathophysiology*
*,[2]Centre for Translational Research and Systems Medicine,*
*[3]Department XII – Obstetrics and Gynecology I,*
*[4]Department XII – Obstetrics and Gynecology III,*
*[5]Department IX Surgery I – Surgical Semiotics I,*
*[6]Centre for Hepato-Biliary and Pancreatic Surgery, "Victor Babeş" University of Medicine and Pharmacy, Timişoara, Romania, Eftimie Murgu Sq. no. 2, 300041 Timişoara, RO*

Received: 18.03.2022.
Accepted: 20.03.2022.

**Corresponding author:**

**Danina M. Muntean, MD, PhD,**
**Claudia Borza, MD, PhD,**

Department III Functional Sciences – Pathophysiology
Centre for Translational Research and Systems Medicine
"Victor Babeş" University of Medicine and Pharmacy of Timişoara, Romania
Eftimie Murgu Sq., no. 2, 300041 Timişoara, RO

E-mail: daninamuntean@umft.ro,
borza.claudia@umft.ro

Phone: +40-256-493085

## ABSTRACT

*Preeclampsia (PE) is a major complication of pregnancy with both mother and fetal adverse outcomes. Pregnancy is a state of increased oxidative stress that has been reported to be exacerbated when complicated with preeclampsia. However, conflicting data are available in literature regarding the systemic oxidative stress in PE pregnancies. The present pilot study was purported to assess systemic oxidative stress in preeclamptic vs healthy pregnancies. To this aim plasma derived compounds of reactive oxygen metabolites (d-ROMs) and the biological antioxidant potential (BAP) were determined in mild and severe preeclamptic pregnancies using the Diacron equipment. Both healthy and preeclamptic pregnancies showed high levels of systemic oxidative stress. Paradoxically, significantly higher values of d-ROMs were found in healthy pregnancies as compared to the PE ones. At variance, in preeclamptic pregnancies, a major increase in the plasma antioxidant capacity occurred. In this pilot study, we report an increase in the systemic antioxidant capacity in preeclamptic pregnancies.*

***Keywords***: *preeclampsia, plasma reactive oxygen species, d-ROM, biological antioxidant potential, BAP, Diacron.*

UDK: 618.3:616.12-008.331.1
618.3:[577.344:546.21
Ser J Exp Clin Res 2022; 23(1): 45-50
DOI: 10.2478/sjecr-2022-0010

## INTRODUCTION

Preeclampsia (PE), the most frequent complication of pregnancy, is a multisystem disorder diagnosed after 20 weeks of gestation. The increased systolic (≥ 140 mmHg) and/or diastolic (≥90 mmHg) blood pressure at two repeated measurements is associated with proteinuria (≥300 mg/24 hours), and/or at least one of the following new-onset dysfunctions: hepatocytolysis, new-onset headache unresponsive to medication, visual symptoms, thrombocytopenia < 100,000/mm3, hemolysis, high risk for disseminated intravascular coagulation, acute kidney injury, pulmonary edema, neurological complications, and also uteroplacental dysfunction (fetal growth restriction, abnormal Doppler ultrasound findings) (1).

The pathogenesis of preeclampsia has been extensively studied, yet the precise underlying molecular mechanism is only partially elucidated. However, oxidative stress has been unequivocally reported to play a major role in both endothelial and placental dysfunction systemic from PE ultimately leading to the specific clinical syndrome (2).

Oxidative stress is defined as the imbalance between reactive oxygen species (ROS) and/or reactive nitrogen species (RNS) generation and the antioxidant defense systems. Preeclampsia has been systematically associated with both increased ROS production and impaired antioxidant capacity (3).

ROS denomination include both free radicals and their non-radical intermediates, which playing important roles in cell physiology as second messengers in many signaling pathways when generated in small amounts. When excessively produced, they become harmful molecules, the most common deleterious free radical being the superoxide anion (O2-) originating from several sources: mitochondrial electron transport chain, NADPH oxidase (nicotinamide adenine dinucleotide phosphate), xanthine oxidase, uncoupled endothelial nitric oxide synthase (eNOS), cytochrome P450 etc.

Antioxidants comprise both enzymatic and non-enzymatic compounds aimed at counteracting the deleterious effects of excessive ROS. The most important enzymatic antioxidants are: superoxide dismutase (SOD), hemoxygenase (HO-1), catalase (CAT), glutathione peroxidase (GPx), and thioredoxin (TRX) (4). Superoxide dismutase enzyme catalyzes the dismutation of superoxide anion (O2-) into hydrogen peroxide, finally, catalase and glutathione peroxidase, will convert it into water (5,6).

It has to be mentioned that increased ROS generation occurs in both hyperoxic and hypoxic states or their alternance as it happens in PE where repetitive episodes of tissue hypoxia-reoxygenation have been described (7).

While pregnancy itself is associated with increased oxidative stress, ROS generation is further exacerbated in all pregnancy complications, such as: PE, gestational diabetes, spontaneous pregnancy loss and fetal growth restriction (4).

The pathogenesis of preeclampsia has been classically described as evolving according to the “two-stage” model, where the stressed syncitiotrophoblast releases factors into the maternal circulation which stimulates the inflammatory response and activation of the maternal endothelial cells (8).

Both local and systemic oxidative stress have been incriminated as underlying pathomechanisms in PE, yet data in the literature are controversial.

Local oxidative stress can be directly assessed in confocal microscopy with the aid of fluorescent probes: 2′,7′-dichlorofluorescein (DCF) and dihydroethidium (DHE) stainin. Systemic oxidative stress can be quantified using a spectrophotometric method of measuring the derivates of reactive oxygen metabolites (d-ROM) using the Diacron equipment. The latter also allows the global assessment of the biological antioxidant potential (BAP) (9,10).

Indirect markers of oxidative stress in plasma (eg, lipid hydroperoxides, malondialdehyde) or urine (F2-isoprostanes and uric acid) were reported to be increased in pregnancies complicated by preeclampsia (11-13).

In preeclampsia, it is the systemic oxidative stress that leads to endothelial dysfunction, generalized vasoconstriction, which are further amplified via the release into the maternal circulation of pro-inflammatory cytokines, exosomes, and cell-free fetal DNA (14-16).

The present study was aimed to quantify the systemic oxidative stress by measuring the plasma reactive oxygen metabolites (d-ROMs) and the biological antioxidant capacity (BAP) in pregnancies complicated or not by preeclampsia.

## PATIENTS AND METHODS

### 2.1 Study population

This cross-sectional, single-site study was conducted according to the Helsinki declaration (1975), as revised in 2008 and its later amendments, and was approved by the Committee for Research Ethics of "Victor Babeș" University of Medicine and Pharmacy, Timișoara, RO (no. 7/30.01.2019 and 28/25.06.2020). All participants provided a written informed consent.

The systemic oxidative stress was assessed in 20 participants evaluated in the third trimester of pregnancy (28-40 weeks of pregnancy), divided into healthy (n=10) and preeclamptic pregnancies (n=10), both mild (n=8) and severe forms (n=2) of preeclampsia were included in the study.

### 2.2 Systemic oxidative stress

Peripheral blood samples were collected in the third trimester of pregnancy (28-40 weeks of gestation). One-step centrifugation was performed and the resulting plasma stored at -80 degrees Celsius for a maximum of 12 months. Systemic oxidative stress was determined in plasma using the Free Radical Analytical System 4 (Diacron, Grosseto, Italy), which evaluates changes in the reactive oxygen metabolites (d-ROMs) and the plasma antioxidant capacity (BAP) as a measure of the non-enzymatic scavengers. d-ROMs are derivates generated from the interaction of free radicals with organic molecules, being more stable. The method assumes biochemical reactions between the hydroperoxides and the reagents, resulting in colored compound which is further measured spectrophotometrically. The results were expressed in Carratelli units (CARR U).

The antioxidant capacity of the plasma is quantified by the reduction of ferric ions ($Fe^{3+}$) to ferrous ions ($Fe^{2+}$), by adding a biological sample which possesses antioxidative defense capacity.

To express differences between antioxidant and pro-oxidant potential, the ratio of BAP to d-ROMs was calculated (BAP/d-ROMs) (17) .

### 2.3 All chemicals were purchased from Diacron International SRL (Ital.)

### 2.4 Statistics

Statistical data processing was performed with the GraphPad Prism Software Version 9.3.1 (GraphPad, USA). Data are presented as mean ± SEM and were analyzed using Student t-test. Values of $P < 0.05$ were considered statistically significant.

The diagnosis of preeclampsia was based on the criteria proposed by The International Society for the Study of Hypertension in Pregnancy (ISSHP), as previously defined (18). The exclusion criteria were: diagnosis of chronic hypertension, coexistent diabetes mellitus, chronic kidney disease, twin pregnancy, inflammatory disorders, malignancies, cardiovascular disease and coagulation disorders. All pregnant women were evaluated in the third trimester (28-40 weeks of pregnancy).

All preeclamptic patients underwent antihypertensive treatment with Methyldopa and/or Nifedipine. Patients who received antiplatelet drugs, anticoagulants or magnesium sulphate therapy were excluded from the study.

## RESULTS

### Characteristics of the study groups

The following demographic and laboratory characteristics of pregnant women (PE and healthy pregnancies) were included: maternal age, gestational age, maternal blood pressure, fetal weight (Table 1). Additionally, the mean arterial pressure - MAP = (Syst BP + 2 X Diast BP)/3 was calculated. The mean arterial pressure (MAP) was significantly increased in the PE pregnancies, as the main diagnostic criteria.

**Table 1.** Patients characteristics

| Parameter | HEALTHY | PREECLAMPSIA |
|---|---|---|
| Gestational age | 35.37 ± 0.33 | 32.66 ± 2.6 |
| Systolic BP | 123.7 ± 3.52 | 144.3 ± 2.33 ** |
| Diastolic BP | 77.33 ± 1.45 | 93.33 ± 1.66 ** |
| MAP | 92.67 ± 1.45 | 110.3 ± 1.45 ** |
| Proteinuria | - | 0,76 |
| Fetal weight | 3423 ± 132.8 | 2350 ± 419.3 |

** $p < 0.01$

**Figure 1.** A) Concentrations of derivatives of reactive oxygen metabolites (d-ROMs) and (B) biological antioxidant potential (BAP) in plasma collected from healthy pregnancies and pregnancies complicated by preeclampsia. (Data is presented as mean±SEM. Unpaired t- was applied. *** p<0.001, **** p<0.0001)

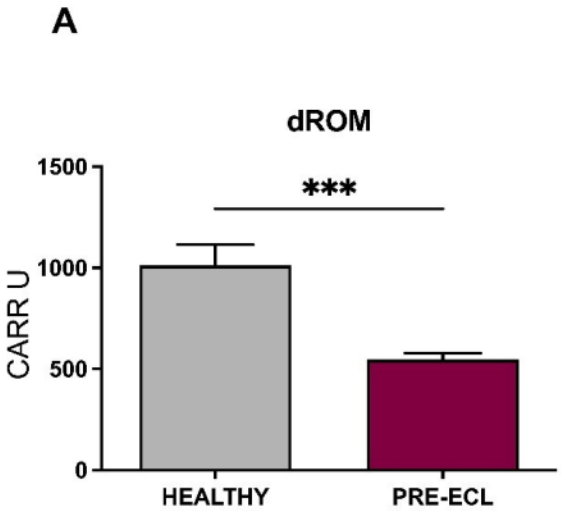

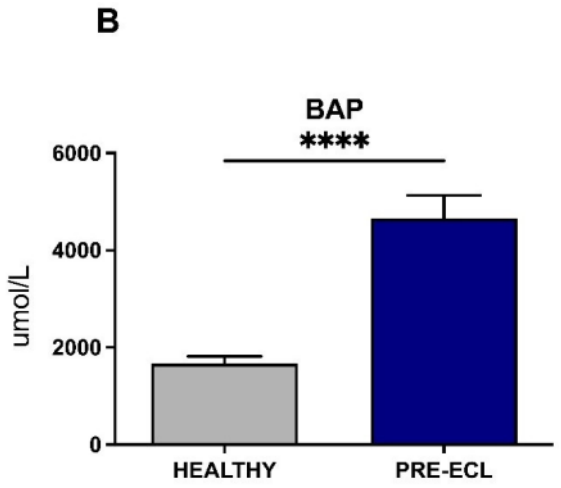


*Preeclampsia was associated with decreased plasma reactive oxygen species and increased antioxidant capacity*

ROS production and the plasma antioxidant capacity were evaluated in preeclamptic pregnancies (mild, n=8 and severe, n=2 forms) and healthy pregnancies. Interestingly, both healthy and preeclamptic pregnancies presented higher levels of oxidative stress, the values being almost double in the control group. Thus dROMs values were 1012±103.3 CARR U in the control group as compared to 546.8 ± 32.22 CARR U in the PE group. At variance, the BAP test was low in the control group (1666 ± 151.3 umol/L) and high in preeclamptic pregnancies (4651 ± 479.9 umol/L). The antioxidant capacity in plasma was significantly increased in the preeclamptic group. No differences were noticed in both dROMs and BAP values between the mild and severe forms of preeclampsia.

*The ratio antioxidants to reactive oxygen metabolites was significantly increased in preeclampsia*

The ratio of BAP to d-ROMs has been calculated (BAP/d-ROMs) and showed significantly increased values in pregnancies complicated by preeclampsia.

**Figure 2.** The ratio BAP test to d-ROMS in healthy vs preeclamptic pregnancies. (**** p<0.0001)

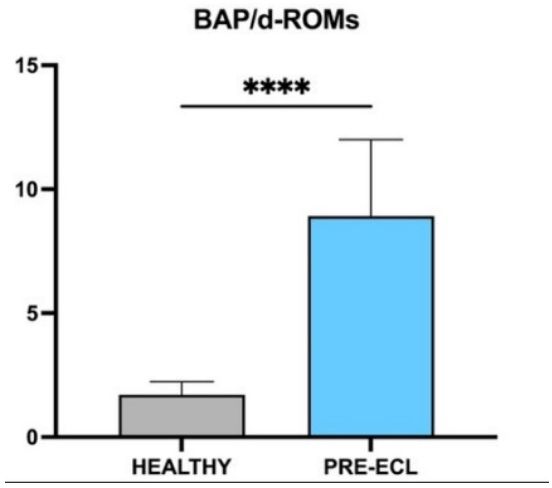


## DISCUSSION

The present study was purported to assess the systemic oxidative stress in pregnancies complicated with preeclampsia by measuring the plasma reactive oxygen metabolites and the antioxidant status.

Preeclampsia is a serious complication of pregnancy remaining a major cause of perinatal morbidity and mortality globally, with an unpredictable evolution. Upon severity, mild and severe forms of preeclampsia are recognized; the latter presents with values of the SBP 160–180mmHg SBP and/or DBP>110 mmHg (19).

The correlation oxidative stress – preeclampsia has been extensively studied in past decades and placenta is the main site of ROS generation with subsequent release into the maternal circulation leading to deleterious effects (4).

The main findings can be summarized as follows: i) the levels of plasma reactive oxygen metabolites (d-ROMS) were above normal limit in all evaluated pregnancies, with significantly higher values in healthy pregnancies; ii) the plasma antioxidant capacity (BAP) was in the normal to high range in preeclampsia but healthy pregnancies associated a deficiency and iii) for a better evaluation the BAP test/d-ROMS ratio was calculated, reflecting a significantly higher state of oxidative stress in healthy pregnancies. No differences were noticed between the mild and severe forms of preeclampsia.

Since ROS have a very short lifespan, the evaluation of reactive oxygen metabolites in form of hydroperoxides, which are stable molecules and can be stored in blood samples is a reliable method of oxidative stress evaluation, being in the last years evaluated in several pathologies. A meta-analysis of four population-based cohort studies suggest that increased d-ROMs levels were associated with cardio-vascular disease and cancer mortality (20). Of note, values above the normal upper limit were also reported in heavy drinkers (10).

In a recent study it has been reported that ultramarathon running induces systemic oxidative stress since the ratio BAP/d-ROMS was significantly decreased 24 hours after the race, due to the proinflammatory state and subsequent muscular and renal injury (21).

The literature regarding the antioxidant capacity (measured globally or as specific enzymes) in preeclampsia is inconclusive, with several studies reporting high values while in others a significant reduction was observed (22). Aris et al established an increased $H_2O_2$ level in plasma and placenta of preeclamptic pregnancies correlated with decreased levels of NO due to the cytotrophoblasts NO synthesis inhibition by $H_2O_2$ (2).

Watanabe et al reported increased levels of dROM in the severe forms of preeclampsia, an observation that was not recapitulated in the mild forms or healthy pregnancies. The

same study found no change in plasma antioxidant capacity in the three study groups (23). In contrast, Kinoshita et al evaluated only the dROM and found significantly higher values in preeclampsia vs normal pregnancies; however, this study included only mild forms of preeclampsia at term (24).

Oxidative stress in preeclampsia was also evaluated in the early *vs* late onset disease, with higher concentration of dROMs in both groups as compared to the control, while no changes in the antioxidant capacity was found (25).

In women with recurrent PE, Rijvers et al determined the plasma antioxidant capacity before pregnancy and at 20 weeks of gestation reporting higher values; however, in this study a latent cardiovascular or metabolic abnormality appeared to interfere with early placental development (26). Specific antioxidant enzymes suc as reduced glutathione, superoxide dismutase, catalase and vitamin E were increased in preeclampsia as compared to healthy pregnancies (27).

Conflicting results reported in the literature are most probably related to the use of different methods to assess the reactive oxygen species (direct or indirect markers) and antioxidant status (specific antioxidative enzymes or total antioxidant capacity).

Last but not least, we should mention that a major influence has also the severity of PE (mild *vs* severe). The lack of higher systemic oxidative stress in the PE group might be related to the fact that most of the consecutive cases were mild (not severe) forms. Of note in a parallel study (under review), we have also assessed the local oxidative stress (placental tissue) and reported it was increased in severe (but not in mild) preeclamptic pregnancies.

We cannot exclude the fact that the higher antioxidant capacity in pregnancies complicated with preeclampsia, is a compensatory mechanism of the triggered as a consequence of placental oxidative stress (and subsequent release of various ROS in the circulation).

## CONCLUSION

Pregnancy is associated with an increased systemic oxidative stress. In this pilot study higher values of d-ROMs were found out in healthy pregnancies as compared to preeclamptic ones whereas the antioxidant capacity was higher in preeclamptic pregnancies. Future studies in larger groups of patients aimed at simultaneously assessing both local and systemic oxidative stress in relation with the severity of the disease are worth to be designed.

## AUTHOR CONTRIBUTIONS:

Conceptualization, A.M.B., C.B. and D.M.M.; Methodology, A.M.B., A.I.A.; Validation, A.M.B., A.I.A..; Formal Analysis, A.M.B, A.V.L; Investigation, D.V.C., A.G.M., E.B., Z.L.P.; Resources, M.L.C..; Data Curation, A.M.B, A.V.L.; Writing - Original Draft Preparation, A.M.B, A.V.L..; Writing - Review & Editing, D.M.M.; Visualization, E.B., Z.L.P.; Supervision, C.B., M.L.C., Z.L.P.; Project Administration, O.M.C; Funding Acquisition, O.M.C.

## FUNDING

Research supported by the university internal funds allocated to the Centre for Translational Research and Systems Medicine. The funder had no role in the design of the study; in the collection, analyses, or interpretation of data; in the writing of the manuscript, or in the decision to publish the results.

## CONFLICTS OF INTEREST

The authors declare no conflict of interest.

## REFERENCES

1. ACOG Practice Bulletin No. 202: Gestational Hypertension and Preeclampsia. Obstet Gynecol 2019, 133, 1.
2. Aris A, Benali S, Ouellet A, Moutquin JM, Leblanc S. Potential biomarkers of preeclampsia: inverse correlation between hydrogen peroxide and nitric oxide early in maternal circulation and at term in placenta of women with preeclampsia. Placenta. 2009;30(4):342-7.
3. Marín R, Chiarello DI, Abad C, Rojas D, Toledo F, Sobrevia L. Oxidative stress and mitochondrial dysfunction in early-onset and late-onset preeclampsia. Biochim Biophys Acta Mol Basis Dis. 2020;1866(12):165961.
4. Aouache R, Biquard L, Vaiman D, Miralles F. Oxidative Stress in Preeclampsia and Placental Diseases. Int J Mol Sci. 2018;19(5):1496.
5. Burton GJ, Jauniaux E. Oxidative stress. Best Pract Res Clin Obstet Gynaecol. 2011;25(3):287-99.
6. Guerby P, Tasta O, Swiader A, et al. Role of oxidative stress in the dysfunction of the placental endothelial nitric oxide synthase in preeclampsia. Redox Biol. 2021;40:101861.
7. Burton GJ. Oxygen, the Janus gas; its effects on human placental development and function. J Anat. 2009;215(1):27-35.
8. Redman CW, Sargent IL. Placental stress and pre-eclampsia: a revised view. Placenta. 2009;30 Suppl A:S38-42.
9. Katerji M, Filippova M, Duerksen-Hughes P. Approaches and Methods to Measure Oxidative Stress in Clinical Samples: Research Applications in the Cancer Field. Oxid Med Cell Longev. 2019;2019:1279250.
10. Trotti R, Carratelli M, Barbieri M. Performance and clinical application of a new, fast method for the detection of hydroperoxides in serum. Panminerva Med. 2002;44(1):37-40.
11. Rani N, Dhingra R, Arya DS, Kalaivani M, Bhatla N, Kumar R. Role of oxidative stress markers and antioxidants in the placenta of preeclamptic patients. J Obstet Gynaecol Res. 2010;36(6):1189-94.

12. Hsieh TT, Chen SF, Lo LM, Li MJ, Yeh YL, Hung TH. The association between maternal oxidative stress at mid-gestation and subsequent pregnancy complications. Reprod Sci. 2012;19(5):505-12.
13. Lee R, Margaritis M, Channon KM, Antoniades C. Evaluating oxidative stress in human cardiovascular disease: methodological aspects and considerations. Curr Med Chem. 2012;19(16):2504-20.
14. Amaral LM, Cunningham MW Jr, Cornelius DC, LaMarca B. Preeclampsia: long-term consequences for vascular health. Vasc Health Risk Manag. 2015 15;11:403-15.
15. Tannetta D, Masliukaite I, Vatish M, Redman C, Sargent I. Update of syncytiotrophoblast derived extracellular vesicles in normal pregnancy and preeclampsia. J Reprod Immunol. 2017;119:98-106.
16. Craige SM, Kant S, Keaney JF Jr. Reactive oxygen species in endothelial function - from disease to adaptation. Circ J. 2015;79(6):1145-55.
17. Alberti A, Bolognini L, Macciantelli D, Caratelli M. The radical cation of N,N-diethyl-para-phenylendiamine: A possible indicator of oxidative stress in biological samples. Res Chem Intermediat. 2000;26:253-267.
18. Brown MA, Magee LA, Kenny LC, et al. International Society for the Study of Hypertension in Pregnancy (ISSHP). Hypertensive Disorders of Pregnancy: ISSHP Classification, Diagnosis, and Management Recommendations for International Practice. Hypertension. 2018;72(1):24-43.
19. Mancia G, De Backer G, Dominiczak A, et al. The task force for the management of arterial hypertension of the European Society of Hypertension, The task force for the management of arterial hypertension of the European Society of Cardiology. 2007 Guidelines for the management of arterial hypertension: The Task Force for the Management of Arterial Hypertension of the European Society of Hypertension (ESH) and of the European Society of Cardiology (ESC). Eur Heart J. 2007;28(12):1462-536..
20. Schöttker B, Brenner H, Jansen EH, et al. Evidence for the free radical/oxidative stress theory of ageing from the CHANCES consortium: a meta-analysis of individual participant data. BMC Med. 2015;13:300.
21. Hoppel F, Calabria E, Pesta DH, Kantner-Rumplmair W, Gnaiger E, Burtscher M. Effects of Ultramarathon Running on Mitochondrial Function of Platelets and Oxidative Stress Parameters: A Pilot Study. Front Physiol. 2021;12:63266.
22. Taravati A, Tohidi F. Comprehensive analysis of oxidative stress markers and antioxidants status in preeclampsia. Taiwan J Obstet Gynecol. 2018;57(6):779-790.
23. Watanabe K, Mori T, Iwasaki A, Kimura C, Matsushita H, Shinohara K, Wakatsuki A. Increased oxygen free radical production during pregnancy may impair vascular reactivity in preeclamptic women. Hypertens Res. 2013;36(4):356-60.
24. Kinoshita H, Watanabe K, Azma T, et al. Human serum albumin and oxidative stress in preeclamptic women and the mechanism of albumin for stress reduction. Heliyon. 2017;3(8):e00369.
25. Watanabe K, Mori T, Iwasaki A, et al. Increased oxidant generation in the metabolism of hypoxanthine to uric acid and endothelial dysfunction in early-onset and late-onset preeclamptic women. J Matern Fetal Neonatal Med. 2012 Dec;25(12):2662-6.
26. Severens-Rijvers CAH, Al-Nasiry S, Vincken A, et al. Early-Pregnancy Circulating Antioxidant Capacity and Hemodynamic Adaptation in Recurrent Placental Syndrome: An Exploratory Study. Gynecol Obstet Invest. 2019;84(6):616-622.
27. Gohil JT, Patel PK, Gupta P. Evaluation of oxidative stress and antioxidant defence in subjects of preeclampsia. J Obstet Gynaecol India. 2011;61(6):638-40.

ORIGINAL SCIENTIFIC ARTICLE

# ANTIOXIDANT AND ANTIMICROBIAL ACTIVITY OF *SANGUISORBA MINOR* L. EXTRACTS

Tijana Cirovic[1], Ana Barjaktarevic[1], Snezana Cupara[1], Violeta Mitic[2], Jelena Nikolic[2] and Vesna Stankov Jovanovic[2]

[1]*University of Kragujevac, the Faculty of Medical Sciences, Department of Pharmacy, Kragujevac, Serbia*
[2]*University of Nis, the Faculty of Science and Mathematics, Department of Chemistry, Nis, Serbia*

Received: 29.08.2019.
Accepted: 10.09.2019.

**Corresponding author:**

**Ana Barjaktarevic**

University of Kragujevac, Faculty of Medical Sciences, Department of Pharmacy
69 Svetozara Markovica Street,
34000 Kragujevac, Serbia

E-mail: ana.radovanovickg@gmail.com

sciendo

UDK: 615.322:582.639.1
Ser J Exp Clin Res 2022; 23(1): 51-57
DOI: 10.2478/sjecr-2019-0044

## ABSTRACT

*The aim of this study was to investigate in vitro antioxidant and antimicrobial potential of methanol and chloroform extracts of Sanguisorba minor L. subsp. muricata Briq. herba (S. minor). Total phenolic and flavonoid content of the investigated extracts were characterized. Antioxidant activity was estimated by five different in vitro assays. Antioxidant potency composite index was calculated also. Antimicrobial activity was tested against nine bacterial and one fungus strains by the micro-well dilution assay. The methanol extract of S. minor contains more phenols and shows the stronger antioxidant and antibacterial activity in comparison to the chloroform extract. However, the chloroform extract was superior to the methanol extract in content of flavonoids. Gram-positive bacteria were more sensitive than Gram-negative, to both extracts, Staphylococcus aureus being the most sensitive. Sanguisorba minor extracts were not considerably active against Candida albicans. The previous research data about Sanguisorba minor are scarce, so this data represent the first report on antimicrobial activity of S. minor. These results indicate that extracts of S. minor subsp. muricata have evidence-based potential for more comprehensive studies.*

***Keywords***: *Sanguisorba minor subsp. muricata, antioxidant activity, antimicrobial activity*

## ABBREVIATIONS

**ABTS**: 2,2'-azino-bis (3-ethylbenzothiazoline-6-sulphonic acid); **ANOVA**: One-way analysis of variance; **CLP**: Cecal Ligation and Puncture; **CUPRAC**: Cupric Reducing Antioxidant Capacity; **FRAP**: Ferric-reducing antioxidant power; **TBARS**: Thiobarbituric Acid Reactive Species; **TFC**: Total Flavonoid Content; **TPC**: Total Phenolic Content; **TRP**: Total Reducing Power.

## INTRODUCTION

*Sanguisorba minor* (little burnet, *S. minor*) is a perennial herbaceous plant, belonging to the genus *Sanguisorba*, family Rosaceae. It is widespread throughout Europe, Africa and Asia. It has been used as a traditional medicine for the treatment of conjunctivitis, fever and diarrhea in the form of infusions and tinctures (1, 2). Different subspecies of *S. minor* have been found in Serbia, including subsp. *muricata* (3).

*Sanguisorba genus* plants expressed a wide range of pharmacological effects - such as hemostatic, antibacterial, anti-inflammatory, antioxidant, hypoglycemic, neuroprotective or anticancer (3). The most investigated *Sanguisorba* species has been *Sanguisorba officinalis,* while *S. minor* species is less explored (4, 5). Among various active compounds isolated from the root and aerial parts of the *S. minor*, phenolic acids, triterpenoids, tannins and flavonoids have been reported as its major components (6-8). The previous research also proved that *S. minor* contains high amount of polyphenols, β-carotene, vitamin E, and vitamin C which has been associated with the antioxidant potential of *S. minor* herba (9-11). The aqueous extract of *S. minor subsp. muricata* herba showed anti-inflammatory and anti-ulcerogenic effects (12, 13), while the ethanol extract of *S. minor* herba inhibits activity of acetylcholinesterase (2). To the best of our knowledge, there have not been any investigations on *S. minor* antimicrobial activity. Since *S. officinalis* has shown antimicrobial properties in the previously published research, we have been encouraged to direct our research in this way (14-16).

## THE AIM OF THE PAPER

An autochthon growing plant from the region of Serbia, *S. minor subsp. muricata* Briq. has not been characterized neither chemically nor biologically. Therefore, the aim of this study was to determine the amount of flavonoids and phenol compounds in methanol and chloroform extracts of *S. minor subsp. muricata* herba as part of the chemical characterization. Biological activity of afore-mentioned extracts was evaluated by the antioxidant and antimicrobial testing of extracts *in vitro*.

## MATERIALS AND METHODS

### Plant material

Aerial parts of *S. minor subsp. muricata* were collected from Kamenica village meadows, located in Sumadija region (Serbia) during a spring sunny day. Plant materials were authenticated at the Institute for Biology and Ecology at the Faculty of Science (University of Kragujevac, Serbia), by standard botanical keys for the plant determination (3, 17). After drying in the shade at room temperature, aerial parts (herba) were ground and extracted with reflux of methanol and chloroform on boiling temperature for four hours. 35 g of the aerial parts of the plant and 300 mL of solvents were used. The yield of the methanol extract was 2.46 g and 0.61 g for the chloroform extract. Dry extracts were obtained by the rotary vacuum evaporator and stored in the desiccator until the experiment.

### Total phenolic and flavonoid content

Total Phenolic Content (TPC) of samples was determined spectrophotometrically at 750 nm according to the Folin-Ciocalteu method. Gallic acid was used as a standard for the calibration curve and results were expressed as μg of gallic acid equivalents per mg of dry weight (μg GAE per mg dw). All the measurements were done in triplicate (18, 19).

Total Flavonoid Content of extracts (TFC) was estimated by the aluminium chloride colorimetric method. The absorbance was measured spectrophotometrically at 510 nm. All the measurements were done in triplicate. Rutin was used to perform the standard curve, and the results were expressed as μg of rutin equivalent per mg dry weigh (μg RE/mg) (20).

### Antioxidant activity assays

### ABTS radical scavenging activity

Free radical scavenging activity of *S. minor* extracts was determined by the ABTS radical cation decolorization assay. The absorbance of the mixture was measured at 734 nm. All the measurements were carried out three times. Results were expressed as μg of Trolox equivalents (TE) per mg extract dry weight (μg TE per mg dw) (19).

### DPPH radical scavenging assay

Free radical scavenging activity of the investigated extracts was determined the application of the DPPH assay. The absorbance of samples was measured at 515 nm spectrophotometrically. All samples were made in triplicate. Trolox was used as a positive control. Results were expressed as μg of Trolox equivalents (TE) per mg dry extract weight (μg TE per mg dw) (19).

### Cupric Reducing Antioxidant Capacity (CUPRAC) assay

The CUPRAC assay was performed according to the Dimitrijevic et al. The absorbance of reaction mixture was measured at 450 nm spectrophotometrically. Results were expressed as μg of Trolox equivalents per mg of dry weight (μg TE per mg dw) (19).

### Ferric-Reducing Antioxidant Power (FRAP) assay

The reducing power was determined by ferricyanide-ferric chloride method. The change of absorbance of the FRAP reagent was monitored at 596 nm 595 nm. All the measurements were done in triplicate. Results were expressed as a μg Fe/mg dw of Fe(II) equivalents per mg of dry weight (μg Fe per mg dw) (19).

### Total Reducing Power (TRP) assay

The method of the reducing power assay was based on the reduction of Fe(III) hexacyanate to Fe(II) hexacyanate. The absorbance of the reaction mixture was measured at 700 nm, spectrophotometrically. All samples were made in triplicate. Results were expressed as µg of the ascorbic acid equivalents per mg of dry extract weight (µg AAE per mg dw) (19).

### Antioxidant Potency Composite Index-ACI

Antioxidant Potency Composite Index (ACI) was calculated according to the following equation: ACI=(sample score/best score)×100 (21).

### Antimicrobial activity assay

Methanol and chloroform extracts of the *S. minor subsp. muricata* herba were used for the evaluation of antimicrobial activity by the micro-well dilution assay *in vitro* (CLSI 2009, with some modifications). The initial concentration of extracts was 100 mg/ml. Antibacterial assays were carried against three Gram-positive bacteria (*Bacillus cereus, Enterococcus faecalis, Staphylococcus aureus*) and six Gram-negative bacteria (*Escherichia coli, Pseudomonas aeruginosa, Enterobacter aerogenes, Proteus mirabilis, Klebsiella pneumoniae, Salmonella enteritidis*). Antifungal activity of the extracts was tested against *Candida albicans*.

Suspensions of test strains were prepared from fresh overnight cultures transferred into normal saline (0.9% NaCl) under aseptic conditions. Density of each suspension was standardized to 0.5 McFarland. The final bacterial suspension was adjusted to $10^6$ CFU/mL. Serial dilutions of extracts were prepared and tested in the concentration range from 0.04 to 100.0 mg/mL in a 96/well microtiter plate with the inoculated Mueller-Hinton brott (for bacterial suspension) or the Sabouraud Dextrose agar (for fungal suspension). For this assay, positive control agents were doxycycline and nystatin in the concentration range of 0.01-20.0 µg/mL. Dimethyl sulfoxide (DMSO, 100%) was taken as a negative control, in the concentration range from 0.02 to 50.0 mg/mL. After adding 20 µL of 0.5% triphenyl tetrazolium chloride solution, bacterial and fungal growth was detected. Results were presented as MIC/MBC or MIC/MFC (in mg/mL). The minimal inhibitory concentration (MIC) was defined as the lowest concentration of samples that produced complete growth inhibition of the tested microorganisms while minimal bactericidal/fungicidal concentration (MBC/MFC) was defined as the lowest concentration of extracts that killed ≥99.9% of the final inoculum. All experiments were independently repeated three times.

### Statistical analysis

All the experiments were performed in triplicate and the experimental data were expressed as mean±standard deviation (SD). Antioxidant activity was analyzed by five different methods which make it difficult to compare results with each other. Because of that, statistical analysis was performed with the Antioxidant Potency Composite Index (ACI) values. Linear regression was used to identify the correlation between antioxidant activity and total phenolic and flavonoid contents of *S. minor* herba extracts.

## RESULTS

### Antioxidant activity assays

The antoxidant activity, the Total Phenolic (TPC) and Total Flavonoid Content (TFC) of the tested *S. minor* herba extracts are shown in Table 1. These results represent mean value±standard deviation of three replicate experiments.

**Table 1.** Antioxidant activity of *S. minor* herba extracts

| *S. minor* extracts | ABTS µg TE/mg | DPPH µg TE/mg | CUPRAC µg TE/mg | FRAP µg Fe/mg | TRP µg AAE/mg | TPC µg GAE/mg | TFC µg RE/mg |
|---|---|---|---|---|---|---|---|
| Methanol | 77.26 ±0.16 | 95.06 ±0.28 | 289.09 ±0.24 | 205.62 ±2.53 | 0.58 ±0.015 | 132.80 ±3.87 | 506.50 ±5.00 |
| Chloroform | 53.83 ±1.35 | 40.31 ±0.54 | 182.90 ±0.55 | 78.22 ±0.44 | 0.06 ±0.005 | 67.87 ±0.77 | 889.00 ±43.30 |

**Antioxidant Potency Composite Index (ACI)**

Antioxidant Potency Composite Index (ACI) values of the methanol and chloroform *S. minor* herba extracts are presented in Table 2.

**Table 2.** ACI for *S. minor* extracts by five different methods

| *S. minor* extracts | ABTS | DPPH | CUPRAC | FRAP | TRP | Average |
|---|---|---|---|---|---|---|
| Methanol | 98.85 | 100 | 100 | 100 | 100 | 99.77 |
| Chloroform | 69.67 | 42.40 | 63.27 | 38.04 | 10.35 | 44.75 |

The correlation between total phenolic/flavonoid content and antioxidant composite index of *Sanguisorbae minor* extracts has been shown in Figures 1 and 2. There is a significant positive correlation between the total phenolic content and antioxidant potency composite index of *S. minor* extracts ($r^2$=0.9979 and r=0.9989). The total flavonoid content and ACI of *S. minor* extracts are significantly negative correlated ($r^2$=0.9972 and r=0.9985)

**Figure 1.** Linear regression between the Total Phenolic Content (µg GAE/mg) and ACI of Sanguisorbae herba extracts

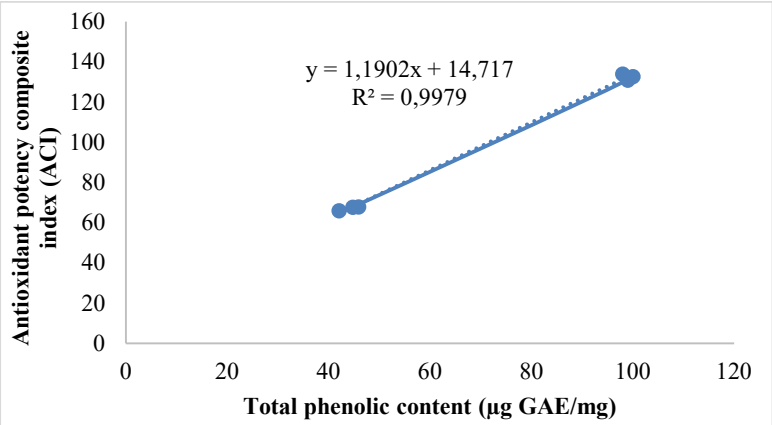


**Figure 2.** Linear regression between the TFC (µg RE/mg) and ACI of Sanguisorbae herba extracts

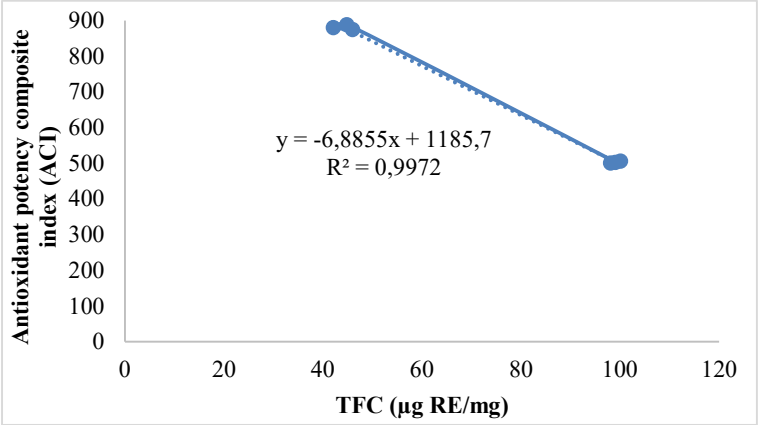

**Antimicrobial activity**

The results of the micro-well dilution assay on *S.minor* herba extracts have been summarized in the Table 3.

**Table 3.** Antimicrobial activity of *S. minor* extracts against bacterial and fungus strains (MIC/MBC in mg/mL)

| Microorganisms | ATCC | *S. minor* extracts | |
|---|---|---|---|
| | | Methanol | Chloroform |
| *Escherichia coli* | 25922 | 3.13/3.13 | 3.13/12.50 |
| *Pseudomonas aeruginosa* | 9027 | 1.56/3.13 | 3.13/6.25 |
| *Salmonella enteritidis* | 13076 | 3.13/3.13 | 3.13/12.50 |
| *Proteus mirabilis* | 12453 | 3.13/3.13 | 6.25/6.25 |
| *Klebsiella pneumoniae* | 10031 | 3.13/3.13 | 6.25/6.25 |
| *Enterobacter aerogenes* | 13048 | 1.56/3.13 | 3.13/25.0 |
| **Gram-positive bacteria** | | | |
| *Bacillus cereus* | 11778 | 0.39/0.39 | 1.56/3.13 |
| *Staphylococcus aureus* | 25923 | 0.10/0.39 | 0.78/12.50 |
| *Enterococcus faecalis* | 19433 | 0.39/0.39 | 0.39/6.25 |
| **Fungi** | | | |
| *Candida albicans* | 14053 | 6.25/12.50 | 6.25/12.50 |

## DISCUSSION

Two different extracts of *S. minor subsp. muricata* herba were investigated and compared to their antioxidant, antimicrobial potential-methanol and chloroform extract. In order to chemically characterize this scarcely researched plant, contents of phenolics and flavonoids were determined and an attempt to understand their possible influence on the antioxidant activity of the extracts was made.

Antioxidant activity of plants has been thoroughly researched by several different methods in order to perform the best possible evaluation of all compounds contributing to this activity. In most cases, the antioxidant activity has been positively correlated to the content of total phenolics, due to their potential to scavenge free radicals (22). In absence of the reference data for this species from Serbia for phenolics, determination of total content of phenolic compounds in investigated extracts seems to have been a prerequisite. In our study we compared content of these antioxidant-contributing compounds in the methanol and chloroform extract. The methanol extract, due to the stronger polarity of its solvent, possessed a higher content of phenolics (132.80±3.87 μg GAE/mg dw) in comparison to the chloroform extract (67.87±0.77 μg GAE/mg dw). These results demonstrate that total phenolic content depends on the polarity of the solvent used. Previous studies also reported methanol as an effective solvent for the extraction of phenolic compounds (22, 16).

Investigations on *S. minor subsp. muricata* are scarce or absent, which limits us to discuss our results in the light of the references data available solely on *S. minor* species, of which *S. officinalis* has been the most investigated. There have not been any reports on the content of total phenolics for *S. minor* herba methanol or chloroform extract. However, the TPC was determined in methanol extract of *S. officinalis* herba (116.96±5.89 mg GAE/100 mg), which is in concordance with the result of TPC in our investigated *S. minor* herba methanol extract (23).

Flavonoids have been documented to be strong scavengers of the most oxidizing molecules, singlet oxygen and/or different free radicals (24). In our study, chloroform extract contained a higher level of flavonoids (889.00±43.30 μg RE/mg), than the methanol extract (506.50±5.00 μg RE/mg). Direct comparison of total flavonoids from our study and previous reports on *S. minor* spp. is not reproducible due to the different equivalents used in the result expression.

The antioxidant potential of *S. minor subsp. muricata* methanol and chloroform extracts was evaluated by five in vitro methods: ABTS, DPPH, CUPRAC, FRAP and TRP assays. Methanol extract showed a significantly higher antioxidant activity than the chloroform extract, determined by all assays (Table 1). That difference may be due to strong difference in the polarity of these two solvents (25). Antioxidant Potency Composite Index values also confirmed that the methanol extract of *S. minor* herba showed much better

antioxidant activity than the chloroform extract in all employed assays (Table 2). Due to the lack of similar data on *S. minor subsp. muricata* that could serve as the reference point, we declare that our results are within the range of antioxidant activity found in *Sanguisorba genus* plants, which has been well documented (4).

The highly significant positive correlations between the TPC and ACI of *S. minor* extracts obtained in this study (Figure 1) support the hypothesis that phenolic compounds contribute significantly to the total antioxidant capacity of plants species (25). The positive correlation between antioxidant activity and total flavonoid content of *S. minor* aerial parts extracts was reported (15). However, we observed an inverse correlation between the ACI and TFC in our extracts (Figure 2). The chloroform extract showed the higher TFC, but the lower antioxidant activity. Therefore, we assume that flavonoids in our investigated *S. minor* extracts do not contribute significantly to the antioxidant activity.

The aim of this study was also to evaluate antibacterial/antifungicidal activity of chloroform and methanol extracts of *S. minor subsp. muricata* aerial parts. Both extracts exhibited considerable antimicrobial activity against all examined strains of bacteria (*B. cereus, E. faecalis, S. aureus, E. coli, P. aeruginosa, E. aerogenes, P. mirabilis, K. pneumoniae, S. enteritidis*) but not against *Candida albicans*. All tested strains, except *C. albicans*, were more susceptible to the methanol extract than the chloroform extract (Table 2). Methanol extract exhibited the stronger bacteriostatic and bactericidal activity than the chloroform extract, with MIC range 0.1-3.13 mg/mL, and MBC range 0.39-3.13 mg/mL (Table 2). Our research confirms previous reports on *Sanguisorba genus* plants which demonstrated that methanol extracts were more active than chloroform extracts (16, 26). Our investigated extracts of *S. minor* were more active against the Gram-positive than Gram-negative bacteria. The most sensitive was the *Staphylococcus aureus* (MIC=0.10 mg/mL, MBC=0.39mg/ml). Since there has not been any research on antimicrobial activity of *S. minor* species, our results represent the first data of this kind. Therefore, in the following discussion we assume as relevant the comparison of antimicrobial activity of *S. minor* to *S. officinalis*, since *S. officinalis* as a plant of *Sangisorba genus* has shown strong antimicrobial activity (16, 26, 27). *S. officinalis* is active against *E. coli, S. aureus, B. cereus, P. aeruginosa* and *Candida albicans* (14, 16, 26). In spite of the most common use of roots *S. officinalis* in traditional medicine, it was proved that *S. officinalis* herba showed a higher antimicrobial activity compared to the root (16). Methanol extract of *S. minor* herba in our study exhibited the stronger antimicrobial activity (MIC=0.10 mg/mL, MBC=0.39 mg/ml) than the methanol extract of *S. officinalis* herba (MIC=0.256 mg/ml, MBC > 1.024 mg/ml) against S. aureus (16). The same relation was observed in comparison of chloroform extracts *S. minor* herba vs. *S. officinalis* herba extract. Chloroform extract of *S. minor* showed better MIC values than chloroform extract of *S. officinalis* (16).

The previous published results indicated similar activity of *S. officinalis* herba extracts against both, the Gram-negative and Gram-positive bacteria (16). However, Shan et al. that suggested in their research that *S. officinalis* herba extract was more active against the Gram-positive bacteria. In our investigation *S. minor* extracts were also more active against the Gram-positive bacteria. We, therefore, share their observation that a possible cause may be different interactions of Sangusiorba sp. extracts with outer layers of the Gram-negative and Gram-positive bacteria, since both plants belonging to *Sanguisorba genus* exhibited the same preference to act stronger against the Gram-positive bacteria (27).

## CONCLUSION

*S. minor* subps. *muricata* was investigated *in vitro* for its antioxidant and antimicrobial properties. Methanol extract of *S. minor* subps. *muricata* herba has a high content of phenols and shows considerable antioxidant activity, measured by all five different methods that were used. Methanol extract is superior to the chloroform extract in the content of phenols and antioxidant activity. Chloroform extract has a higher content of flavonoids. Methanol extract was stronger than the chloroform extract against all investigated bacterial strains and it is also stronger against the Gram-positive bacteria. *S. minor* subps. *muricata* is active mostly against *Staphylococcus aureus.* The obtained data indicate that *S. minor subsp. muricata* has evidence-based potential for further more comprehensive studies.

## ACKNOWLEDGMENTS

This work was supported by the projects: No. MFVMA 04/19-21 of the University of Defense, Serbia and No. OI 172051, No. OI 172047, No. OI 175014 of the Ministry of Education, Science and Technological Development of Serbia.

## REFERENCES

1. Viano J, Masotti V, Gaydou EM. Nutritional value of Mediterranean sheep's burnet (Sanguisorba minor ssp. muricata). J Agric Food Chem. 1999; 47(11): 4645-8
2. Ferreira A, Proença C, Serralheiro ML, Araújo ME. The in vitro screening for acetylcholinesterase inhibition and antioxidant activity of medicinal plants from Portugal. J Ethnopharmacol. 2006; 108(1): 31-7.
3. Josifovic, M. (1972). Flora of Serbia. Volume 4. Rosaceae family. Belgrade: SANU. pp. 66-71.
4. Zhao Z, He X, Zhang Q, Wei X, Huang L, Fang JC, et al. Traditional Uses, Chemical Constituents and Biological Activities of Plants from the Genus Sanguisorba L. Am J Chin Med. 2017; 45(2): 199-224.
5. Jang E, Inn KS, Jang YP, Lee KT, Lee JH. Phytotherapeutic Activities of Sanguisorba officinalis and its Chemical Constituents: A Review. Am J Chin Med. 2018; 46(2): 299-318.

6. Ayoub NA. Unique phenolic carboxylic acids from Sanguisorba minor. Phytochem 2003; 63(4): 433-6.
7. Reher G, Reznicek G, Baumann A. Triterpenoids from Sarcopoterium spinosum and Sanguisorba minor. Planta Med. 1991; 57(5): 506.
8. el-Mousallamy AM. Polyphenols of Egyptian Rosaceae plants-two new flavonoid glycosides from Sanguisorba minor. Scop. Pharmazie. 2002; 57(10): 702-4.
9. Guarrera PM, Savo V. Wild food plants used in traditional vegetable mixtures in Italy. J Ethnopharmacol. 2016; 185: 202-34.
10. Vanzani P, Rossetto M, De Marco V, Sacchetti LE, Paoletti MG, Rigo A. Wild Mediterranean plants as traditional food: a valuable source of antioxidants. J Food Sci. 2011; 76(1): C46-51.
11. Romojaro A, Botella MÁ, Obón C, Pretel MT. Nutritional and antioxidant properties of wild edible plants and their use as potential ingredients in the modern diet. Int J Food Sci Nutr. 2013; 64(8): 944-52.
12. Arıhana O, Özbekb H, Mine A, Özkand G. Anti-inflammatory effects of Sanguisorba minor Scop. subsp. muricata (Spach) Briq. and Cirsium libanoticum DC. subsp. lycaonicum (Boiss. & Heldr.) Davis & Parris in rat. EJM 2015; 20: 81-85.
13. Gürbüz I, Ozkan AM, Yesilada E, Kutsal O. Anti-ulcerogenic activity of some plants used in folk medicine of Pinarbasi (Kayseri, Turkey). J Ethnopharmacol. 2005; 101(1-3): 313-8.
14. Chen X, Shang F, Meng Y, Li L, Cui Y, Zhang M, et al. Ethanol extract of Sanguisorba officinalis L. inhibits biofilm formation of methicillin-resistant *Staphylococcus aureus* in an ica-dependent manner. J. Dairy Sci. 2015; 98: 1-6.
15. Gawron-Gzella A, Witkowska-Banaszczak E, Bylka W, Dudek-Makuch M, Odwrot A Skrodzka N. Chemical composition, antioxidant and antimicrobial activities of Sanguisorba officinalis L. extracts. Pharmaceutical Chemistry Journal. 2016; 50(4): 244-9.
16. Ginovyan M, Petrosyan M, Trchounian A. Antimicrobial activity of some plant materials used in Armenian traditional medicine. BMC Complement Altern Med. 2017; 17(1): 50.
17. Tutin TG, Heywood VH, Burges NA, et al. Rosaceae to Umbelliferae. In: Flora Europaea, Vol. 2. Cambridge: Cambridge University press. 1968, p. 33- 4.
Rajurkar NS, Hande SM. Estimation of phytochemical content and antioxidant activity of some selected traditional Indian medicinal plants. Indian J Pharm Sci. 2011; 73: 146.
18. Dimitrijevic M, Jovanovic VS, Cvetkovic J, Mihajilov-Krstev T, Stojanovic G, Mitic V. Screening of antioxidant, antimicrobial and antiradical activities of twelve selected Serbian wild mushrooms. Anal Methods. 2015; 7: 4181-91.
19. Baba SA, Malik SA. Determination of total phenolic and flavonoid content, antimicrobial and antioxidant activity of a root extract of Arisaema jacquemontii Blume. J Taibah Univ Sci. 2015; 9: 449-54.
20. Seeram NP, Aviram M, Zhang Y, Henning SM, Feng L, Dreher M et al. Comparison of antioxidant potency of commonly consumed polyphenol-rich beverages in the United States, J Agric Food Chem. 2008; 56:1415-22.
21. Singh M, Pandey N, Agnihotri V, Singh KK, Pandey A. Antioxidant, antimicrobial activity and bioactive compounds of Bergenia ciliata Sternb.: A valuable medicinal herb of Sikkim Himalaya. J Tradit Complement Med. 2016; 7(2): 152-7.
22. Arnold E, Benz T, Zapp C, Wink M. Inhibition of Cytosolic Phospholipase A2α(cPLA2α) by Medicinal Plants in Relation to Their Phenolic Content. Molecules. 2015; 20(8): 15033-48.
23. Saeed N, Khan MR, Shabbir M. Antioxidant activity, total phenolic and total flavonoid contents of whole plant extracts Torilis leptophylla L. BMC Complement Altern Med. 2012; 12: 221.
24. Li S, Li SK, Gan RY, Song FL, Kuang L, Li HB. Antioxidant capacities and total phenolic contents of infusions from 223 medicinal plants. Ind Crops Prod. 2013; 51: 289-98.
25. Kokoska L, Polesny Z, Rada V, Nepovim A, Vanek T. Screening of some Siberian medicinal plants for antimicrobial activity. J Ethnopharmacol. 2002; 82: 51-3.
26. Shan B, Cai YZ, Brooks JD, Corke H. The in vitro antibacterial activity of dietary spice and medicinal herb extracts. Int J Food Microbiol. 2007; 117: 112-9.

ORIGINAL SCIENTIFIC ARTICLE

# THE INCIDENCE OF ADOLESCENT PREGNANCY AT CLINIC OF GYNECOLOGY AND OBSTETRICS OF CLINICAL CENTER KRAGUJEVAC

Marija Bicanin Ilic[1] and Aleksandra Dimitrijevic[1]

[1] *Clinic of Gynecology and Obstetrics, Clinical Centre Kragujevac, Kragujevac, Serbia*

Received: 26.04.2019.
Accepted: 03.05.2019.

**Corresponding author:**

**Marija Bicanin Ilic, MD**

Clinic of Gynecology and Obstetrics,
Clinical Centre Kragujevac
30 Zmaj Jovina Street, Kragujevac, Serbia

Phone: +381 642210218
E-mail: abahelica@hotmail.com

sciendo

UDK: 618.2-053.6(497.11)"2007/2019"
Ser J Exp Clin Res 2022; 23(1): 59-66
DOI: 10.2478/sjecr-2019-0028

## ABSTRACT

*Adolescent pregnancy belongs to a group of high-risk pregnancies with high maternal and fetal mortality and morbidity rate with high prevalence globally (11%). The aim of this observational study is to show the incidence of adolescent deliveries in relation to the total number of births in the twelve-year period from 2007 to 2019 at the Department of Gynecology and Obstetrics of Clinical Center in Kragujevac from medical protocols and patients' medical records. By evaluating the data of our research, we noticed a continuing decrease in the percentage of adolescents that give births each year. The total number of births in our clinic in this twelve-year period was 26544, and the number of teenage deliveries was 390 (1.74%), which is in accordance with the results of a similar research which was conducted in our clinic in the period from 2002 to 2007 (16.1%). However, despite the increase in the number of caesarean sections, Apgar score of newborn babies was similar to the results of previous tests - 8.31 which proves that the increase in caesarean sections is not correlated with growth of Apgar score. The average pregnancy duration of adolescents is similar as in the previous five-year period (37.5 w.g.), while in the general population of pregnant women it is 39.2 w.g which represents a statistically significant difference. The main causes of poor outcomes of adolescent pregnancies are biological immaturity of mothers, poor health care, that comes from poor socio-demographic conditions, as well as emotional stress. It is necessary to change the attitude of society towards these young people, give them support in the environment they live and provide them with better health care and social treatment.*

***Keywords***: *Adolescent pregnancy, teenage pregnancy, young age childbirth.*

## INTRODUCTION

According to the World Health Organization (WHO) definition, adolescence presents forming full sexual maturity, maturing of person from the psyche of the child to the psyche of an adult and transition from full social and economic dependence to the relative independence (1). This life period of a woman is followed by turbulent psychosocial events and often complicated by dyscoordination of mental and physical maturation. Modern hygiene and dietary conditions have led to the occurrence of girl's menarche earlier, that together, followed by the customs and attitudes of the surroundings, results in sexual relations at the early age. Adolescents are usually not aware of the risks and dangers of unprotected sexual behavior and they are not mentally mature to face the consequences of the act. Adolescent pregnancy is usually the product of the mentioned factors. It belongs to a group of high-risk pregnancies with high maternal and fetal mortality and morbidity rate. Pregnancy at this age has been reported as the leading cause of death in adolescent girls in low- and middle-income countries (2).

Insufficient biological maturity of pregnant girls, poor socio epidemiological living conditions and inadequate medical care are key factors of pregnancy complications amongwhich the most common are: premature birth, intrauterine growth restriction, pregnancy induced hypertension (PIH), anemia, infections and fetal anomaly (1). Partial progesterone resistance that persists into adolescent years may compromise the physiological transformation of the spiral arteries and predispose for defective placentation in the case of pregnancy. The major obstetric syndromes caused by impaired placental bed spiral artery remodeling are prevalent in teenage pregnancies, including preeclampsia, fetal growth restriction, and spontaneous preterm labor (3). Some studies report that the adverse outcomes are due to physiological and anatomical factors associated with young maternal age, while others report that they are due to external factors such as socioeconomic status, social support, inadequate antenatal care and other behavioural determinants associated with adolescence (4). Almost all assessments of adolescent pregnancies are based on chronological age. Gynecologic age is defined as age in years at conception minus age at menarche and it is an indicator of physiological maturity. Low gynecologic age is associated with an increased rate of obstetric and perinatal complications in adolescent pregnancies. Although the main aim is the prevention of adolescent pregnancies, a detailed evaluation of such pregnancies including determination of the gynecological age together with a multidisciplinary approach may decrease potential complications (5).

According to WHO statistics, about 16 million girls aged 15 to 19 give birth each year, mostly in low- and middle-income countries, and about 3 million have an abortion. Complications during pregnancy and childbirth are the second cause of death of girls in this age group. Young mothers, and particularly teenage mothers, are a vulnerable group at high risk of poor mental health outcomes compared to mothers aged 25 and above (6).

About 11% of all pregnancies globally belong to adolescent pregnancies (7). Since 1990 there has been a downward trend in adolescent pregnancies which is associated with more massive educating youth about the risks and consequences of unprotected sexual relation and massive use of condoms.

The aim of this study is to determine the incidence of adolescent deliveries in relation to the total number of births in the twelve-year period from 2007 to 2019 at the Department of Gynecology and Obstetrics of Clinical Center in Kragujevac by collecting the data about the maternal age, body weight and Apgar score of newborns, indications for instrumental delivery and frequency of caesarean section.

## METHODOLOGY

### Ethical concerns

This observational study was performed in accordance with all relevant ethical principles.

### Design of the study

This study was designed as retrospective cross-sectional observational clinical study which evaluated the incidence of adolescent pregnancy during twelve-year period from 2007 to 2019 at the Department of Gynecology and Obstetrics of Clinical Center in Kragujevac from medical protocols and patients' medical records.

### Population of the study

The study included all medical data regarding adolescent pregnancy from birth protocols and caesarean sections protocols and patients' medical records during past twelve years. The main inclusion criteria were adolescent age (12-18 years old) and confirmed pregnancy.

### Data processing and analysis

All data were processed in Excel, presented in tables and charts, statistically expressed by mean and by percentile.

## RESULTS

### Prevalence of adolescent births

During past twelve years, the highest number of adolescent births occurred in 2009, then in 2007 and 2008 in eighteen years old mothers. On the other hand, the smallest count of adolescent pregnancies was in last two years (2017 and 2018) in the youngest mothers (Table 1).

In percent, from all pregnancies over past twelve years, the highest incidence was in 2009, then in 2007 and 2008. On the other hand, 2017 and 2018 were years with the lowest incidence (Figure 1).

Comparative presentation of the total number of births and births by adolescents by age shows that the first four years have the highest frequency compared with other years and that the dynamics of frequency was different over the twelve years study period (Table 2).

**Table 1.** Total number of adolescent deliveries classified by age of mothers

| | 2007 | 2008 | 2009 | 2010 | 2011 | 2012 | 2013 | 2014 | 2015 | 2016 | 2017 | 2018 |
|---|---|---|---|---|---|---|---|---|---|---|---|---|
| **12** | 1 | 0 | 0 | 0 | 0 | 0 | 0 | 0 | 0 | 0 | 0 | 0 |
| **13** | 0 | 0 | 0 | 0 | 0 | 0 | 0 | 0 | 0 | 0 | 0 | 0 |
| **14** | 1 | 0 | 0 | 1 | 2 | 0 | 0 | 0 | 0 | 0 | 0 | 0 |
| **15** | 0 | 2 | 4 | 1 | 1 | 3 | 3 | 2 | 0 | 0 | 1 | 0 |
| **16** | 4 | 9 | 6 | 9 | 4 | 2 | 3 | 4 | 4 | 0 | 1 | 2 |
| **17** | 18 | 14 | 15 | 11 | 9 | 7 | 9 | 8 | 5 | 10 | 4 | 1 |
| **18** | 28 | 26 | 30 | 21 | 17 | 22 | 16 | 11 | 10 | 15 | 5 | 8 |
| **Σ** | **52** | **51** | **55** | **43** | **33** | **34** | **31** | **25** | **19** | **25** | **11** | **11** |

**Figure 1.** Frequency of adolescent deliveries

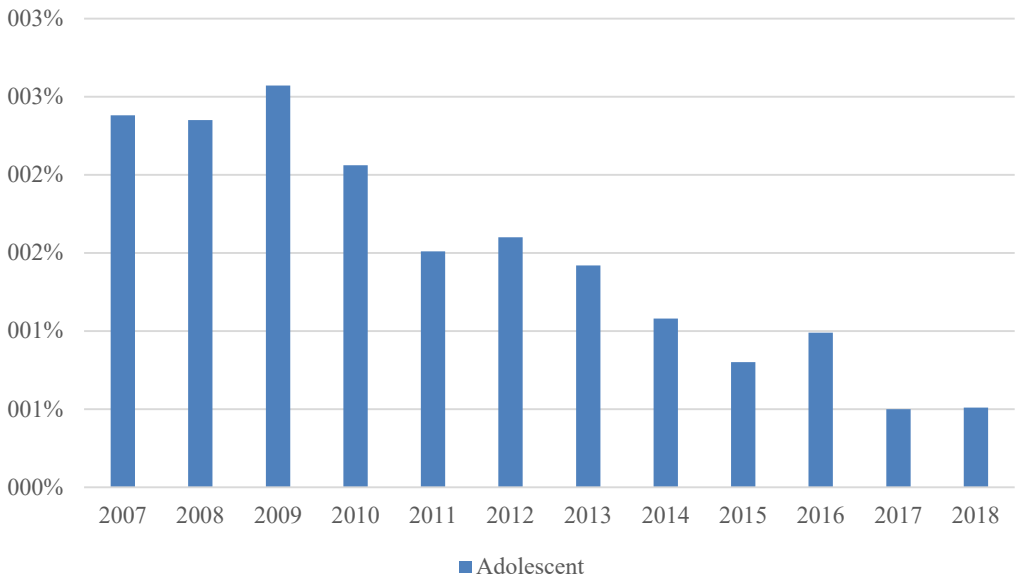

**Table 2.** Comparative presentation of the total number of births and deliveries by adolescents from 2007 to 2018

| | 2007 | 2008 | 2009 | 2010 | 2011 | 2012 | 2013 | 2014 | 2015 | 2016 | 2017 | 2018 |
|---|---|---|---|---|---|---|---|---|---|---|---|---|
| **Total number of births** | 2180 | 2171 | 2138 | 2088 | 2185 | 2121 | 2181 | 2302 | 2352 | 2511 | 2170 | 2151 |
| **adolescents** | 52 | 51 | 55 | 43 | 33 | 34 | 31 | 25 | 19 | 25 | 11 | 11 |
| **percentage** | 2.38 | 2.34 | 2.57 | 2.06 | 1.51 | 1.60 | 1.42 | 1.08 | 0.80 | 0.99 | 0.50 | 0.51 |

**Apgar score of newborns from adolescent pregnancies**

Table 3 shows distribution of Apgar scores of newborns in adolescent pregnancies during twelve-year period. Most newborns were born with 8-10 Apgar score (91.3%) (Table 3).

**Table 3.** Apgar score of newborns from adolescent pregnancies

| | 2007 | 2008 | 2009 | 2010 | 2011 | 2012 | 2013 | 2014 | 2015 | 2016 | 2017 | 2018 |
|---|---|---|---|---|---|---|---|---|---|---|---|---|
| **≤ 7 (8.97%)** | 8 | 8 | 4 | 2 | 1 | 3 | 1 | 2 | 1 | 1 | 3 | 1 |
| **8-10 (91.3%)** | 44 | 43 | 51 | 41 | 32 | 31 | 30 | 23 | 18 | 24 | 8 | 10 |
| **Total number** | 52 | 51 | 55 | 43 | 33 | 34 | 31 | 25 | 19 | 25 | 11 | 11 |

**Gestational age of newborns from adolescent pregnancies at the moment of childbirth**

Table 4 shows distribution of gestational age of adolescent pregnancies at the moment of childbirth. The highest frequency of adolescent pregnancies resulted in birth at 32-42 g.w. (62.82%), then 37-38 g.w. (21.28%) and ≤36.6 g.w. (15.64%) (Table 4).

**Table 4.** Gestational age of adolescent pregnancies at the moment of childbirth

| | 2007 | 2008 | 2009 | 2010 | 2011 | 2012 | 2013 | 2014 | 2015 | 2016 | 2017 | 2018 | Total % |
|---|---|---|---|---|---|---|---|---|---|---|---|---|---|
| **≤36.6** | 9 | 5 | 8 | 6 | 3 | 6 | 1 | 3 | 4 | 8 | 4 | 4 | (15.64%) |
| **37-38 g.w.** | 5 | 9 | 9 | 7 | 5 | 5 | 12 | 7 | 3 | 12 | 4 | 5 | (21.28%) |
| **39-42 g.w.** | 38 | 37 | 38 | 30 | 25 | 23 | 17 | 15 | 12 | 5 | 3 | 2 | (62.82%) |

**Ratio of average body weight of newborns from adolescent pregnancies with body weights of newborns according to anthropometric standards**

Figure 2 shows ratio of the average body weight of newborns from adolescent pregnancies with body weights of newborns according to anthropometric standards. The averages of body mass of newborns are higher in higher g.w. (Figure 2).

**Figure 2.** Ratio of average body weight of newborns from adolescent pregnancies with body weights of newborns according to anthropometric standards. (11)

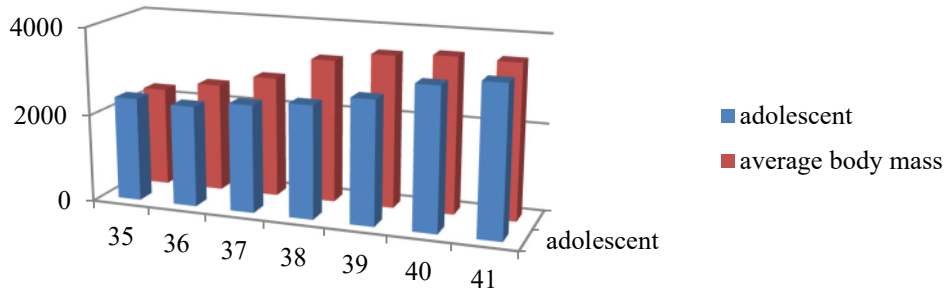


**Distribution of caesarean section in adolescents compared to general population of women**

In Table 5 and Figure 3 are presented distribution of caesarean section in adolescents compared to general population of women. The highest ratio was observed in 2015, then in 2009, and the lowest ratio in 2011 (*Table 5*).

Table 5. The ratio of births by caesarean section in adolescents and in the general population of women.

| | *2007* | *2008* | *2009* | *2010* | *2011* | *2012* |
|---|---|---|---|---|---|---|
| *Adolescent* | 52 | 51 | 55 | 43 | 33 | 34 |
| *C- sections (Total 8.97%)* | 4 (7.69%) | 3 (5.88%) | 6 (10.99%) | 1 (2.35%) | 0 (0%) | 4 (11.74%) |
| | 2013 | 2014 | 2015 | 2016 | 2017 | 2018 |
| *Adolescent* | 31 | 25 | 19 | 25 | 11 | 11 |
| *C- sections (Total 8.97%)* | 3 (9,67%) | 3 (12%) | 4 (21.05%) | 5 (20%) | 1 (9.09%) | 1 (9.09%) |

**Figure 3.** The ratio of births by caesarean section in adolescents and in the general population of women.

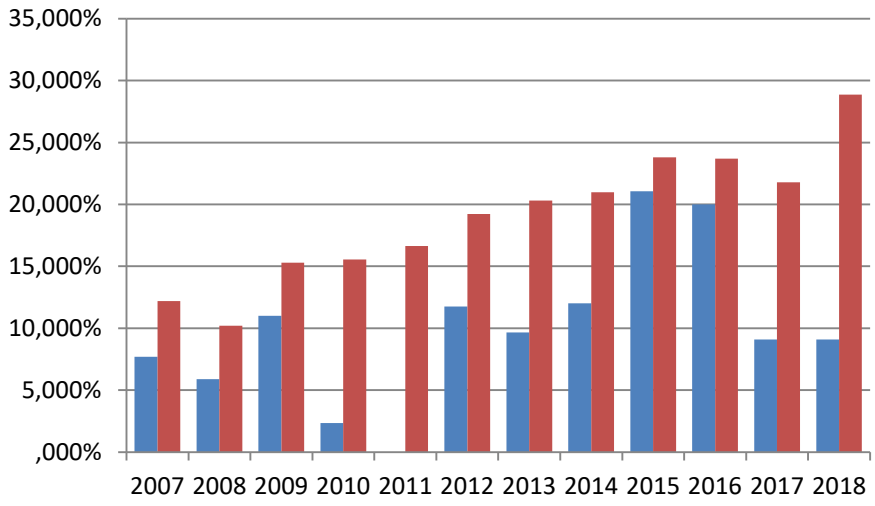

## DISCUSSION

By evaluating the data of our research, we noticed a continuing decrease in the percentage of adolescents that give births each year (Fig. 1).

The total number of births in our clinic in this twelve-year period was 26544, and the number of teenage births was 390 (1.46%), which is in accordance with results of a similar research which was conducted in our clinic in the period from 2002 to 2007 (16.1% expressed in percentage) (8). Both studies showed a significant decrease in the percentage of these deliveries compared to the 90' of the last century when this percentage was reaching 4.13%. It is far below the world level, which reaches 11% (9).

We would like to claim that the cause of this trend is better health care provided for young people, education about the risks of early entry into sexual relationships and massive use of condoms among young people. However, more likely cause is greater availability of abortions in private practice that young people easily decide to do. Data on the number of pregnancies terminated in this way do not exist, because they do not report abortions despite legal obligations. Young people terminate pregnancy without being aware of the possible complications of the interventions and health consequences. Emotionally immature young people who do not have adequate support from families and environment, seeking a way out of their unenviable situation, decide for available solutions, which is often an abortion.

Percentage of deliveries completed by caesarean section was 8.97%, which is closer to the results of studies from the 90' (6.86%), while in the period from 2002 to 2007 it was 4.51% (8). This increase in the number of caesarean sections in a group of adolescents follows the increase in the number of operative deliveries in the general population of pregnant women, but remains far below this percentage. The explanation for this increase can be found in more liberal indications for operative delivery. (9) In the general population of pregnant women, there has been an increase of pregnancies from *in vitro* fertilization in mature generative age of women and the surgical completion of these pregnancies contributes to the constant increase in the number of caesarean sections.

The percentage of caesarean sections in a group of adolescentsis smaller (Fig. 3) because there is a very small number of the leading indication for surgical termination of a pregnancy that apply to the general population of pregnant women, and those are repeated cesarean section and disproportion. In the group of deliveries by adolescents, most often is vaginal delivery with episiotomy.

However, despite the increase in the number of caesarean sections, Apgar score of newborn babies was similar to the results of previous tests which was 8.31 while in the last twelve-year period it was 8.23, which proves that the increase in caesarean sections is not correlated with growth of Apgar score.

Among the indications for operative completion of labor in the group of adolescents, leading places belong to Preterm Premature rupture of membranes (PPROM), dystocia, PIH, and fetal asphyxia (9).

The average pregnancy duration of adolescents was similar as in the previous five-year period (37.5 w.g.), while in the general population of pregnant women it is 39.2 w.g. which represents a statistically significant difference.

Preterm delivery together with insufficient body weight and death cases in newborns are the main issues in obstetrics. About 40% of preterm delivery is caused by infections (10). Even 15.64% of pregnancies ended giving birth before 37 weeks which is significantly higher than the data from the world literature, which is 10%.

Newborns' body weight from adolescents' pregnancies, expressed by weeks of gestation, significantly deviates from the average weight of newborns in the territory of Šumadija district (Fig. 2), and belongs to the 10 percentile of the body mass of newborns in the territory of Sumadija district (11). Low birth weight is a result of intrauterine growth retardation that occurs in pregnancies complicated by hypertension, malnutrition, genetic anomalies of fetus, etc. Poor prenatal health care is directly related to these complications.

The main causes of poor outcomes of adolescent pregnancies are biological immaturity of mothers, poor health care, that comes from poor socio-demographic conditions, as well as emotional stress. The well-recognized factors of socioeconomic disadvantage, disrupted family structure and low educational level and aspiration appear consistently associated with teenage pregnancy (12).

In European Union countries, this percentage has been declining since 2001, although the trend differs between countries and regions. In Eastern Europe, this percentage is the highest and amounts to 4.17%, while in the North, West and South Europe it amounts to 3.07%, 1.82% and 1.76%, respectively. (13). In the USA, rates for other vulnerable groups, such as runaway and homeless adolescents, adolescents in foster care, and adolescents living in rural areas, are higher than those of the general adolescent population (14).

The biological immaturity of mothers in pregnancy means "young gynecological age" (before the age of two years from menarche) and growth and development of the mother. In our study, the youngest mother was only 12 years old. Incomplete A case of adolescent multiparty, a 18-year-old quadripara, was also recorded. Underdeveloped cervix bloodstream can lead to subclinical infections, early production of prostaglandins and consequently premature birth (12). This datum, according to our research, shows that leading complications during pregnancy were premature ruptures of membranes, and that leading complications after childbirth were retained placenta and fetal membranes that were

associated with intrauterine infection (15). Pregnant women who have not completed the physical growth and development are competitors in the developing fetus for nutrients and if we add to that the bad social conditions that they usually come from, malnutrition is mandatory companion of these pregnancies. In addition to these evident medical consequences, pregnancy in adolescence also leads to social isolation, delay or neglect of education, and consequent depression of young mothers (16).

## CONCLUSION

Pregnancy in adolescent period is a major medical, psychological and social problem that society faces. Parent-child communication about sexuality issues is extremely difficult and leads to anxiety and neglecting of the problem, despite the fact that this type of communication as well as sexual education is proven to be associated with postponing sexual intercourse and more consistent use of contraception (17). Firstly, it is necessary to change the attitude of society towards these young people, give them support in the environment they live and provide them with better health care and social treatment. Educating young people about the consequences of risky sexual behavior, as well as presenting them methods of contraception is the best way to prevent serious complications at the beginning of women's generative age.

The necessary steps that society should take are the introduction of education on sexual behavior through elementary education, as well as the involvement of doctors, gynecologists, pediatricians and social workers in the implementation of this education. The role of the gynecologist is to provide the necessary information and to choose adequate contraceptives with the emphasis on the use of long-acting reversible contraceptives (LARC) (18). Improvements in contraceptive use including increases in the use of long-acting reversible contraception and withdrawal in combination with another method-appear to be driving recent declines in adolescent birth and pregnancy rates (19).

Adolescent mothers who initiate a LARC method within 8 weeks of delivery are less likely to have a repeated pregnancy within 2 years than those who choose other methods or no method. First time adolescent mothers should be counseled about the advantage of using LARC (20).

## CONFLICT OF INTEREST

The authors declare that there is no conflict of interest.

## REFERENCE


1. Fraser AM, Brockert JE, Ward RH. Association of Young Maternal Age with Adverse Reproductive Outcomes. The New England Journal of Medicine. 1995; 332(17):1113-1117
2. Demirci O, Yılmaz E, Tosun Ö, Kumru P, Arınkan A, Mahmutoğlu D, Tarhan N. (2016). Effect of Young Maternal Age on Obstetric and Perinatal Outcomes: Results from the Tertiary Center in Turkey. Balkan medical journal, 2016; 33(3):344–349.
3. Brosens I, Benagiano G, Brosens JJ. The potential perinatal origin of placentation disorders in the young primigravida. Am J Obstet Gynecol. 2015;212(5): 580-5.
4. Kang G, Lim JY, Kale AS, Lee LY. Adverse effects of young maternal age on neonatal outcomes. Singapore Med J. 2015;56(3):157-63. doi:10.11622/smedj.2014194
5. Kaplanoglu M, Bülbül M, Konca C, Kaplanoglu D, Tabak MS, Ata B. Gynecologic age is an important risk factor for obstetric and perinatal outcomes in adolescent pregnancies. Women Birth. 2015;28(4):e119-23.
6. Aitken Z, Hewitt B, Keogh L, LaMontagne AD, Bentley R, Kavanagh AM. Young maternal age at first birth and mental health later in life: Does the association vary by birth cohort? Soc Sci Med. 2016;157:9-17.
7. Treffers PE, Olukoya AA, Ferguson BJ, Liljestrand J. Care for adolescent pregnancy and childbirth. Int J Gynecol Obstet 2001;75:111–121.
8. Varjacic M, Lukic G, Sazdanovic P, Protrka Z, Babic G. Childbirth in adolescence. Gynecology and perinatology 2007;40(3-4):12-4.
9. Varjacic M, Ristic P, Sazdanovic P, Babic G. Adolescent delivery and cesarean section. 7th European congress on Pediatric and Adolescent gynecology, Vienna, Austria .12 – 15 Marth 1997(185).
10. Mijović G, Lukić G, Jokmanović N, Crnogorac S, Kuljić-Kapulica N, Gajić M, Kulauzov M, Bujko M. [Impact of vaginal and cervical colonisation/infection on preterm delivery]. Vojnosanit Pregl. 2008;65 (4):273-80.
11. Durutovic Gligorovic S. Anthropometric newborn norms. Medical Faculty of the University of Belgrade. 2000.
12. D Silva AAM, Simeos VMF, Barbieri MA, Betioll H, Lamz Filho F, Coimbra LC and Alves. Young maternal age and preterm birth, Paediatric and Perinatal Epidemiology. 2003;17(4):332-339
13. Part K, Moreau C, Donati S, Gissler M, Fronteira I, Karro H. Teenage pregnancies in the European Union in the context of legislation and youth sexual and reproductive health services. Acta Obstet Gynecol Scand. 2013;92(12):1395-1406.
14. Burrus BB. Decline in Adolescent Pregnancy in the United States: A Success Not Shared by All. Am J Public Health. 2018;108:S5-S6.

15. Socolov DG, Iorga M, Carauleanu A, Ilea C, Blidaru I, Boiculese L, Socolov RV. Pregnancy during Adolescence and Associated Risks: An 8-Year Hospital-Based Cohort Study (2007-2014) in Romania, the Country with the Highest Rate of Teenage Pregnancy in Europe. Biomed Res Int. 2017;2017:9205016.
16. Leftwich HK, Alves MV. Adolescent Pregnancy. Pediatr Clin North Am. 2017;64(2):381-388.
17. Amie M. Ashcraft, MPHaPamela J.Murray, MHPb Talking to Parents About Adolescent Sexuality. Pediatr Clin North Am. 2017;64(2): 305–320.
18. Powell A. Choosing the Right Oral Contraceptive Pill for Teens. Pediatr. Clin. North. Am. 2017;64:343–358.
19. Laura D. Lindberg, John S. Santelli, Sheila Desai. Changing Patterns of Contraceptive Use and the Decline in Rates of Pregnancy and Birth Among U.S. Adolescents, 2007–2014, Journal of Adolescent Health. 2018;63:253-256.
20. Damle LF, Gohari AC, McEvoy AK, Desale SY, Gomez-Lobo V. Early initiation of postpartum contraception: does it decrease rapid repeat pregnancy in adolescents? J Pediatr Adolesc Gynecol. 2015;28(1):57-62.

ORIGINAL SCIENTIFIC ARTICLE

# NUMBER AND DISTRIBUTION OF MAST CELLS IN REPRODUCTIVE SYSTEMS OF GRAVID AND NON-GRAVID FEMALE MICE

Mila Glavaski[1], Pavle Banovic[1,2] and Dusan Lalosevic[1,2]

[1] *University of Novi Sad, Faculty of Medicine, AP Vojvodina, Serbia*
[2]*Pasteur Institute in Novi Sad, AP Vojvodina, Serbia*

Received: 28.04.2019.
Accepted: 29.06.2019.

**Corresponding author:**

**Mila Glavski**

Faculty of Medicine, University of Novi Sad, AP Vojvodina, Serbia

E-mail: milaglavaski@yahoo.com

UDK: 612.014
Ser J Exp Clin Res 2022; 23(1): 67-73
DOI: 10.2478/sjecr-2019-0047

## ABSTRACT

*Mast cells are mainly distributed in tissues exposed to the external environment, but they are also found in ovaries, oviducts and uterus. We determined the difference in the number and distribution of Alcian Blue (+) and Safranine O (+) mast cells in reproductive systems of gravid and non-gravid female mice by histological examination. We showed that the number of mast cells is significantly higher in the reproductive system of gravid mice than in the reproductive system of non-gravid mice. Mast cells are unevenly distributed in ovaries, oviducts and uterus in both gravid and non-gravid mice. A large number of mast cells reside close to blood vessels throughout the entire reproductive system.*

**Keywords**: *mast cells, gestation, ovary, oviduct, uterus.*

## INTRODUCTION

Mast cells, the so-called unicellular glands, are mainly distributed in tissues exposed to the external environment, such as skin and airways (1). Each mast cell contains about 500,000 secretory granules that contain a large number of biologically active molecules (2). Mast cells are activated by allergens, anaphylatoxins (C3a, C5a), hormones, physical stimuli (pressure and temperature change), cytokines and neuropeptides (2).

Mast cell stimulation leads to the release of vasoactive and proinflammatory mediators (2). Some mediators are produced before stimulation and activation of mast cells and are kept in cytoplasmic granules: histamine, serotonin, heparin, tryptase, chymase, TNFα. Other mediators are synthesized *de novo* only when mast cells are stimulated and activated: leukotrienes, cytokines, and chemokines (1). Mast cells are able to selectively release the contents of individual granules or mediators without degranulation (like in the case of serotonin). That enables them to participate in many processes, without starting allergic or inflammatory reactions (2).

The difference in mast cells granules content is connected with their maturation: through the maturation of mast cells with tryptase granules only ($MC_T$), mast cells with both tryptase and chymase granules ($MC_{TC}$) are produced (3). Local factors cause mast cells to change their phenotype (4).

Uterine mast cells differ substantially from mast cells in other tissues (5). They hold 3-5% of the total endometrial cell number (6). Number, maturation and degranulation of mast cells are controlled by female sex hormones (1). The hormone modulation prepares the uterus for possible implantation (7).

The number of mast cells increases during the fertile period of the estrous cycle in mice and reaches its maximum during estrus when the female is sexually receptive, and when the endometrium is prepared for nidation. If fertilization does not occur, the number of mast cells decreases rapidly (8).

The number of mast cells in the uterus is relatively constant during the menstrual cycle. Mast cells are dispersed and moderately present in the uterus (9). They are placed in close proximity to fibroblasts and collagen fibers during the menstrual cycle, which may indicate that they have an important role in uterine tissue reconstitution (10). During the late secretory phase, extracellular tryptase expression increases, probably because of the intensification of mast cell activation during this period. Tryptase and other mast cells mediators (such as histamine, cytokines and growth factors) induce tissue edema and have a role in extracellular matrix degradation via proteolytic enzymes and metalloproteinases activation. Mast cell and metalloproteinases activity persist during the menstrual phase of the cycle. Metalloproteinases make the endometrial lining easier. However, most of the lining happens before menstrual bleeding - during the menstrual phase, when mechanisms of endometrial repair are already established (9).

After menopause, the number of mast cells declines in all parts of the uterus (10).

The application of luteinizing hormone (LH), follicle-stimulating hormone (FSH) or estradiol in mice increases mast cell degranulation in the ovaries (11). In the ovaries of rats, significantly larger number of mast cells are seen at estrus and diestrus. There is a possible involvement of mast cells products in vascularization of *corpora lutea* (12). Ovarian mast cells change their histamine content during the rat estrus cycle (11).

## AIM OF THE STUDY

The aim of this study was to determine the difference in the number and distribution of Alcian Blue (+) and Safranine O (+) mast cells in the reproductive systems of gravid and non-gravid NMRI mice.

## MATERIALS AND METHODS

### Experimental animals

The experimental group consisted of five adult NMRI mice: one male, and four non-gravid females. The control group consisted of four adult non-gravid female NMRI mice. Mice were bred at Pasteur Institute, Novi Sad, Serbia. Mice were housed under standard vivarium conditions: exposed to a 12:12-hour light:dark cycle, the ambient temperature of 25±2ºC, with food and water provided ad libitum.

The experiment was approved by the Ethical Committee of Pasteur Institute, Novi Sad, Serbia.

### Experiment

Four female mice from the experimental group were marked with a saturated picric acid water solution for proper identification and then placed in a cage with the male mouse. Every morning, vaginal flushes were performed, by pumping technique with distilled water. The flushes were used for smear preparation, fixed with methanol, and then stained with Eriochrome cyanine R-Eosin Y method by Stefanović and coauthors (13). The day when the smear was sperm positive was considered as the zero-day of the experiment. 10 days later, female mice were sacrificed by cervical dislocation. Ovaries, oviducts and uteri were dissected out, examined macroscopically, and fixed in 10% formalin. After gradient ethanol dehydration and xylene clearing, the organs were molded into paraffin, and 7µm slices were cut using Leica RT350 rotary microtome. The slices were deparaffinized by heating to 60ºC and then stained with Alcian Blue and Safranine O. Alcian Blue-Safranin O staining was conducted according to the protocol of Tas and coauthors (14).

The experiment was conducted in the laboratory of Pasteur Institute, Novi Sad, Serbia.

**Analysis**

Histological examination was performed using Leica DM 2500 light microscope with a camera connected to a computer and it included morphological analysis and description using free software ImageJ. In every group, mast cell presence was analyzed in 15 high-power fields (HPF) at a magnification $^{x}$ 400.

Results from the experimental and control group were compared using two-tailed Student t-test; a significant difference was considered at $p<0.05$.

**Chemicals**

- DPX mountant for histology- Fluka, Sigma-Aldrich Chemie GmbH, Germany
- Picric acid ($(O_2N)_3C_6H_2OH$)- Fluka, Sigma-Aldrich Chemie GmbH, Germany
- Formalin (37% formaldehyde solution) - Centrohem, Stara Pazova, Serbia.
- 70%, 80%, 90%, 96%, and absolute ethanol- Centrohem, Stara Pazova, Serbia
- Xylene, HCl, FeCl3·6H20 - Centrohem, Stara Pazova, Serbia
- Alcian Blue 8GX (Sigma-Aldrich Chemie GmbH, Germany, 861006), as 0.5%(w/v) stain powder solution, and 3% (v/v) acetic acid solution, pH=2.4
- Safranine O (Sigma-Aldrich Chemie GmbH; Germany; 50240), as 0.3%(w/v) solution with dissolvent 0.125M HCl, pH=0.9
- Eosin Y (Fluka Sigma-Aldrich Chemie GmbH, Germany; HT110116), as 0.5%(w/v) ethanol solution.

Eriochrome cyanine R working solution was prepared as follows: 450 ml distilled water was acidified by HCl to pH 1.5, 1 g of Eriochrome cyanine R powder (Magnacol Ltd.; Wales, Great Britain) and 1.12 g FeCl3·6H20 were added to the solution, followed by mixing and filtering. Water was added to a final volume of 500 ml. The pH of the final solution was adjusted to 1.5.

Distilled water was prepared in Pasteur Institute, Novi Sad, Serbia, cooled to 25ºC and buffered by ion exchange resin.

## RESULTS

During histological preparations, Alcian Blue (+) mast cells and Safranine O (+) mast cells were detected in both experimental and control group. They preserved their structure and were unevenly distributed in the tissue - individually or in small groups. Their shape ranged from spherical to oval and slightly spindle. Intracellular metachromatic granules were detected in mast cells, but their nuclei were poorly marked. In some places, mast cell degranulation was observed (Figures 1 and 2).

In both experimental and control group, mast cells were found in the ovaries - in interstitial stroma and medulla, and in follicles and cortex. In oviducts of the experimental females, Alcian Blue (+) mast cells were observed. However, Safranine O (+) mast cells were absent or detected in a small number. In uteri, mast cells were distributed around uterine glands, in basal and deeper layers of endometrial stroma, and also in the myometrium, where they were predominantly detected in close proximity to smooth muscle cells in both experimental and control group. A large number of mast cells were found around blood vessels throughout the entire reproductive tract (Figure 3).

A highly significant difference between the mean number of mast cells in the experimental and the control group ($p<0.001$) has been found, with a significantly higher number of mast cells in the reproductive systems of the experimental group (Table 1, Figures 4 and 5).

**Figure 1.** a: Perivascular Safranine O (+) mast cell are marked with pointed arrow in uterus of control group. b: Alcian Blue (+) mast cells are marked with arrows, degranulated mast cells are marked with 5-point stars in uterus of experimental group (Alcian Blue-Safranine O staining, x400)

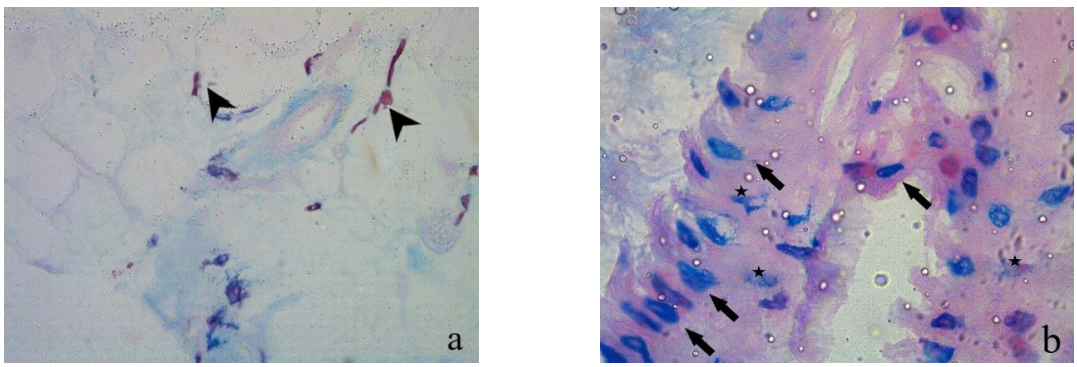

**Figure 2.** a: Safranine O (+) mast cell are marked with pointed arrow in uterus of control group. b: Alcian Blue (+) mast cells are marked with arrows, Safranine O (+) mast cell are marked with pointed arrow, degranulated mast cells are marked with 5-point stars in uterus of experimental group (Alcian Blue-Safranine O staining, x 400)

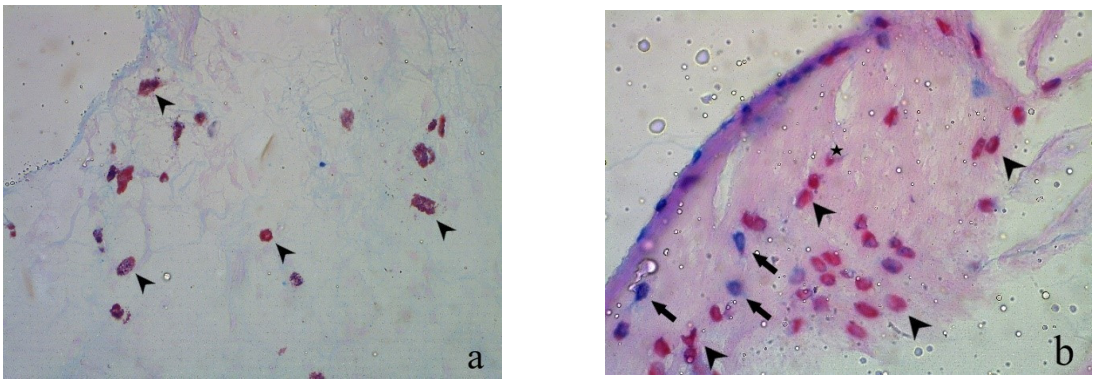


**Figure 3.** a,b: Distribution and density of the mast cells in the uterus tissue of the control group. Presence of mast cells is noticed in extremely small number, where the highest percentage is taken by Safranine O (+) mast cells; note Safranine O (+) cells surrounding blood vessels marked with X. c,d: Distribution and density of mast cells in the experimental group in the uterine tissue. Note the presence of a large number of Alcian Blue (+) and Safranine O (+) mast cells, unevenly distributed, presented individually or in groups; note majority of Alcian (+) cells surrounding blood vessels marked with X (Alcian Blue-Safranine O staining, x 200)

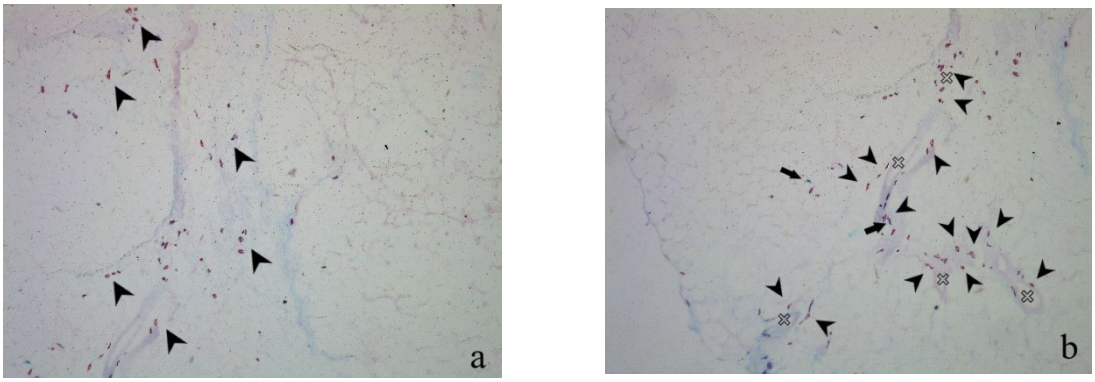


**Figure 4.** Comparison of Alcian blue (+) mast cells mean number in the control and the experimental group per HPF. Significantly higher number of Alcian blue (+) mast cells was found in each analyzed reproductive organ of gravid mice

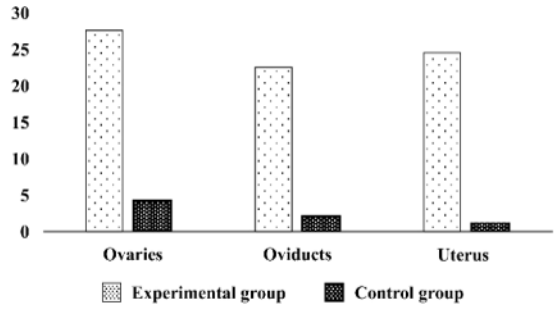


**Figure 5.** Comparison of Safranine O (+) mast cells mean number in control and experimental group per HPF. Significantly higher number of Safranine O (+) mast cells was found in each analyzed reproductive organ of gravid mice.

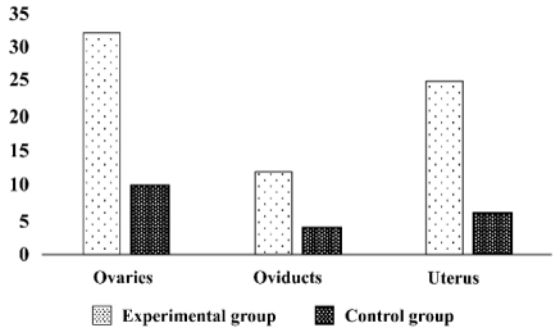

**Table 1**. Mast cell count (stated as mean±SD) in 15 high-power fields (x400). Each preparation included ovaries, oviducts, and uterus.

| | Experimental group | Control group |
|---|---|---|
| **Alcian Blue (+)** | 26.40±6.47 | 2.20±2.46 |
| **Safranine O (+)** | 18.33±6.16 | 6.00±5.41 |

## DISCUSSION

In this study, we determined the difference in the number and distribution of Alcian Blue (+) and Safranine O (+) mast cells in the reproductive systems of non-gravid and gravid NMRI mice. Alcian Blue (+) mast cells and Safranine O (+) mast cells were detected in both non-gravid and gravid NMRI mice, but a substantially larger number of mast cells was present throughout the reproductive systems of gravid mice. In comparison with non-gravid mice, a larger number of mast cells was also found in each analyzed organ of gravid mice - ovary, oviduct and uterus. The observed presence of mast cells indicates their probable role in the homeostasis of a non-gravid reproductive system. Larger number of mast cells in the reproductive systems of gravid mice could mean that mast cells have an important physiological role in the reproductive system during gestation. Their abundance could also be explained by changing levels of female sex hormones during pregnancy, which affect the number, maturation and degranulation of mast cells. Mast cells are fruitful sources of biologically active molecules, which could mediate, determine, or enable processes in the reproductive tract during pregnancy. The magnitude of increase of mast cells' number in ovaries, oviducts and uteri might reflect their importance in those organs during pregnancy. We found a large number of mast cells around blood vessels in the reproductive systems of gravid mice. Mast cells might contribute to angiogenesis in the reproductive system during pregnancy and that could be a reason for their proximity to blood vessels. We observed mast cell degranulation in uteri of gravid mice, which showed that some of the mast cells had been activated.

Woidacki and coauthors previously showed that uterine mast cell number increases in mice if gestation takes place and stays high (higher than in estrus) during pregnancy. In abortus-prone gravid mice, the number of mast cells in the gravid uterus is similar to the number of mast cells in metestrus (and is far smaller than in normal pregnancies). The same study showed that during the middle of pregnancy, mast cells are numerous on the maternal side of the feto-maternal barrier and are usually close to blood vessels. Detailed characterization of mast cells in uterus showed that it is a heterogenic population consisting of connective tissue mast cells and mucosal mast cells, and also mast cells in different phases of differentiation and transdifferentiation. Mast cells in the uterus are mast cells protease 8 (Mcpt8) and CD117 positive, and 5-20% of mast cells in the uterus are also mast cells protease 5 (Mcpt5) positive (8). Padilla and coauthors found that mast cells are more numerous in myometrium than in endometrium in pregnant mice uteri (15).

Batth and coauthors showed that in the ovaries of rats, the number of mast cells was high during gestation, with a positive correlation between mast cell count and embryo number. After parturition, the mast cell count declined significantly (12). During late gestation, mast cells activation led to angiogenesis in the cervix of the rat. Mast cells degranulation modulated cervix contractility in guinea pigs (2).

Jeziorska and coauthors conducted a study on 107 women during normal menstrual cycle. There was a similar number of mast cells in the functional and basal endometrial layers and in the myometrium (16). In the study of De Leo and coauthors in tissue samples of 20 women, mast cells with both tryptase and chymase expression were identified in all three layers of the non-gravid uterus. In the same study, in the basal endometrium and myometrium, rare mast cells with chymase expression only (without tryptase expression), $MC_C$, were found (17). Mori and coauthors in a study on 24 non-pregnant women with different gynecological disorders observed that mast cells were located mainly in the inner half of the myometrium and the majority of them were $MC_T$ (18). According to Gomez-Lopez and coauthors in humans, mast cells count is higher in gravid than in non-gravid uteri (19). Ivanišević and coauthors showed that the number of tryptase-positive mast cells in the myometrium of the non-gravid human uterus was significantly higher than in the myometrium of the gravid uterus (20). Garfield and coauthors showed that the number of mast cells in the myometrium was higher during human pregnancy, with more $MC_T$ than $MC_{TC}$ (21).

During degranulation, mast cells release various mediators that are very important for embryo implantation (such as histamine, proteases, metalloproteinases, and proangiogenic factors) (1). Angiogenesis and tissue remodeling are necessary for successful implantation. Many mediators involved in those processes are synthesized in mast cells (8). Histamine causes muscle contraction, exocrine glands cause secretion and vasodilatation (2). Histamine created in the uterus is a key regulator of implantation due to its ability to influence vascular permeability and induce decidualization. Before the implantation, human embryos provoke histamine release by histamine-releasing factor secretion (7). Mast cells and their products regulate trophoblast invasion and growth (3).

Mast cells in uteri positively affect placentation, spiral artery remodeling, size of the placenta and fetal growth. Spiral artery remodeling is necessary for oxygen and nutrients delivery to the fetus. Inadequate spiral artery remodeling is

associated with preeclampsia, slower fetal growth, miscarriages and preterm deliveries (22).

Mast cells affect the myometrium by proliferation and smooth muscle cell regulation (3). They play a central role in the initiation and progression of uterine contractions. Their activation increases contractility of the myometrium (2). Pregnant women with systemic mastocytosis or asthma often give birth before the term (8). In strong allergic reactions, there is a sufficient degree of mast cells activation to induce preterm labor. If antihistamines and steroid drugs are given, uterine contractions stop. During anaphylaxis, strong contractions of the uterus occur as a result of mast cells degranulation (3).

An especially large number of mast cells in the uterus is placed in close proximity to nerves, blood or lymph vessels (23). Stress significantly increases the number of mast cells in pregnant mice uteri (for about 55.6-76.9%) (24).

According to some authors, estrogens and progesterone are able to attract mast cells in the uterus *in vitro* and *in vivo* (4), individually and in combination, by modulation of receptor expression for chemokines on their surface (7). If ovaries are removed from mice, estradiol and progesterone are almost absent, and those mice have a lower number of mast cells compared to control (mice that do have ovaries). When mice without ovaries receive estradiol replacement or combination of estradiol and progesterone, the number of mast cells reaches control level. Application of these hormones also increases expression of mast cells proteases in the uterus and increases the degranulation degree (1).

Human mast cells express estrogen receptors and their activation increases mast cells stimulation and degranulation. Human mast cells express receptors for progesterone and testosterone, but activation of these receptors has an inhibitory effect (2). Progesterone prevents mast cells migration in response to chemokines, e.g. downregulates the expression of superficial chemokines receptors. Progesterone inhibits secretion of histamine from mast cells. It is possible that mast cells during pregnancy are inhibited by high levels of progesterone, and that transit of mast cells from circulation to uterus is limited. As the term of delivery approaches, functional sensitivity on estrogens is higher than on progesterone, and that is the reason why estrogens' effect on mast cells dominate (3). Estradiol and progesterone dose-dependently increase degranulation level in immature mast cells *in vitro*. The combination of these two hormones significantly increases degranulation compared to situations when each hormone is applied individually (7).

Corticotropin-releasing hormone (CRH) might be involved in endometrial mast cell activation (3).

Mast cells create and release galectin-1. It mediates fetal growth and aids in placentation, angiogenesis, syncytium synthesis, and trophoblast growth (8).

Myometrial stretching during fetal growth causes release of stem cell factor (SCF) and other chemokines, which attract mast cells progenitors and mature mast cells from the blood. Possibly, the release of mast cells mediators causes migration of other immune cells to the uterus (3). A high level of tryptase is associated with spontaneous abortions, probably as a result of inflammation induction. A high level of chymase is associated with severe preeclampsia. In the case of preeclampsia, the placenta contains high concentrations of histamine and a high number of mast cells (3). Decreasing the number of mast cells during pregnancy could prevent the creation of a critical quantity of proinflammatory mediators which induce preterm delivery. Since human myometrium sensitivity to mast cells mediators increases towards the end of pregnancy, the myometrium might be stimulated even if mast cells density is low (20).

Mast cells tryptase is a potent angiogenic factor (25). Chymase contributes to matrix degradation, tissue remodeling and angiogenesis (2). Chymase is also a potent proinflammatory mediator (26). Mast cells are involved in angiogenesis. Their accumulation is found in many conditions such as tumor growth, rheumatoid arthritis, ovulation, wounds healing and tissue renewal. Mast cells metalloproteinases degrade connective tissue to make space for neovascularization onset (10). *In vivo* exposition to mast cells stabilizers, which inhibit their degranulation, decreases uterine endothelial cells proliferation and vascular endothelial growth factor A (VEGF-A) secretion (8).

A limitation of this study was sample size. All our conclusions were based on one experiment with 9 mice. However, the difference observed between the number of mast cells in reproductive systems of gravid and non-gravid female mice was so significant that the sample size should not affect the study's findings. In addition, our results are in line with other published studies of mast cells' number and distribution in reproductive systems during pregnancy. The small sample size in our study opens a possibility for larger studies to validate our findings. Likewise, more research about the role of mast cells in the gravid and non-gravid uterus is needed, including examination of the molecular mechanisms of their activity. The definitive role of mast cells during successful and pathological pregnancy remains to be determined.

## CONCLUSION

The number of mast cells is significantly higher in the reproductive systems of gravid mice than in the reproductive systems of non-gravid mice. Mast cells are unevenly distributed in ovaries, oviducts and uteri in both gravid and non-gravid mice. A large number of mast cells reside close to blood vessels throughout the entire reproductive system.

## ACKNOWLEDGMENT

The authors would like to thank Michelle Li for proofreading the paper.

## REFERENCES


1. Zierau O, Zenclussen AC, Jensen F. Role of female sex hormones, estradiol and progesterone, in mast cell behavior. Front Immunol 2012; 3: 169.
2. Theoharides TC, Stewart JM. Genitourinary mast cells and survival. Transl Androl Urol 2015; 4(5): 579-86.
3. Menzies FM, Shepherd MC, Nibbs RJ, Nelson SM. The role of mast cells and their mediators in reproduction, pregnancy and labour. Hum Reprod Update 2011; 17(3): 383-96.
4. Woidacki K, Jensen F, Zenclussen AC. Mast cells as novel mediators of reproductive processes. Front Immunol 2013; 4: 29.
5. Zenclussen AC, Hämmerling GJ. Cellular regulation of the uterine microenvironment that enables embryo implantation. Front Immunol 2015; 6: 321.
6. Lee SK, Kim CJ, Kim DJ, Kang JH. Immune cells in the female reproductive tract. Immune Netw 2015; 15(1): 16-26.
7. Jensen F, Woudwyk M, Teles A, Woidacki K, Taran F, Costa S, et al. Estradiol and progesterone regulate the migration of mast cells from the periphery to the uterus and induce their maturation and degranulation. PLoS ONE 2010; 5(12): e14409.
8. Woidacki K, Popovic M, Metz M, Schumacher A, Linzke N, Teles A, et al. Mast cells rescue implantation defects caused by c-kit deficiency. Cell Death Dis 2013; 4(1): e462.
9. Berbic M, Fraser IS. Immunology of normal and abnormal menstruation. Womens Health (Lond) 2013; 9(4): 387-95.
10. Pansrikaew P, Cheewakriangkrai C, Taweevisit M, Khunamornpong S, Siriaunkgul S. Correlation of mast cell density, tumor angiogenesis, and clinical outcomes in patients with endometrioid endometrial cancer. Asian Pac J Cancer Prev 2010; 11(2): 309-12.
11. Theoharides TC. Neuroendocrinology of mast cells: challenges and controversies. Exp Dermatol 2017; 26(9): 751-9.
12. Batth BK, Parshad RK. Mast cell dynamics in the house rat (Rattus rattus) ovary during estrus cycle, pregnancy and lactation. Eur J Morphol 2000; 38(1): 17-23.
13. Stefanović D, Stefanović M, Lalošević D. Use of eriochrome cyanine R in routine histology and histopathology: is it time to say goodbye to hematoxylin? Biotech Histochem 2015; 90(6): 461-9.
14. Tas J. The Alcian Blue and combined Alcian Blue-Safranin O staining of glycosaminoglycans studied in a model system and in mast cells. Histochem J 1977; 9(2): 205-30.
15. Padilla L, Reinicke K, Montesino H, Villena F, Asencio H, Cruz M, et al. Histamine content and mast cells distribution in mouse uterus: the effect of sexual hormones, gestation and labor. Cell Mol Biol 1990; 36: 93-100.
16. Jeziorska M, Salamonsen LA, Woolley DE. Mast cell and eosinophil distribution and activation in human endometrium throughout the menstrual cycle. Biol Reprod 1995; 53(2): 312-20.
17. De Leo B, Esnal-Zufiaurre A, Collins F, Critchley HOD, Saunders PTK. Immunoprofiling of human uterine mast cells identifies three phenotypes and expression of ERβ and glucocorticoid receptor. F1000Res 2017; 6: 667.
18. Mori A, Zhai YL, Toki T, Nikaido T, Fujii S. Distribution and heterogeneity of mast cells in the human uterus. Hum Reprod 1997; 12(2): 368-72.
19. Gomez-Lopez N, StLouis D, Lehr MA, Sanchez-Rodriguez EN, Arenas-Hernandez M. Immune cells in term and preterm labor. Cell Mol Immunol 2014; 11(6): 571-81.
20. Ivanisevic M, Segerer S, Rieger L, Kapp M, Dietl J, Kämmerer U, et al. Antigen-presenting cells in pregnant and non-pregnant human myometrium. Am J Reprod Immunol 2010; 64(3): 188-96.
21. Garfield RE, Irani AM, Schwartz LB, Bytautiene E, Romero R. Structural and functional comparison of mast cells in the pregnant versus nonpregnant human uterus. Am J Obstet Gynecol 2006; 194(1): 261-7.
22. Woidacki K, Meyer N, Schumacher A, Goldschmidt A, Maurer M, Zenclussen AC. Transfer of regulatory T cells into abortion-prone mice promotes the expansion of uterine mast cells and normalizes early pregnancy angiogenesis. Scientific Reports [Internet] 2015 Nov [cited 2019 Feb 20]; 5(1). Available from: http://www.nature.com/articles/srep13938
23. Alan E, Liman N. Involution dependent changes in distribution and localization of bax, survivin, caspase-3, and calpain-1 in the rat endometrium. Microsc Res Tech 2016; 79(4): 285-97.
24. Liu G, Dong Y, Wang Z, Cao J, Chen Y. Restraint stress alters immune parameters and induces oxidative stress in the mouse uterus during embryo implantation. Stress 2014; 17(6): 494-503.
25. Goksu Erol AY, Tokyol C, Ozdemir O, Yilmazer M, Arioz TD, Aktepe F. The role of mast cells and angiogenesis in benign and malignant neoplasms of the uterus. Pathol Res Pract 2011; 207(10): 618-22.
26. Paula R, Oliani AH, Vaz-Oliani DCM, D'Ávila SCGP, Oliani SM, Gil CD. The intricate role of mast cell proteases and the annexin A1-FPR1 system in abdominal wall endometriosis. J Mol Histol 2015; 46(1): 33-43.

ORIGINAL SCIENTIFIC ARTICLE

# EXO-D-MAPPS ATTENUATES PRODUCTION OF INFLAMMATORY CYTOKINES AND PROMOTED GENERATION OF IMMUNOSUPPRESSIVE PHENOTYPE IN PERIPHERAL BLOOD MONONUCLEAR CELLS

Carl Randall Harrell[1], Bojana Simovic Markovic[2], Crissy Fellabaum[1], Dragica Miloradovic[2], Aleksandar Acovic[3], Dragana Miloradovic[4], Nebojsa Arsenijevic[2] and Vladislav Volarevic[2]

*[1]Regenerative Processing Plant, LLC, Palm Harbor, Florida, United States of America*
*[2]University of Kragujevac, Faculty of Medical Sciences, Department of Microbiology and Immunology, Center for Molecular Medicine and Stem Cell Research, Kragujevac, Serbia*
*[3]University of Kragujevac, Faculty of Medical Sciences, Department of Dentistry, Kragujevac, Serbia*
*[4]University of Kragujevac, Faculty of Medical Sciences, Department of Genetics, Kragujevac, Serbia*

Received: 14.08.2019.
Accepted: 31.08.2019.

**Corresponding author:**

**PhD Vladislav Volarevic**

University of Kragujevac, Faculty of Medical Sciences
Department of Microbiology and Immunology,
Center for Molecular Medicine and Stem Cell Research
69 Svetozara Markovica Street, 34000 Kragujevac,
Serbia

Phone: +38134306800
E-mail: drvolarevic@yahoo.com

sciendo

UDK: 602.9
Ser J Exp Clin Res 2022; 23(1): 75-82
DOI: 10.2478/sjecr-2019-0045

## ABSTRACT

*Mesenchymal stem cells (MSCs) produce immunomodulatory factors that regulate production of cytokines and chemokines in immune cells affecting their functional properties. Administration of MSCs-sourced secretome, including MSC-derived conditioned medium (MSC-CM) and MSC-derived exosomes (MSC-Exos), showed beneficial effects similar to those observed after transplantation of MSCs. Due to their nano-size dimension, MSC-Exos easily penetrate through the tissue and in paracrine and endocrine manner, may deliver MSC-sourced factors to the target immune cells modulating their function. MSCs derived from amniotic fluid (AF-MSCs) had superior cell biological properties than MSCs derived from bone marrow. We recently developed "Exosomes Derived Multiple Allogeneic Proteins Paracrine Signaling (Exo-d-MAPPS)", a biological product in which the activity is based on AF-MSC-derived Exos capable to deliver immunomodulatory molecules and growth factors to the target cells. Herewith, we analyzed immunosuppressive capacity of Exo-d-MAPPS against human peripheral blood mononuclear cells (pbMNCs) and demonstrated that Exo-d-MAPPS efficiently suppressed generation of inflammatory phenotype in activated pbMNCs. Exo-d-MAPPS attenuated production of inflammatory cytokines and promoted generation of immunosuppressive phenotype in Lipopolysaccharide-primed pbMNCs. Exo-d-MAPPS treatment reduced expansion of inflammatory Th1 and Th17 cells and promoted generation of immunosuppressive T regulatory cells in the population of Concanavalin A-primed pbMNCs. Similarly, Exo-d-MAPPS treatment suppressed pro-inflammatory and promoted anti-inflammatory properties of α-GalCer-primed pbMNCs. In summing up, due to its capacity for suppression of activated pbMNCs, Exo-d-MAPPS should be further explored in animal models of acute and chronic inflammatory diseases as a potentially new remedy for the attenuation of detrimental immune response.*

***Keywords***: *mesenchymal stem cells, amniotic fluid, secretome, immunosuppression, mononuclear cells.*

## INTRODUCTION

Mesenchymal stem cells (MSCs) are the plastic adherent, fibroblast-like multipotent cells capable to self-renew and under appropriate culture conditions, differentiate into cells of the mesodermal, endodermal and ectodermal lineage (1-4). MSCs are present in virtually all postnatal tissues and organs and after isolation (from the bone marrow, umbilical cord blood, placenta, adipose tissue, amniotic fluid, Wharton's jelly) may be easily propagated to reach appropriate cell number for autologous or allogeneic transplantation (2, 3). Therefore, large number of experimental and clinical studies indicated that MSCs could be considered as new remedy in cell-based therapy of degenerative diseases (5).

Additionally, MSCs are able to modulate phenotype of immune cells and may suppress detrimental, local and systemic immune response (6). In juxtacrine, the cell to cell contact-dependent manner and paracrine manner (through the production of soluble mediators), MSCs alter the function of all immune cells (macrophages, dendritic cells (DCs), natural killer (NK), natural killer T cells (NKT), T and B lymphocytes) that have essential role in the pathogenesis of autoimmune, acute and chronic inflammatory diseases (7-9).

Production of immunoregulatory factors in MSCs and their capacity for immunosuppression was identified by Haynesworth and co-workers (10). They reported that MSCs produce and release a broad repertoire of growth factors, chemokines, and cytokines that modulate production of inflammatory cytokines in immune cells affecting their functional properties (10). Additionally, further studies revealed that MSC-sourced factors promote neo-angiogenesis, reduce apoptosis and enhance survival of parenchymal cells, regulate remodeling of extracellular matrix and prevent fibrosis in injured tissues, enabling the enhanced tissue repair and regeneration (11, 12).

Among immunomodulatory factors, MSCs produce transforming growth factor-β (TGF-β), hepatic growth factor (HGF), nitric oxide (NO), indolamine 2,3-dioxygenase (IDO), IL-10, IL-6, leukocyte inhibitory factor (LIF), IL-1 receptor antagonist (IL-1Ra), tumor necrosis factor a-stimulated gene 6 (TSG-6), human leukocyte antigen-G (HLA-G), hemeoxygenase-1 (HO-1), and prostaglandin E2 (PGE2) (6, 13, 14). Therefore, local as well as systemic administration of MSCs-sourced secretome, including MSC-derived conditioned medium (MSC-CM) and MSC-derived exosomes (MSC-Exos), showed beneficial effects similar to those observed after transplantation of MSCs. Due to their nano-size dimension, MSC-Exos easily penetrate through the tissue and in paracrine and endocrine manner, deliver MSC-sourced factors to the target immune cells modulating their function (15).

Several lines of evidence suggested that MSCs derived from amniotic fluid (AF-MSCs) had superior cell biological properties than MSCs derived from the bone marrow (BM-MSCs) (16-19). Roubelakis and colleagues revealed that AF-MSCs have 78 unique proteins which are responsible for their increased proliferation rate and plasticity (20). Furthermore, AF-MSCs more efficiently suppressed detrimental T cell-driven immune response than BM-MSCs (21). In line with these findings, we recently developed: "Exosomes Derived Multiple Allogeneic Proteins Paracrine Signaling (Exo-d-MAPPS)", a biological product in which activity was based on AF-MSC-derived Exos capable of delivering immunomodulatory molecules and growth factors to the target cells (22). Herewith, we analyzed immunosuppressive capacity of Exo-d-MAPPS against activated human peripheral blood mononuclear cells (pbMNCs) and demonstrated that Exo-d-MAPPS efficiently down-regulated production of inflammatory cytokines and enhanced production of immunosuppressive cytokines in pbMNCs, suggesting its potential therapeutic use in the treatment of acute and chronic inflammatory diseases.

## MATERIALS AND METHODS

### Preparation of AF and Exo-d-MAPPS samples

Amniotic fluid and tissues were collected from healthy, full-term, scheduled cesarean sections. Samples of collected material were tested by laboratories certified under the Clinical Laboratory Improvement Amendments (CLIA) and were found negative using United States (U.S) Food and Drug Administration (FDA) licensed tests for detection of at minimum: Hepatitis B Virus, Hepatitis C Virus, Human Immunodeficiency Virus Types 1/2, Treponema Pallidum. All samples were obtained with patient consent as well as institutional ethical approval, as previously described (23). Exo-d-MAPPS samples were engineered as AF-derived sterile product containing AF-MSC-Exos, manufactured under current Good Manufacturing Practices (cGMP), regulated and reviewed by the FDA (22). Sterile Exo-d-MAPPS incorporate Regenerative Processing Plant's (RPP) proprietary patented sterilization process to provide for a safe, sterile product. Exo-d-MAPPS samples, used in this study, were manufactured under specific conditions in order to be applicable for bioavailability testing and for different therapeutic use.

### Isolation of pbMNCs

Serum samples (2 ml) were obtained from healthy volunteers at the Center for Molecular Medicine and Stem Cell Research, the Faculty of Medical Sciences of the University of Kragujevac, and pbMNCs were isolated by the use of Histopaque (Sigma-Aldrich, Munich, Germany) density gradient centrifugation. Briefly, the serum was diluted by equal volume of Dulbecco's modified Eagle's medium (DMEM) supplemented with 10% fetal bovine serum, 2 mmol/L of L- glutamine, 1 mmol/L penicillin-streptomycin, and 1 mmol/L of mixed nonessential amino acids, (Sigma Aldrich, Munich, Germany). Heparinized peripheral blood (10 ml) was centrifuged at 400 g for 10 min to separate plasma and cells. Lymphocyte separation liquid (3 ml) was filled into a 10-ml centrifuge tube. After 10 min, the mononuclear cell layer was transferred to a sterile tube by a fresh sterile pipette (capillary tube), gently mixed with five volumes of DMEM and

centrifuged at 2700 r/min for 20 min, then washed with DMEM twice. After the supernatant was discarded, cells were resuspended in DMEM containing the 10% fetal bovine serum (Gibco, United States) for lymphocyte count. Then the cell suspensions were diluted to $1^x10^6$ cells/ml for further *in vitro* experiments.

**Activation of pbMNCs**

After isolation, pbMNCs were plated in a 24-well plate ($1^x10^6$ cells per well) and subsequently primed with 10 ng/ml Lipopolysaccharides (LPS) (24), or 5 μg/ml Concanavalin A (Con A)-potent activator of T cells (25), or 100 ng/ml of alpha galactosyl ceramide (α-GalCer)-selective stimulator of NKT cells (8, 25, 26). Isolated pbMNCs were cultured in complete DMEM for 48h in the presence or in the absence of Exo-d-MAPPS and AF. After 48 hours of culture, activated pbMNCs were harvested for the ELISA assay or flow cytometry.

**Measurement of cytokines in supernatants**

The ELISA assay was conducted according to the handbook provided by the ELISA kit (R&D Systems Minneapolis, MN for IL-12, IL-17 and IL-10; BD Biosciences San Diego, CA for IFN-γ). The optical density of each sample at 450 nm was detected by an ELISA microplate reader (Zenyth, 3100) and the concentrations of IL-12, IL-17, IFN-γ and IL-10 levels in supernatants were determined.

**Flow cytometry analysis of pbMNCs**

To detect the cell surface expression of a variety of molecules, isolated pbMNCs were analyzed by the flow cytometry (FACS) using standard staining methods (27). Briefly, the prepared cell suspension fluid (1 ml) was centrifuged at 250 g for 5 min and rinsed twice with suspension fluid. The supernatant was discarded and cells were suspended with PBS to 10 μl, adding human CD14, CD56, HLA-DR and CD4 antibody conjugated with fluorescein isothiocyanate (FITC; BD Biosciences, Franklin Lakes, NJ), phycoerythrin (PE; BD Biosciences) or allophycocyanin (APC; BD Biosciences or isotype-matched controls (BD Pharmingen/BioLegend) (about 1.25 μg, suggested by the manual) respectively, and incubated at 4°C in the dark for 30 min. Then, the cell suspension was supplemented with 2 ml PBS, centrifuged at 250 g 5 minutes, and washed with suspension fluid followed by staining with flow cytometry staining buffer. For the intracellular staining, cells were previously stimulated with phorbol myristate acetate (PMA) and ionomycin for 4 h at 37 °C with the addition of 1 μg/mL Golgi plug. Intracellular staining for forkhead box P3 (Foxp3), IL-10, tumor necrosis factor alpha (TNF-α), IL-17, interferon gamma (IFN-γ) was performed using the BD Bioscience fixation/permeabilization buffer kit. Flow cytometric analysis was conducted on a BD Biosciences FACSCalibur and analyzed by the application of the flowing software analysis program.

**Statistical analysis**

Results were analyzed using the Student's t test. All data in this study were expressed as the mean ± standard error of the mean (SEM). Values of $p<0.05$ were considered as statistically significant.

## RESULTS

Exo-d-MAPPS attenuated production of inflammatory cytokines and promoted generation of immunosuppressive phenotype in LPS-primed pbMNCs

LPS significantly enhanced production of inflammatory IL-12 in pbMNCs (Fig.1A). Exo-d-MAPPS significantly attenuated concentration of IL-12 in supernatants of LPS-primed pbMNCs (Fig.1A). Importantly, both room temperature (RT) and fridge (4°C) stored Exo-d-MAPPS suppressed production of IL-12 more efficiently than RT and 4°C stored AF (Fig.1A). Since LPS mainly activates CD14-expressing macrophages, we analyzed whether Exo-d-MAPPS affected percentage of this cell population. As it is shown in Fig.1B, the percentage of LPS-primed pbMNCs that expresses CD14 was significantly lower after Exo-d-MAPPS treatment. Additionally, Exo-d-MAPPS down-regulated expression of HLA-DR molecule and production of inflammatory TNF-α in CD14-expressing pbMNCs (Fig.1C-D). In similar manner as it was observed in the attenuation of IL-12 production, Exo-d-MAPPS-treated LPS-primed CD14+pbMNCs produced lower amount of TNF-α than AF-treated LPS-primed CD14+pbMNCs (Fig. 1C-D). In line with these findings, Exo-d-MAPPS treatment induced generation of immunosuppressive phenotype in LPS-primed CD14+pbMNCs (Fig.1E). Significantly higher percentage of IL-10-producing CD14+ cells and significantly higher concentration of IL-10 was observed in supernatants of Exo-d-MAPPS treated LPS-primed pbMNCs than in supernatants of AF-treated LPS-primed pbMNCs (Fig.1E)

Exo-d-MAPPS treatment reduced expansion of inflammatory Th1 and Th17 cells and promoted generation of immunosuppressive Tregs in the population of Con A-primed pbMNCs

Con A treatment induced expansion of CD4+ cells and, particularly, inflammatory, IFN-γ-producing Th1 and IL-17-producing Th17 CD4+ T cells within the population of pbMNCs (Fig.2A-C). Exo-d-MAPPS significantly attenuated expansion of CD4+ cells and alleviated production of IFN-γ and IL-17 in Con A-primed CD4+ T cells (Fig.2A-C). Importantly, treatment with either RT or 4°C stored Exo-d-MAPPS more efficiently reduced expansion of inflammatory Th1 and Th17 cells than AF (Fig.2A-C), indicating superior immunosuppressive properties of Exo-d-MAPPS over AF. Additionally, Exo-d-MAPPS promoted generation of immunosuppressive phenotype in CD4-expressing pbMNCs, as evidenced by higher percentage of FoxP3-expressing and IL-10-producing CD4+ cells in the population of Exo-d-MAPPS-treated Con A-primed pbMNCs compared to Con A-only and AF+Con A-treated pbMNCs (Fig.2D-E). In line

with these findings, significantly lower concentration of IL-17 and higher concentration of IL-10 were noticed in supernatants of Exo-d-MAPPS+Con A-treated pbMNCs compared to Con A-only and AF+Con A-treated pbMNCs (Fig.2F-G).

Exo-d-MAPPS treatment suppressed pro-inflammatory and promoted anti-inflammatory properties of α-GalCer-primed pbMNCs

As it is shown in Fig.3A, α-GalCer treatment stimulated expansion of inflammatory, IFN-γ-producing and IL-17-producing CD56-expressing cells within population of pbMNCs. Both RT and 4°C stored Exo-d-MAPPS more efficiently reduced proliferation of IFN-γ-producing and IL-17-producing CD56+ cells than RT or 4°C stored AF (Fig.3B-C). In similar manner as it was observed with Con A-primed pbMNCs, Exo-d-MAPPS treatment promoted generation of immunosuppressive phenotype in α-GalCer-activated pbMNCs (Fig.3D-E). Significantly higher percentage of FoxP3-expressing and IL-10-producing CD56+cells were observed in the population of α-GalCer+Exo-d-MAPPS-treated pbMNCs than in α-GalCer-only and α-GalCer+AF treated pbMNCs (Fig.3D-E). In line with these findings, significantly lower concentration of immunosuppressive IL-10 was measured in supernatants of α-GalCer+Exo-d-MAPPS-treated pbMNCs than in supernatants of α-GalCer-only and α-GalCer+AF-treated pbMNCs (Fig.3F).

**Figure 1.** Exo-d-MAPPS decreased production of proinflammatory cytokines and promoted generation of immunosuppressive phenotype in LPS-primed pbMNCs

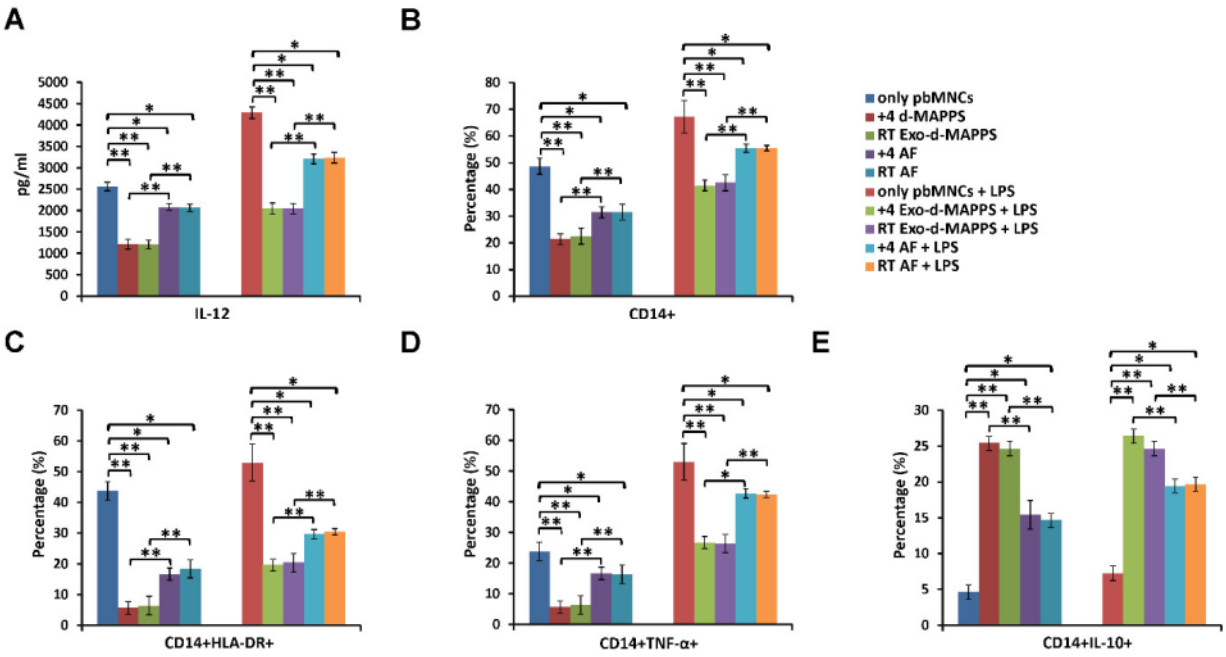


**(A)** Level of pro-inflammatory IL-12 in supernatants of pbMNCs
**(B-E)** Percentage of CD14+, CD14+HLA-DR+, CD14+TNF-α+ and CD14+IL-10+ pbMNCs primed with LPS after treatment with Exo-d-MAPPS and AF.
Values are mean ± SEM; *p<0.05, **p<0.01, ***p<0.001.

**Figure 2.** Treatment with Exo-d-MAPPS diminished expansion of inflammatory Th1 and Th17 cells and promoted generation of immunosuppressive Tregs in the population of Con A-primed pbMNCs.

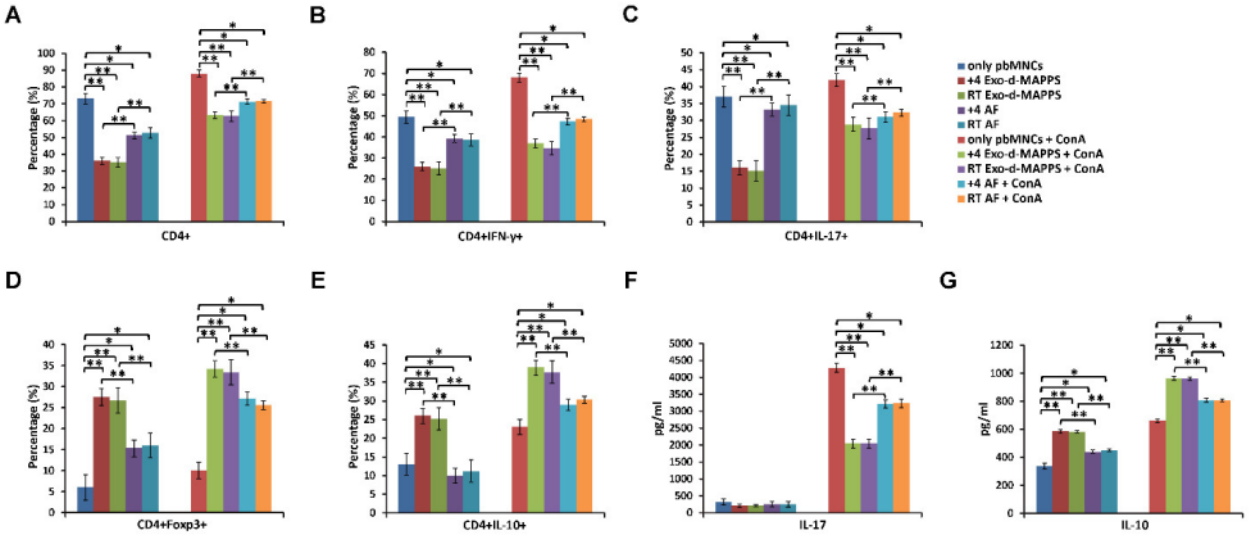


**(A-C)** Flow cytometry data showing decrease in percentage of CD4+ T cells as well as IFN-γ and IL-17-producing CD4+ T cells after Exo-d-MAPPS treatment. **(D, E)** Significant increase in percentage of regulatory CD4+ cells (Foxp3+ and IL-10+) after Exo-d-MAPPS treatment. **(F, G)** Level of the pro-inflammatory IL-17 and anti-inflammatory IL-10 in supernatants of ConA-primed pbMNCs.
Data presented as mean ± SEM; *p<0.05, **p<0.01, ***p<0.001.

**Figure 3.** Exo-d-MAPPS treatment suppressed pro-inflammatory and promoted anti-inflammatory properties of α-GalCer-primed pbMNCs

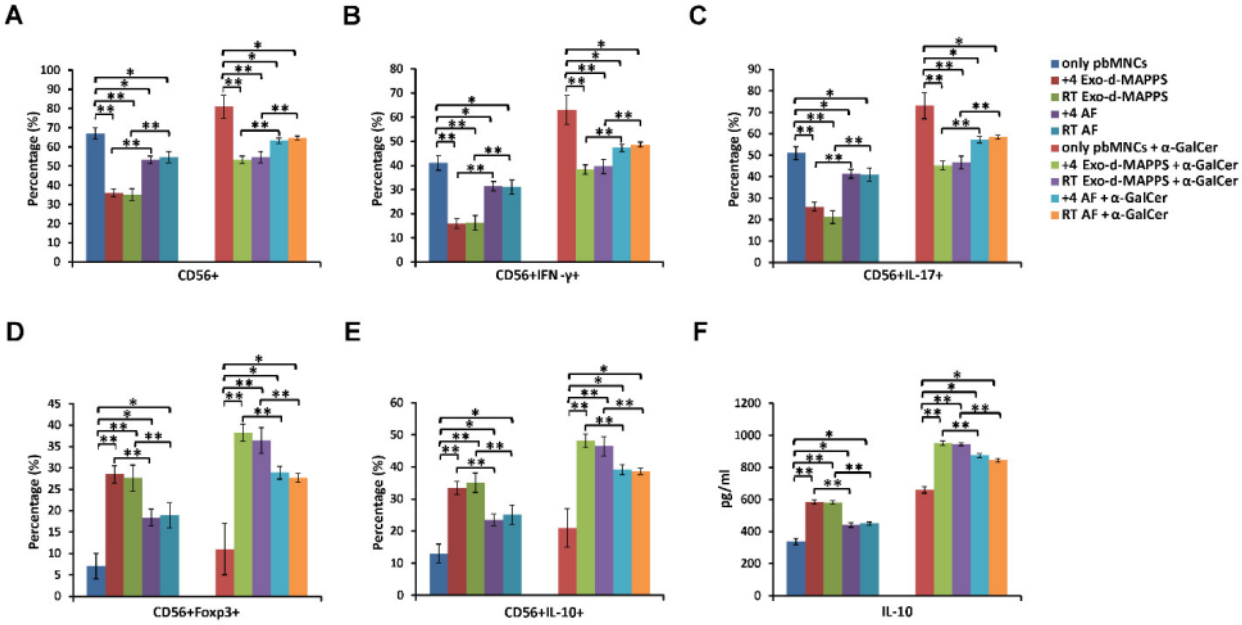


**(A-C)** The percentage of CD56+ cells as well as IFN-γ and IL-17-producing CD56+ cells after Exo-d-MAPPS and AF treatment. **(D, E)** Significant increase in the percentage of regulatory CD56+ cells (Foxp3+ and IL-10+) after Exo-d-MAPPS treatment. **(F)** Level of anti-inflammatory IL-10 in supernatants of α-GalCer-primed pbMNCs. Values are mean ± SEM; *p<0.05, **p<0.01, ***p<0.001.

## DISCUSSION

A large number of experimental and clinical evidences suggested that MSCs, due to their immunomodulatory properties, should be considered as new therapeutic agents for the treatment of autoimmune and incurable inflammatory diseases (28-31). Despite promising results observed after autologous and allogeneic transplantation of MSCs, safety issues regarding MSCs-based therapy are still a matter of debate (32). Due to their multipotency, MSCs may spontaneously differentiate into the undesired cell type, particularly osteocytes and chondrocytes (32). Although malignant transformation of transplanted MSCs has not been validated, the high proliferation rate and the capacity for self-renewal indicate possible risk of mutations which may result in tumor development and therefore the long-term follow up of patients that received MSCs is required (32). Several studies revealed that despite of low engraftment rate therapeutic effects of MSCs remained long after transplantation, suggesting that beneficial effects of MSC-based therapy were relied on the activity of MSC-sourced factors rather than on the differentiation of engrafted MSCs (33-35). Recently published studies indicated that MSC-derived immunosuppressive factors might be delivered to the target immune cells within MSC-Exos which, due to their nano-sized dimension and lipid envelope, easily avoid biological barriers in the body (28). In line with these findings, herewith we demonstrated that Exo-d-MAPPS, soluble product which contains a broad number of MSC-derived immunomodulatory factors (22), efficiently suppress inflammatory properties of pbMNCs and could be considered as a potentially new agent for the treatment of acute and chronic inflammatory diseases.

Capacity of LPS-primed CD14-expressing monocytes for the production of inflammatory cytokines (TNF-α and IL-12) was significantly attenuated by Exo-d-MAPPS treatment (Fig.1). CD14 is a LPS-binding protein, expressed on the membrane of macrophages and DCs, playing crucial role in the immune recognition of the microbial cell wall components from Gram-negative bacteria (36). Cross-talk between LPS-activated, CD14-expressing monocytes and IFN-γ-producing CD4+ Th1 cells has crucially important role in the pathogenesis of many autoimmune and chronic inflammatory diseases (diabetes mellitus, multiple sclerosis, Crohn's disease, etc.) (37-38). CD14-expressing macrophages and DCs, through the production of "pro-Th1 cytokines" (TNF-α and IL-12), induce generation of IFN-γ-producing CD4+ Th1 effector cells, which in turn, through the secretion of IFN-γ promote the phagocytic activity and capacity for antigen presentation of CD14-expressing monocytes (37, 38). Exo-d-MAPPS treatment resulted in attenuated production of TNF-α and IL-12 in activated CD14-expressing monocytes (Fig.1A, D) and alleviated production of IFN-γ in activated CD4+ cells (Fig.2B), indicating its capacity for suppression of CD4+Th1: the macrophage crosstalk and therapeutic potential for the treatment of chronic inflammatory diseases. Additionally, Exo-d-MAPPS significantly attenuated production of IL-17 in activated CD4+T cells (Fig.2F) and inhibited expansion of Th17 cells (Fig.2C). IL-17 and Th17 cells have important pathogenic role in the chronic organ-specific and systemic inflammatory disorders and, therefore, alleviation of IL-17-driven immune response has been responsible for beneficial effects of MSCs and MSC-derived secretome in the therapy of liver fibrosis, multiple sclerosis, systemic lupus erythematosus and rheumatoid arthritis (39-42). Several lines of evidence indicated that MSCs in IDO/Kynurenine, TGF-β and PGE2-dependent manner increased Tregs/Th17 ratio by promoting generation of immunosuppressive Tregs during the differentiation process of Th17 cells (42-44). In line with these findings, Exo-d-MAPPS, containing MSC-derived Treg-promoting factors (22), concomitantly suppressed proliferation of Th17 cells and induced enhanced expansion of IL-10-producing Tregs (Fig.2C-D).

Similarly, Exo-d-MAPPS induced expansion of FoxP3-expressing and IL-10-producing CD56+ cells and suppressed proliferation of inflammatory IFN-γ and IL-17 α-GalCer-primed pbMNCs (Fig.3). Having in mind that most of α-GalCer-primed CD56-expressing pbMNCs are NKT cells that play crucially an important role in the development of fulminant hepatitis, Exo-d-MAPPS might be considered as a potentially new remedy for the attenuation of NKT cell-dependent acute liver failure.

Since there was not a significant difference in immunomodulatory potential of RT and 4ºC Exo-d-MAPPS samples (Fig.1-3), Exo-d-MAPPS may be used either as RT or 4ºC storage soluble product. Importantly, although Exo-d-MAPPS is an AF-MSC-derived product, Exo-d-MAPPS-suppressed generation of inflammatory phenotype in pbMNCs is significantly better than AF (Fig.1-3). Exo-d-MAPPS contains AF-MSC-derived Exos, extracellular vesicles which diameter is smaller than 100 nm and do not contain apoptotic bodies (22). During the production of Exo-d-MAPPS, due to the centrifugation and filtration, large extracellular vesicles (with diameter bigger than 100 nm), including apoptotic bodies and microvesicles, were removed from the secretome (22). Since apoptotic bodies may induce an activation of inflammatory cascade in immune cells (45), we believe that their deficiency in Exo-d-MAPPS samples resulted in their better immunosuppressive potential compared to the AF samples (Fig.1-3).

## CONCLUSION

Due to its capacity for suppression of activated pbMNCs, Exo-d-MAPPS should be further explored in animal models of acute and chronic inflammatory diseases as the potentially new remedy for the attenuation of detrimental immune response.

## ACKNOWLEDGMENT

This study was supported by the Faculty of Medical Sciences of the University of Kragujevac (Grant MP 01/18).

## REFERENCES


1. Friedenstein AJ, Petrakova KV, Kurolesova AI, Frolova GP. Heterotopic of bone marrow. Analysis of precursor cells for osteogenic and hematopoietic tissues. Transplantation. 1968; 6: 230-247.
2. Bieback K, Kern S, Kluter H, Eichler H. Critical parameters for the isolation of mesenchymal stem cells from umbilical cord blood. Stem Cells. 2004; 22: 625-634.
3. Yanez R, Lamana ML, Garcia-Castro J, Colmenero I, Ramirez M, Bueren JA. Adipose tissue-derived mesenchymal stem cells have in vivo immunosuppressive properties applicable for the control of the graft-versus-host disease. Stem Cells. 2006; 24: 2582-2591.
4. Anversa P, Perrella MA, Kourembanas S, Choi AM, Loscalzo J. Regenerative pulmonary medicine: potential and promise, pitfalls and challenges. Eur J Clin Invest. 2012; 42: 900-913.
5. Volarevic V, Ljujic B, Stojkovic P, Lukic A, Arsenijevic N, Stojkovic M. Human stem cell research and regenerative medicine-present and future. Br Med Bull. 2011; 99: 155-168.
6. Harrell CR, Jankovic MG, Fellabaum C, Volarevic A, Djonov V, Arsenijevic A, Volarevic V. Molecular Mechanisms Responsible for Anti-inflammatory and Immunosuppressive Effects of Mesenchymal Stem Cell-Derived Factors. Adv Exp Med Biol. 2019 Jun 8. doi: 10.1007/5584_2018_306.
7. Simovic Markovic B, Gazdic M, Arsenijevic A, Jovicic N, Jeremic J, Djonov V, Arsenijevic N, Lukic ML, Volarevic V. Mesenchymal Stem Cells Attenuate Cisplatin-Induced Nephrotoxicity in iNOS-Dependent Manner. Stem Cells Int. 2017; 2017: 1315378.
8. Gazdic M, Simovic Markovic B, Vucicevic L, Nikolic T, Djonov V, Arsenijevic N, Trajkovic V, Lukic ML, Volarevic V. Mesenchymal stem cells protect from acute liver injury by attenuating hepatotoxicity of liver natural killer T cells in an inducible nitric oxide synthase- and indoleamine 2,3-dioxygenase-dependent manner. J Tissue Eng Regen Med. 2018; 12: e1173-e1185.
9. Simovic Markovic B, Nikolic A, Gazdic M, Nurkovic J, Djordjevic I, Arsenijevic N, Stojkovic M, Lukic ML, Volarevic V. Pharmacological Inhibition of Gal-3 in Mesenchymal Stem Cells Enhances Their Capacity to Promote Alternative Activation of Macrophages in Dextran Sulphate Sodium-Induced Colitis. Stem Cells Int. 2016; 2016: 2640746.
10. Haynesworth SE, Baber MA, Caplan AI. Cytokine expression by human marrow-derived mesenchymal progenitor cells in vitro: Effects of dexamethasone and IL-1Î±. J Cell Physiol. 1996; 166: 585-92.
11. Caplan AI, Dennis JE. Mesenchymal stem cells as trophic mediators. J Cell Biochem. 2006; 98: 1076-84.
12. Moravej A, Karimi M-H, Geramizadeh B, Azarpira N, Zarnani A-H, Yaghobi R, Khosravi M, Kalani M, Gharesi-Fard B. Mesenchymal stem cells upregulate the expression of PD-L1 but not VDR in dendritic cells. Immunol Invest. 2017; 46: 80-96.
13. Volarevic V, Gazdic M, Simovic Markovic B, Jovicic N, Djonov V, Arsenijevic N. Mesenchymal stem cell-derived factors: Immuno-modulatory effects and therapeutic potential. Biofactors. 2017; 43: 633-644.
14. Harrell CR, Fellabaum C, Jovicic N, Djonov V, Arsenijevic N, Volarevic V. Molecular Mechanisms Responsible for Therapeutic Potential of Mesenchymal Stem Cell-Derived Secretome. Cells. 2019; 8(5). pii: E467. doi: 10.3390/cells8050467.
15. Mohammadipoor A, Antebi B, Batchinsky AI, Cancio LC. Therapeutic potential of products derived from mesenchymal stem/stromal cells in pulmonary disease. Respir Res. 2018; 19: 218.
16. Hass R, Kasper C, Böhm S, Jacobs R. Different populations and sources of human mesenchymal stem cells (MSC): A comparison of adult and neonatal tissue-derived MSC. Cell Commun Signal. 2011; 9: 12.
17. Kil K, Choi MY, Kong JS, Kim WJ, Park KH. Regenerative efficacy of mesenchymal stromal cells from human placenta in sensorineural hearing loss. Int J Pediatr Otorhinolaryngol. 2016; 91: 72-81.
18. Cho JS, Lee J, Jeong DU, Kim HW, Chang WS, Moon J, Chang JW. Effect of Placenta-Derived Mesenchymal Stem Cells in a Dementia Rat Model via Microglial Mediation: a Comparison between Stem Cell Transplant Methods. Yonsei Med J. 2018; 59: 406-415.
19. Jiang H, Zhang Y, Tian K, Wang B, Han S. Amelioration of experimental autoimmune encephalomyelitis through transplantation of placental derived mesenchymal stem cells. Sci Rep. 2017; 7: 41837.
20. Roubelakis MG, Pappa KI, Bitsika V, Zagoura D, Vlahou A, Papadaki HA, Antsaklis A, Anagnou NP. Molecular and proteomic characterization of human mesenchymal stem cells derived from amniotic fluid: comparison to bone marrow mesenchymal stem cells. Stem Cells Dev. 2007; 16: 931-952.
21. Mareschi K, Castiglia S, Sanavio F, Rustichelli D, Muraro M, Defedele D, Bergallo M, Fagioli F. Immunoregulatory effects on T lymphocytes by human mesenchymal stromal cells isolated from bone marrow, amniotic fluid, and placenta. Exp Hematol. 2016; 44: 138-150.e1.
22. Harrell CR, Fellabaum C, Simovic Markovic B, Arsenijevic A, Volarevic V. Therapeutic potential of “Exosomes derived Multiple Allogeneic Proteins Paracrine Signaling: Exosomes d-MAPPS” is based on the effects of exosomes, immunosuppressive and trophic factors. Ser J of Exp Clin Res. 2017; 1: 1.
23. Miron PM. Preparation, Culture, and Analysis of Amniotic Fluid Samples. Curr Protoc Hum Genet. 2018: e62.
24. Meng F, Lowell CA. Lipopolysaccharide (LPS)-induced macrophage activation and signal transduction in the absence of Src-family kinases Hck, Fgr, and Lyn. J Exp Med. 1997; 185: 1661-70.

25. Volarevic V, Milovanovic M, Ljujic B, Pejnovic N, Arsenijevic N, Nilsson U, Leffler H, Lukic ML. Galectin-3 deficiency prevents concanavalin A-induced hepatitis in mice. Hepatology. 2012; 55: 1954-1964.
26. Pejnovic NN, Pantic JM, Jovanovic IP, Radosavljevic GD, Milovanovic MZ, Nikolic IG, Zdravkovic NS, Djukic AL, Arsenijevic NN, Lukic ML. Galectin-3 deficiency accelerates high-fat diet-induced obesity and amplifies inflammation in adipose tissue and pancreatic islets. Diabetes. 2013; 62: 1932-1944.
27. Volarevic V, Zdravkovic N, Harrell CR, Arsenijevic N, Fellabaum C, Djonov V, Lukic ML, Simovic Markovic B. Galectin-3 Regulates Indoleamine-2,3-dioxygenase-Dependent Cross-Talk between Colon-Infiltrating Dendritic Cells and T Regulatory Cells and May Represent a Valuable Biomarker for Monitoring the Progression of Ulcerative Colitis. Cells. 2019; 8.
28. Rad F, Ghorbani M, Mohammadi Roushandeh A, Habibi Roudkenar M. Mesenchymal stem cell-based therapy for autoimmune diseases: emerging roles of extracellular vesicles. Mol Biol Rep. 2019; 46: 1533-1549.
29. Harrell CR, Sadikot R, Pascual J, Fellabaum C, Jankovic MG, Jovicic N, Djonov V, Arsenijevic N, Volarevic V. Mesenchymal Stem Cell-Based Therapy of Inflammatory Lung Diseases: Current Understanding and Future Perspectives. Stem Cells Int. 2019; 2019: 4236973.
30. Markovic BS, Kanjevac T, Harrell CR, Gazdic M, Fellabaum C, Arsenijevic N, Volarevic V. Molecular and Cellular Mechanisms Involved in Mesenchymal Stem Cell-Based Therapy of Inflammatory Bowel Diseases. Stem Cell Rev. 2018; 14: 153-165.
31. Gazdic M, Arsenijevic A, Markovic BS, Volarevic A, Dimova I, Djonov V, Arsenijevic N, Stojkovic M, Volarevic V. Mesenchymal Stem Cell-Dependent Modulation of Liver Diseases. Int J Biol Sci. 2017; 13: 1109-1117.
32. Volarevic V, Markovic BS, Gazdic M, Volarevic A, Jovicic N, Arsenijevic N, Armstrong L, Djonov V, Lako M, Stojkovic M. Ethical and Safety Issues of Stem Cell-Based Therapy. Int J Med Sci. 2018; 15: 36-45.
33. Gnecchi M, Danieli P, Malpasso G, et al. Paracrine mechanisms of mesenchymal stem cells in tissue repair. Methods Molecular Biol (Clifton, NJ). 2016; 1416: 123-146.
34. Liang X, Ding Y, Zhang Y, et al. Paracrine mechanisms of mesenchymal stem cell-based therapy: current status and perspectives. Cell Transplant. 2014; 23: 1045-1059.
35. Wang A, Brown EG, Lankford L, et al. Placental mesenchymal stromal cells rescue ambulation in ovine myelomeningocele. Stem Cells Transl Med. 2015; 4: 659-669.
36. Zamani F, Zare Shahneh F, Aghebati-Maleki L, Baradaran B. Induction of CD14 Expression and Differentiation to Monocytes or Mature Macrophages in Promyelocytic Cell Lines: New Approach. Adv Pharm Bull. 2013; 3: 329-332.
37. Xu Y, Liu Y, Yang C, Kang L, Wang M, Hu J, He H, Song W, Tang H. Macrophages transfer antigens to dendritic cells by releasing exosomes containing dead-cell-associated antigens partially through a ceramide-dependent pathway to enhance CD4(+) T-cell responses. Immunology. 2016; 149: 157-171.
38. Hirahara K, Nakayama T. CD4+ T-cell subsets in inflammatory diseases: beyond the Th1/Th2 paradigm. Int Immunol. 2016; 28: 163-171.
39. Mills KH. Induction, function and regulation of IL-17-producing T cells. Eur J Immunol. 2008; 38: 2636-2649.
40. Bunte K, Beikler T. Th17 Cells and the IL-23/IL-17 Axis in the Pathogenesis of Periodontitis and Immune-Mediated Inflammatory Diseases. Int J Mol Sci. 2019; 20.
41. Chehimi M, Vidal H, Eljaafari A. Pathogenic Role of IL-17-Producing Immune Cells in Obesity, and Related Inflammatory Diseases. J Clin Med. 2017; 6.
42. Harrell CR, Simovic Markovic B, Fellabaum C, Arsenijevic A, Djonov V, Arsenijevic N, Volarevic V. Therapeutic Potential of Mesenchymal Stem Cell-Derived Exosomes in the Treatment of Eye Diseases. Adv Exp Med Biol. 2018; 1089: 47-57.
43. Wang D, Huang S, Yuan X, Liang J, Xu R, Yao G, Feng X, Sun L. The regulation of the Treg/Th17 balance by mesenchymal stem cells in human systemic lupus erythematosus. Cell Mol Immunol. 2017; 14: 423-431.
44. Luz-Crawford P, Kurte M, Bravo-Alegría J, Contreras R, Nova-Lamperti E, Tejedor G, Noël D, Jorgensen C, Figueroa F, Djouad F, Carrión F. Mesenchymal stem cells generate a CD4+CD25+Foxp3+ regulatory T cell population during the differentiation process of Th1 and Th17 cells. Stem Cell Res Ther. 2013; 4: 65.
45. Tannetta D, Dragovic R, Alyahyaei Z, Southcombe J. Extracellular vesicles and reproduction-promotion of successful pregnancy. Cell Mol Immunol. 2014; 11: 548-563.

REVIEW PAPER

# BONE QUALITY ASSESSMENT OF DENTAL IMPLANT RECIPIENT SITES

Miroslav Vasovic, Lena Jovanovic and Aleksandrija Djordjevic
*Faculty of Medical Sciences, University of Kragujevac, Serbia*

Received: 24.05.2015.
Accepted: 06.06.2015.

**Corresponding author:**

**Miroslav Vasovic**

University of Kragujevac, Faculty of Medical Sciences
Kragujevac, Serbia

E-mail: miki_vasovic@yahoo.com

sciendo

UDK: 616.314-77-089.843
Ser J Exp Clin Res 2022; 23(1): 83-87
DOI: 10.1515/sjecr-2015-0052

## ABSTRACT

*The term bone quality is not clearly defined and depends on many factors, such as bone density, bone vascularity, bone metabolism and other factors that may affect implant outcome. The assessment of bone volume and bone density is most common in planning the treatment of dental implants. Bone quality is an important predictor of primary implant stability, which influences the future implant osseointegration. Numerous classifications have been described for the evaluation of bone density. Th e most commonly used has been the one proposed by Lekholmu and Zarb. For the objective evaluation of bone density, conventional computed tomography (CT) or Cone Beam Computed tomography (CBCT), have been proposed. Both methods are reliable for the measurement of bone density, but preference is given to CBCT, due to the lower radiation doses, greater comfort for the patient and the lower prices. Pre-operatively defined bone density is a good indicator of the future success of implant therapy. In addition to the bone density, vascularity of the jawbone is an important factor of the quality of the bone for the osseointegration of dental implants. Laser Doppler is a simple method that can determine the vascularity of bone during implant insertion. Th e development of modern diagnostic methods for assessing the quantity and quality of the jawbone has enabled easier implant planning and has provided a secure outcome.*

***Keywords:*** *Bone quality, implant stability, computed tomography, cone beam computed tomography, jawbone vascularity.*

## INTRODUCTION

The insertion of dental implants has become an increasingly common procedure in the oral rehabilitation of partially and totally edentulous patients. This trend has certainly contributed to the positive results of numerous clinical studies regarding implant survival rates (1,2,3,4). The success of any implant procedure depends on a series of patient-related and procedure dependent parameters, including general health conditions, biocompatibility of the implant material, the features of the implant surface, the surgical procedure, and the quality and quantity of the local bone (5,6). Based on the literature data, the success rate of implants is higher in the lower jaw than the upper jaw (4,5,6,7). This discrepancy may arise from the bone conditions around the implants. It is evident that, when compared with the maxilla, the bone surrounding the implant has a better volume and quality in the mandible (6).

There is no clear definition of bone quality, but it is generally presented as the sum of all of the characteristics of bone that influence its resistance to fracture (8). Many authors define bone quality as equivalent to bone mineral density. This includes physiological and structural aspects and the degree of bone tissue mineralization (9,10,11). Aspects such as bone metabolism, cell turnover, maturation, intracellular matrix and vascularity were also emphasized. Although the clinical outcome of an implant is influenced by many factors, including the implant body, the skill of the surgeon, and the oral environment, the key factor for success is the primary stability at the implant placement. Some studies have demonstrated that the quality of the alveolar bone is the most important factor for achieving good primary stability (12,13).

Primary implant stability has been acknowledged as an essential criterion for later achievement of osseointegration (14). The primary stability could be increased with increased bone quality, which would improve the osseointegration and increase the survival probability of the dental implant. Poor bone quantity and especially poor bone quality are the main risk factors for implant failure using the standard protocol for implant insertion (15). The primary stability depends on the quality of the local bone, the implant geometry and the applied surgical techniques (16). By applying additional surgical techniques, such as the absence of threads at the implant site; the use of a profile borer at a reduced diameter; the use of a larger implant of greater diameter and length; and the presence of bicortical stabilization, can make for greater primary implant stability (17,18,19). Detailed preoperative analysis of the jawbone helps therapists in making decisions about the type of surgical procedure and the type of implants.

### Bone density

Bone density seems to be of great importance not only in primary implant stability but also in the predictability for oral implant outcomes (10). The literature describes a large number of classifications and procedures for the determination of jawbone density (20,21,22). The most commonly used classification has been the one proposed by Lekholmu and Zarb (1985), based on the amount of cortical and trabecular bone shown in preoperative panoramic and cephalometric radiographs. They classified bone density as Q1 to Q4 according to the ratio of cortical bone to spongy bone (10) (table 1). This method provides information on bone density but is considered to be a subjective method (23). Misch suggested that computed tomography (CT) can be used for the objective quantification of direct density measurements of bone, expressed in Hounsfield units (HU) (table 1). HU represent the relative density of body tissues according to a calibrated grey-level scale.

CT bone density

The introduction of new radiographic procedures that allow 3D analysis of the jawbone significantly facilitated the work of therapists and ensures a better treatment outcome.

In a CT scan, HU is proportional to the degree of x-ray attenuation, and it is allocated to each pixel to show the image that represents the density of the tissue. This method for pre-operative quantitative and qualitative assessment of dental implant sites is objective and reliable. The dental literature has numerous studies on the usefulness of CT for assessing bone volume and morphology and on the relationship between CT values and primary implant stability (7,9,12,14,16,19). It has been shown that there is a strong correlation between the pre-operative bone density

**Table 1.**Bone classifications and bone densities in Hounsfield units (HU)

| **Lekholm and Zarb clasiffication** | | | |
|---|---|---|---|
| Type1 | Type2 | Type3 | Type4 |
| Large homogenous cortical bone | Thick cortical layer surrounding a dense medullar bone | Thin cortical layer surrounding a dense medullar bone | Thin cortical layer surrounding a sparse medullar bone |

| **Misch clasification** | | | | |
|---|---|---|---|---|
| **D1** | **D2** | **D3** | **D4** | **D5** |
| > 1250 HU | 850 to 1250 HU | 350 to 850 HU | 150 to 350 HU | < 150 HU |
| Dense cortical bone | Thick dense to porous cortical bone on crest and coarse trabecular bone | Thin porous cortical bone on crest and fine trabecular bone within | Fine trabecular bone | Immature, non-mineralized bone |

**Table 2.** Bone densities in HU in diferent jaw regions

| Jawbone region | Turkyilmaz et al. (2007) | de Oliveira et al. (2008) | Fun et al. (2010) |
|---|---|---|---|
| **Anterior mandible** | 945 ± 207 | 383 ± 243 | 530 ± 161 |
| **Anterior maxilla** | 716 ± 190 | 370 ± 176 | 516 ± 132 |
| **Posterior mandible** | 674 ± 227 | 306 ± 187 | 359 ± 150 |
| **Posterior maxilla** | 455 ± 122 | 255 ± 184 | 332 ± 136 |

values and the primary stability measured after implant insertion (5,6,11,14,16)

The available literature indicates that the implant location greatly affects the implant success, which is approximately 4% higher in the mandible than in the maxilla, and it is higher in the anterior region than in the posterior region (approximately 12% and 4% in the maxilla and mandible, respectively). This might be explained by the mean bone density being highest in the anterior mandible, followed by the anterior maxilla, posterior mandible, and posterior maxilla (7, 24,25) (table 2).

There is also a difference in bone density between females and males, which may be explained by the hormonal peculiarities in females and the generally higher bone mass in males (25).

HU derived by CT can be used as a diagnostic parameter to predict possible implant stability. Thus, preoperative assessment of bone densities by HU is very important for optimizing primary implant stability. The use of CT has continued to grow, although its systematic use in clinical practice has been limited by concerns about high radiation doses and the relatively high cost.

Cone beam CT bone density

In recent years, due to the need for less expensive image acquisition protocols and scanners with a lower radiation dose, cone beam computed tomography (CBCT) has become widely used for oral and maxillofacial imaging. CBCT is a new medical imaging technique that generates 3-D images at a lower cost and at a lower absorbed dose compared with conventional computed tomography. This imaging technique is based on a cone-shaped X-ray beam centred on a 2-D detector that performs one rotation around the object, producing a series of 2-D images. These images are re-constructed in 3-D using a modification of the original cone-beam algorithm developed by Feldkamp et al. in 1984 (26).

In recent years, CBCT has been used for preoperative diagnosis in implant treatments. CBCT is superior because of its high definition, reduction of the exposure dose, low cost, and usability compared with CT. With the use of the CBCT, the dimensional accuracy is also comparable with CT, but in contrast to CT; the grey density values of the CBCT images (voxel value [VV]) are not absolute. In CBCT, the degree of one x-ray attenuation is shown by a grey scale (voxel value) (27). Some studies have shown good correlation between HU and VV and suggest that CBCT can be used in pre-operative evaluation of jawbone density in planning for implants (28,29).

Many articles from the literature suggest that bone quality evaluated by CBCT has a high correlation with the primary stability of the implants (30,31,32). Hence, preoperative density value estimations by CBCT may allow clinicians to predict implant stability.

**Bone vascularity**

Bone vascularity is an important factor in the process of osseointegration. After implant site preparation and implant insertion, tissue repair requires the development of a vascular system for a complete healing process (33,34). The early phase of healing proceeds from haematoma formation to woven bone formation. The late phase of healing results in bone remodelling and the formation of new bone, leading to osseointegration of the implant (35,36).

For assessment of tissue vascularity at the level of microcirculation, laser Doppler Flowmetry (LDF) is an appropriate method (37).This method has been used for the detection of blood flow in oral mucosal, pulpal, muscular and gingival tissues (38,39,40,41,42,43,44).

Recent animal and clinical studies showed that LDF is a reliable method for bone vascularity assessment during implant insertion (45,46). The method is based on a phenomenon known as the Doppler Effect i.e., a change in the frequency of light upon reflection from blood cells in motion.

Using the laser Doppler device software, the electronic impulse is expressed in perfusion units (PU), representing the number of cells multiplied by their average speed. Because the red blood cells are the majority of the mobile cells in the tissue, this means that the perfusion units are the blood velocity in the tissue (47). In their clinical study, Kokovic et al. showed that there is a statistically significant correlation between LDF measured during implant insertion and the changing values of implant stability in the late phase of osseointegration of dental implants in posterior mandibles (48).

Dental implant therapy requires an accurate preoperative assessment of the patient's hard and soft tissues. Clinicians should understand the indications, applications, and limitations of different imaging techniques to obtain information while keeping radiographic risks to a minimum. The use of CBCT with interactive planning software appears to meet the standard of care required for planning dental implant therapy (49). Bone density assessment using CBCT is an efficient method and significantly correlated with implant stability parameters and the Lekholm and Zarb index (50).

It can be concluded that CT and CBCT scanning are useful tools, providing not only morphological information but also bone density data, enabling the evaluation of the adequacy of potential dental implant sites prior to

implant placement. Keeping in mind the advantages of CBCT over conventional CT, it has to be used for the preoperative evaluation of bone quality.

Vascularity at the implant site has been identified as an important factor for the successful outcome of dental implant treatment (51). LDF is a reliable method for the determination of bone vascularity prior to implant insertion and might determine future implant stability.

## REFERENCES


1. Stellingsma K, Slagter AP, Stegenga B, Raghoebar GM, Meijer HJA. Masticatory function in patients with an extremely resorbed mandible restored with mandibular implant-retained overdentures: comparison of three types of treatment protocols. J Oral Rehabil. 2005;32:403–410.
2. Visser A, Geertman ME, Meijer HJA, Raghoebar GM, Kwakman JM, Creuger NHJ, Van Oort RP. Five years of aftercare of implant-retained mandibular overdentures and conventional dentures. J Oral Rehabil. 2002;29:113–120.
3. Geertman ME, Slagter AP, Van't Hof MA, Van Wass MAJ, Kalk W. Masticatory performance and chewing experience with implant-retained mandibular overdentures. J Oral Rehabil. 1999;26:7–13.
4. Comfort MB, Chu FCS, Chai J, Wat PYP, Chow TW. A 5-year prospective study on small diameter screw-shaped oral implants. J Oral Rehabil. 2005;32:341–345.
5. Turkyilmaz I. Clinical and radiological results of patients treated with two loading protocols for mandibular overdentures on Branemark implants. J ClinPeriodontol. 2006;33:233–238.
6. Beer A, Gahleitner A, Holm A, Tschabitscher M, Homolka P. Correlation of insertion torques with bone mineral density from dental quantitative CT in the mandible. Clin Oral Implants Res 2003; 14:616–20.
7. Turkyilmaz I, Tözüm TF, Tumer C. Bone Density Assessments of Oral Implant Sites Using Computerized Tomography. J Oral Rehabil. 2007;34:267–72.
8. Fyhrie DP. Summary – Measuring "bone quality". J Musculoskelet Neuronal Interact. 2005;5:318–320.
9. Bergkvist G, Koh KJ, Sahlholm S, Klintstrom E, Lindh C. Bone density at implant sites and its relationship to assessment of bone quality and treatment outcome. International Journal of Oral and Maxillofacial Implants 2010; 25: 321–28.
10. Molly L. Bone density and primary stability in implant therapy. Clinical Oral Implants Research 2006; 2:124–35.
11. Marquezan M, Oso´rio A, Sant'Anna E, Souza MM, Maia L. Does bone mineral density influence the primary stability of dental implants? A systematic review. Clin. Oral Impl. Res. 2012; 23(7):767-74
12. Tolstunov L. Implant zones of the jaws: implant location and related success rate. J Oral Implantol. 2007;33:211–20.
13. Ozan O, Turkyilmaz I, Yilmaz B. A preliminary report of patients treated with early loaded implants using computerized tomography-guided surgical stents: flapless versus conventionalflapped surgery. J Oral Rehabil. 2007;34:835–40.
14. Merheb J, Van Assche N, Coucke w, Jacobs R, Naert I, Quirynen M. "Relationship between cortical bone thicknessor computerized tomography-derived bone density values andimplant stability,".Clinical Oral Implants Research 2010;21(6):612-17.
15. Herrmann I, Lekholm U, Holm S, Kultje C. Evaluation of patient and implant characteristics as potential prognostic factors for oral implant failures. International Journal of Oral and Maxillofacial Implants 2005; 20: 220–230.
16. Turkyilmaz I, Tumer C, Ozbek EN, TÖzüm TF. Relations between the bone density values from computerized tomography, and implant stability parameters: a clinical study of 230 regular platform implants. J Clin-Periodontol 2007; 34: 716–22.
17. Ostman PO, Hellman M, Wendelhag I, Sennerby L. Resonance frequency analysis measurements of implants at placement surgery. Int J Prosthodont 2006; 19:77–83.
18. O'Sullivan D, Sennerby L, Jagger D, Meredith N. A comparison of two methods of enhancing implant primary stability. Clin Implant Dent Relat Res 2004; 6:48–57.
19. O'Sullivan D, Sennerby L, Meredith N. Influence of implant taper on the primary and secondary stability of osseointegrated titanium implants. Clin Oral Implants Res 2004; 15:474–80.
20. Lekholm U, Zarb GA. Patient selection and preparation. In: Branemark PI, Zarb GA, Albrektsson T, eds.Tissue integrated prostheses: osseointegration in clinical dentistry. Chicago, IL: Quintessence, 1985;199–209.
21. Norton RM, Gamble C. Bone classification: an objective scale of bone density using the computerized tomography scan. Clin Oral Implants Res. 2001; 12:79–84.
22. Misch CE. Density of bone: effect on surgical approach, and healing. In: Misch CE, ed. Contemporary implant dentistry. St Louis, MO: Mosby, 1999; 371–84.
23. de Oliveira RC,Leles CR,Normanha LM, Lindh C, Ribeiro-Rotta RF, "Assessments of trabecular bone density at implant sites on CT images," Oral Surgery, Oral Medicine, Oral Pathology, Oral Radiology and Endodontology, 2008;105(2):231–38.
24. Turkyilmaz I, Aksoy U, McGlumphy EA. Two alternative surgical techniques for enhancing primary implant stability in the posterior maxilla: a clinical study including bone density, insertion torque, and resonance frequency analysis data. Clin Implant Dent Relat Res. 2008 ; 10(4):231-7.
25. Fun LJ, Huang HL, Chen CS, Fu KL, Shen YW, Tu MG, Shen WC. Hsu T.Variations in bone density at dental implant sites in differentregions of the jawbone Journal of Oral Rehabilitation 2010 37; 346–351

26. Almog DM, LaMar J, LaMar FR, LaMar F. Cone beam computerized tomographybased dental imaging for implant planning and surgical guidance, Part 1: Single implant in the mandibular molar region. J Oral Implantol. 2006;32(2):77-81.
27. Cassetta M, Stefanelli LV, Di Carlo S, Pompa G, Barbato E. The accuracy of CBCT in measuring jaws bone density. Eur Rev Med Pharmacol Sci. 2012;16(10):1425-9.
28. Razi T, Niknami M, Ghazani FA. Relationship between Hounsfield Unit in CT Scan and Gray Scale in CBCT. J Dent Res Dent Clin Dent Prospects. 2014; 8(2): 107–110.
29. Cassetta M, Stefanelli LV, Pacifici A, Pacifici L, Barbato E. How accurate is CBCT in measuring bone density? A comparative CBCT-CT in vitro study. Clin Implant Dent Relat Res. 2014;16(4):471-8.
30. Wada M, Tsuiki Y, Suganami T, Ikebe K, Sogo M, Okuno I, Maeda Y. The relationship between the bone characters obtained by CBCT and primary stability of the implants. International Journal of Implant Dentistry (2015) 1:3.
31. Fuster-Torres MÁ, Peñarrocha-Diago M, Peñarrocha-Oltra D, Peñarrocha-Diago M. Relationships between bone density values from cone beam computed tomography, maximum insertion torque, and resonance frequency analysis at implant placement: a pilot study Int J Oral Maxillofac Implants. 2011;26(5):1051-6.
32. Salimov F, Tatli U, Kürkçü M, Akoğlan M, Oztunç H, Kurtoğlu C. Evaluation of relationship between preoperative bone density values derived from cone beam computed tomography and implant stability parameters: a clinical study. Clin Oral Implants Res. 2014;25(9):1016-21.
33. Cooper LF. Biologic determinants of bone formation for osseointegration: clues for future clinical improvements. J Prosthet Dent 1998; 80:439-49.
34. Arnold F, West DC. Angiogenesis in wound healing. PharmacolTher 1991;52:407–22.
Puleo DA, Nanci A. Understanding and controlling the bone implant interface. Biomaterials 1999;20:2311-21.
35. Kuzyk PR, Schemitsch EH. The basic science of periimplant bone healing. Indian J Orthop 2011;45:108-15.
36. GrgaDj, Dzeletovic B, Zivkovic S, Krsljak E. Blood Flow Measurement by Laser Doppler Method in Orofacial Region. Serbian Dental Journal.2010;57(3):141-48.
37. Retzepi M, Tonetti M, Donos N. (2007) Comparison of gingival blood flow during healing of simplified papilla preservation and modified Widman flap surgery: a clinical trial using laser Doppler flowmetry. Journal of Clinical Periodontology 2007; 34: 903-11.
38. Mavropoulos A, Brodin P, Rösing CK, Aass AM, Aars H. Gingival blood flow in periodontitis patients before and after periodontal surgery assessed in smokers and non-smokers. Journal of Periodontology 2007; 78: 1774–82.
39. Barta A, Nagy G, Csiki Z, Márton S, Madléna M. Changes in Gingival Blood Flow during Orthodontic Treatment. Cent Eur J Med 2010; 5(6) :758-65.
40. Singh DB, Stansby G, Harrison DK. Assessment of oxygenation and perfusion in the tongue and oral mucosa by visible spectrophotometry and laser Doppler flowmetry in healthy subjects. Advances in Experimental Medicine and Biology 2008; 614: 227–33.
41. Røe C, Damsgård E, Knardahl S. Reliability of bloodflux measurements from the upper trapezius muscle during muscle contractions. European Journal of Applied Physiology 2008; 102: 497–503.
42. Kijsamanmith K, Timpawat S, Vongsavan N, Matthews B. Pulpal blood flow recorded from human premolar teeth with a laser Doppler flow meter using either red or infrared light.Archives of oral biology 2011; 56: 629-33.
43. Chen E, Goonewardene M, Abbott P. Monitoring dental pulp sensibility and blood flow in patients receiving mandibular orthognathic surgery. International Endodontic Journal 2012; 45:215–23.
44. Verdonck HWD, Meijer GJ, Laurin T, Nieman FH, Stoll C, Riediger D, Stoelinga PJW, de Baat C. Assessment of vascularity in irradiated and non-irradiated maxillary and mandibular alveolar minipig bone using laser Doppler flowmetry. International Journal of Oral & Maxillofacial Implants 2007; 22: 774–78.
45. Verdonck HWD, Meijer GJ, Kessler P, Nieman FH, de Baat C, Stoelinga PJW. Assessment of bone vascularity in the anterior mandible using laser Doppler flowmetry.Clin. Oral Impl. Res 2009; 20:140–44.
46. Monteiro AA, Svensson H, Bornmyr S, Arbolerius M, Kopp S. Comparison of ta3Xe clearance and laser dopplerflowmetry in assessment of blood flow changes in human masseter muscle induced by isometric contraction. Arch Oral Biol. 1989; 34:779-86.
47. Kimura Y, Wilder-Smith P, Matsumoto K. Lasers in endodontics: a review. IntEndod J. 2000; 33:173-85.
48. Kokovic V, Krsljak E, Andric M, Brkovic B, Milicic B, Jurisic M, Rahman MM, Hämmerle CH. Correlation of bone vascularity in the posterior mandible and subsequent implant stability: a preliminary study. Implant Dent. 2014; 23(2):200-5.
49. Adam Shui-Cheong Siu, Frederick Cho-Shun Chu, Thomas Ka-Lun L, Tak-Wah Chow, Fei-Long Deng. Imaging modalities for preoperative assessment in dental implant therapy: an overview. Hong Kong Dent J. 2010;7:23-30.
50. Salimov F, Tatli U, Kurkcu M, Akoglan M, Oztunc H, Kurtoglu C. Evaluation of relationship between preoperative bone density values derived from cone beam computed tomography and implant stability parameters: a clinical study. Clin Oral Implants Res. 2014; 25(9): 1016-21
51. Boonsiriseth K., Suriyan N., Min K., Wongsirichat N. Bone and soft tissue healing in dental implantology. J. Med. Med. Sci.2014; 5(5):121-126

# HYPERTENSIVE CRISIS IN PATIENTS WITH ACUTE INTERMITTENT PORPHYRIA

Olivera Andrejic[1], Rada Vucic[2,3], Violeta Iric Cupic[2,3] and Goran Davidovic[2,3]

[1] *Clinical Centre Kragujevac, Clinic of Pulmology,*
[2] *Clinical Centre Kragujevac, Clinic of Cardiology, Kragujevac, Serbia*
[3] *University of Kragujevac, Faculty of Medical Sciences, Department of Internal Medicine, Kragujevac, Serbia*

Received: 25.11.2014.
Accepted: 17.07.2017.

**Corresponding author:**

**Olivera Andrejic**

Clinical Centre Kragujevac, Department of Pulmology
Kragujevac, Serbia

Phone: + 381 638828476
E-mail: olivera.andrejic@gmail.com

sciendo

UDK: 616-008.9-083.98
Ser J Exp Clin Res 2022; 23(1): 89-92
DOI: 10.2478/sjecr-2017-0039

## ABSTRACT

***Introduction****: Acute intermittent porphyria (AIP) is the most common and the most severe form of acute hepatic porphyria.* ***Case report:*** *Patient, 39 years old, was admitted to the Emergency Department because of abdominal pain. Abdominal pain started 5 days before the admission. The diagnostic research in his hospital showed presence of a stone in the right kidney, and the patient was transported to the other Clinical Centre, where a common urine test showed: high values of delta - aminolevulinic acid and porphobilinogen. The patient was transported to our Clinical Centre. At the admission, abdominal pain decreased, but the patient had a hypertensive crisis with a headache, tearing eyes, swelling, anxiety.Common laboratory tests were in reference range, except creatinine, CRP, arterial blood gas analysis, urine test. The hypertensive crisis was treated by beta blockers and diuretics in maximal doses, but without a positive effect, so we decided to try with Glyceryl trinitrate intravenously. Control blood pressure was 170/100mmHg....130/80mmHg.* ***Discussion:*** *Porphyria can be a diagnostic problem, because one of the manifestations can be abdominal pain.* ***Conclusions:*** *Comorbidities can be critical in the therapy of life threating conditions.*

***Keywords****: porphyria, abdominal pain, hypertensive crisis.*

## INTRODUCTION

Acute intermittent porphyria (AIP) is the most common and the most severe form of acute hepatic porphyria. It is an autosomal dominant inborn error characterized by a decreased activity (less than 50% (1)) of porphobilinogen (PBG) deaminase (also known as hydroxymethylbilane synthase or uroporphyrinogen I synthetase), leading to increased levels of the hem precursors, namely aminolevulinic acid (ALA) and PBG (2).

It can be activated by drugs (barbiturates, sulfonamide antibiotics, anti-seizure drugs, rifampicin, metoclopramide and alcohol), hormones (in women, it may occur after ovulation and during the last part of the menstrual cycle when progesterone levels are high), dietary changes (as an effort to lose weight) (3), as well as infections, surgery, and stressful situations. Sometimes, the activating factors can not be identified (1).The risk for developing chronic renal disease and liver cancer (hepatocellular carcinoma) is increased in AIP (4).

AIP manifests after puberty, especially in women (due to hormonal influences). The symptoms usually come as discrete intermittent attacks which develop over two or more days, that are sometimes life-threatening. They are due to the effects on the visceral, peripheral, autonomic and central nervous systems (5). Abdominal pain, neurological dysfunction and psychiatric disturbances form the classic triad of AIP. Abdominal pain, which is associated with nausea, can be severe and occurs in most cases (90%) (2,6). Presentation like respiratory failure necessitates admission to the intensive care unit. Other symptoms may include (7):

- nausea
- vomiting
- constipation
- pain in the back, arms and legs
- muscle weakness (due to the effects on nerves supplying the muscles)
- urinary retention
- palpitation (due to a rapid heart rate and often accompanied by an increased blood pressure)
- confusion, hallucinations and seizures
- peripheral polyneuropathy, primarily motor with flaccid paresis of the proximal musculature, with or without autonomic involvement

Because this disease is rare and can mimic a host of other more common conditions, its presence is often not suspected (8). On the other hand, the diagnosis of AIP and other types of porphyria is sometimes made incorrectly in patients who do not have porphyria at all, particularly if laboratory tests are improperly done or misinterpreted. The finding of increased levels of ALA and PBG in urine establishes that one of the acute porphyrias is present (2), but some studies have shown that acute attacks are more reflected by plasma PBG than plasma ALA or urinary PBG and ALA (9). The avoidance of precipitating factors and the use of hem preparations and intravenous dextrose form the basis of management (6,10).

## CASE REPORT

Patient, 39 years old was admitted do the Emergency Department because of abdominal pain. In previous history, he did not have any hereditary illness, he is a smoker (40 cigarettes per day). Six months earlier, he had had a surgical intervention after which he experienced similar abdominal pain.

Abdominal pain started 5 days before the admission. The pain was diffuse, sharp, followed by loss of appetite, nausea, vomiting. The diagnostic research in his hospital showed presence of a stone in the right kidney, and the patient was transported to the other Clinical Centre. The common urine test showed: higher values of delta - aminolevulinic acid and porphobilinogen. The patient was transported to our Clinical Centre.

At the admission, abdominal pain decreased in intensity, but the patient had a headache, tearing eyes, swelling, anxiety. He was afebrile, with rhythmic heart beats, referent breathing sounds, diffuse abdominal pain without a peritoneal reaction. Legs were without edema. Blood pressure was 220/120mmHg. Electrocardiogram (Figure 1): sinus rhythm, 80 beats per minute, Q wave in III. Abdominal echo was without any abnormalities. The common laboratory tests were in reference range, except creatinine, CRP, arterial blood gas analysis, urine test (Table 1.)

**Figure 1.** Electrocardiogram

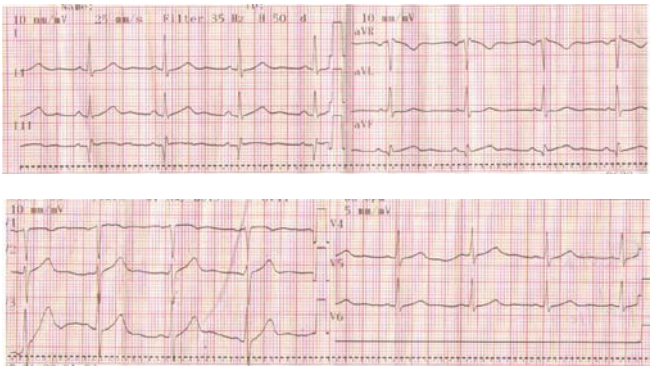

The diagnosis was a hypertensive crisis. Acute intermittent porphyria. Abdominal pain. A surgeon observed the patient for abdominal pain, and Ranitidine was administrated. We were limited in using drugs for the hypertensive crisis. We used Furosemide and Metoprolol intravenously, in maximal doses but without a positive effect. In absence of other safe drugs for the hypertensive crisis in the patients with porphyria, we decided to try with Glyceryl trinitrate intravenously. The control value of blood pressure was 170/100mmHg ….130/80mmHg. The therapy was followed by a slow intravenous administration of glucose.

**Table 1.** Laboratory tests

| Analysis | | Value | Reference value |
|---|---|---|---|
| arterial blood gas analysis | pH | 7.46 | 7.35-7.45 |
| | pCO2 (kPa) | 5.2 | 4.66-6.38 |
| | pO2(kPa) | 10.5 | 11.4-14.36 |
| | $Na^+$ (mmol/L) | 132 | 132 |
| | $K^+$ (mmol/L) | 3.8 | 3.4-4.5 |
| | $Ca^{2+}$ (mmol/L) | 1.04 | 1.15-1.35 |
| | Hematocrit (%) | 48 | 35-51 |
| | $HCO3^-$ (mmol/L) | 27.7 | 18-23 |
| | SpO2 (%) | 96 | 95-98 |
| CRP (mg/L) | | 21.2 | 0.0-5.0 |
| Creatinine (umol/L) | | 114 | 49-106 |
| Urine test | Leukocytes | 15-20 | <0 |
| | Erythrocytes | 2-3 | <0 |
| | Ketones | ++ | <0 |

Explanatory notes: CRP- C reactive protein; $K^+$ – potassium; $Na^+$ – sodium; $Ca^{2+}$ – calcium; $HCO3^-$- bicarbonate, SpO2-oxygen saturation, pO2- arterial oxygen tension pCO2-arterial carbon dioxide tension

## DISCUSSION

The word "porphyria" is derived from the Greek word *porphuros*, which means red or purple. The porphyrias are the group of rare metabolic disorders arising from the reduced activity of enzymes in the hem biosynthetic pathway. These deficiencies disrupt the normal hem production, with symptoms especially prominent when the increased hem is required. The porphyrin precursors, overproduced in response to the synthetic pathway blockages, accumulate in the body, cause diverse pathologic changes, and become the basis for diagnostic tests (11).

A specific enzyme catalyzes each step of the hem biosynthetic pathway. Eight enzymes are involved in the synthesis of hem and, except for the first enzyme (δ-aminolevulinate synthase), the low activity of any of these can disrupt the normal pathway, especially when a stimulus occurs to increase the hem production. The suboptimal activity of any one of these seven enzymes, due to either a defective gene or a toxic chemical effect, results in the overproduction and accumulation of the preceding intermediates, known as porphyrins or the porphyrin precursors. Although these intermediates have no known useful physiologic function, they act as highly reactive oxidants, and deficiencies of seven enzymes are linked to specific types of porphyria (12).

Clinical manifestations are variable. The symptoms may vary considerably in the same patient during different episodes, as well as among the patients with the same porphyria subtype. Because the clinical course can vary from acute, self-limiting attacks to attacks that result in chronic or progressive deficits, the attacks may mimic many other psychiatric or medical disorders, making the potential for a misdiagnosis great (8).

In our case, the patient had abdominal pain which was evaluated for acute abdomen. The common laboratory tests confirmed acute intermittent porphyria, but acute abdomen couldn't be excluded immediately. The administration of some drugs in the patients with porphyria can be dangerous. Unfortunately, the information for most drugs is insufficient to allow them to be classified as definitely harmful or safe.

Pantoprazole is recommended to be used with caution, as other agents in this class. H2 receptor antagonists (Ranitidine and Famotidine) are considered to be safer, even though certain studies proposed that they can be used with caution (13). We decided to use Ranitidine intravenously.

After the admission, the patient had the hypertensive crisis. Hypertension is common in patients with AIP, but the hypertensive crisis is rare. Most antihypertensive drugs are unsafe because they can precipitate attack or they are porphyrinogenic (14). Safe antihypertensive drugs are limited to beta adrenergic blockers (15). Diuretics can be used too (Furosemide, Hydrochlorthiazide). There are contradictory reports about the safety of calcium channels blockers, especially Almodipine (16). The use of Nifedipine is unsafe or it can be used with extreme caution. In some cases, using these drugs in maximal doses can precipitate attack. ACE inhibitor, such as Enalapril is unsafe because it greatly increases the porphyrin accumulation, while Captopril, Lisinopril, Losartan slightly increase. (17)

The administration of glucose and the hem therapy is the basis of treatment, but some studies have shown that

glucoseis not sufficient to achieve the clinical and biochemical remission in more serious attacks in contrast to the hem therapy (9).

In our case, after the administration of beta blockers and diuretics, blood pressure was still high. Of available drugs, Glyceryl trinitrate was alternative, as the drug whose safety has not been proved, but it can probably be used. After its administration, blood pressure was lower, and the patient didn't have any adverse effects, as well as after Ranitidine use.

Porphyria is a rare condition, and clinical trials about it are insufficient. This is one case more which justifies the use of Glyceryl trinitrate and Rantidine in patients with porphyria.

## CONCLUSION

Comorbidities can be critical in the therapy of life treating conditions.

## REFERENCES


1. Sassa S. Modern diagnosis and management of the porphyrias. British Journal of Haematology, 2006; 135: 281–292
2. Mehta M., Rath G.P., Padhy U.P., Marda M., Mahajan C. and Dash H.D. Intensive care management of patients with acute intermittent porphyria: clinical report of four cases and review of literature. Indian J Crit Care Med. 2010; 14(2): 88–91.
3. Handschin, C., Lin, J., Rhee, J., et al. Nutritional regulation of hepatic heme biosynthesis and porphyria through PGC-1alpha. Cell, 2005;122: 505–515.
4. Innala E., Andersson C. Screening for hepatocellular carcinoma in acute intermittent porphyria: a 15-year follow-up in northern Sweden. Journal of Internal Medicine. 2011; 269(5):538-545
5. Stölzel U., Stauch T., Doss M.O. Porphyrias. Internist (Berl). 2010; 51(12): 1525-33
6. Kovačević Z., Janićijević Petrovic M., Šarenac T., Mladenović V., Stojilković T. Acute intermittent Porphyria. PONS Med J. 2012; 9 (3):110-113.
7. Balwani M., Desnick R.J. The porphyrias: advances in diagnosis and treatment. Hematology 2012;120: 19-27
8. Anderson K.E., Bloomer J.R., Bonkovsky H.L., et al. Recommendations for the diagnosis and treatment of the acute porphyrias. Ann Intern Med. 2005 Mar 15;142(6):439-50.
9. Sardh E., Harper P., Andersson D.E., Floderus Y. Plasma porphobilinogen as a sensitive biomarker to monitor the clinical and therapeutic course of acute intermittent porphyria attacks. Eur J Intern Med. 2009 Mar;20(2):201-7.
10. Harper P., Wahlin S. Treatment options in acute porphyria, porphyria cutanea tarda, and erythropoietic protoporphyria. Curr Treat Options Gastroenterol. 2007 Dec;10(6):444-55.
11. González-Arriaza H.L., Bostwick J.M. Acute Porphyrias: A Case Report and Review. Am J Psychiatry 2003; 160 (3):450-8.
12. Puy H., Gouya L., Deybach J.C. Porphyrias. Lancet. 2010 Mar.13;375(9718): 924-37.
13. Jose J, Saravu K, Shastry B A, Jimmy B. Drug use in porphyria: a therapeutic dilemma. Singapore Med J 2008; 49(10): e272-e275
14. Andersson C., Lithner F. Hypertension and renal disease in patients with acute intermittent porphyria. Journal of Internal Medicine. 1994; 236(2):169-175
15. Singh V., Sud K., Kohli H.S., Gupta K.L., Sakhuja V. Acute Intermittent Porphyria : An Unusual Cause of Malignant Hypertension. JAPI. 2003; (51): 225-226.
16. Cinemre H, Korkmaz U, Alcelik A, Onder E, Gungor A. Safety of amlodipine use in patients with acute intermittent porphyria. Br J Clin Pharmacol 2007;64(2): 246–247
17. Lambrecht R.W., Gildemeister O.S., Williams A., Pepe J.A., Tortorelli K.D., Bonkovsky H.L. Effects of selected antihypertensives and analgesics on hepatic porphyrin accumulation: implications for clinical porphyria. Biochem Pharmacol. 1999 Sep 1;58(5):887-96

# THE IMPORTANCE OF PHYSICAL THERAPY IN THE TREATMENT OF UNILATERAL CONGENITAL BELL PARALYSIS – A CASE REPORT

Jelena Milosevic[1], Danijela Pavicevic[2], Katarina Parezanovic-Ilic[1,2] and Zoran Milenkovic[3]

[1] *University of Kragujevac, Faculty of Medical Sciences, Department of Physical medicine and rehabilitation, Serbia*
[2] *Department of Physical medicine and rehabilitation, Clinical Center of Kragujevac, Serbia 2*
[3] *Department of Orthopedics and Traumatology, Clinical Centre of Kragujevac, Serbia*

Received: 31.05.2018.
Accepted: 27.06.2018.

**Corresponding author:**

**Jelena Milosevic**

Department of Physical medicine and rehabilitation, Faculty of Medical Sciences, University of Kragujevac, Svetozara Markovića 69, 34000 Kragujevac, Serbia

Phone: + 381 64 27 509 27
E-mail: jecas0109@gmail.com

UDK: 616.833.17-009.11-085-053.31
Ser J Exp Clin Res 2022; 23(1): 93-97
DOI: 10.2478/sjecr-2018-0062

## ABSTRACT

*Peripheral paralysis of facial nerve in the newly-born can be congenital and developed. In clinical sense, paralysis of facial nerve is characterised by paralysis of mimic face muscles that are controlled by a facial nerve. A female newly-born, delivered by caesarean section was clinically diagnosed weakness on the right side of the face. Thirteen days after the birth the newly-born was examined by a physiatrist for the first time due to the weakness of the right facial side. During the first year of life a severe congenital lesion of facial nerve was diagnosed. Rehabilitation treatments were administered during the first year of life, with partialclinical improvement. The seriousness of facial nerve lesion hasa significant influence on the degree of recovery. It is very important to identify the type of lesion by using efficient technology,since it is the only way to provide early and adequate therapy*

***Keywords***: *facial nerve, newly born, paralysis, physical therapy.*

## ABBREVIATIONS

**EMNG** – electromyeloneurography

**MR** – magnetic resonance

**CRP** – C-reactive protein

**CNS** – central nervous system

## INTRODUCTION

Facial muscle paralysis is defined as inability of a controlled movement of mimic muscles; it occurs due to dysfunction of facial nerve (of the seventh cranial nerve) that is responsible for their innervation (1, 2). The dysfunction of muscle is usually unilateral; it is characterised by asymmetrical face and difficulties in frontal muscle movements, eyelid muscles, cheeks, lips and chin (2, 3). Both sides of the face are rarely affected (4). Facial nerve paralysis can be congenital and developed (1, 3). Congenital paralysis of facial nerve is idiopathic in most cases, but it can often be found in combination with some syndromes as well (1, 5, 6). Developed paralysis in a newly-born can occur due to bad intrauterine position, delivery trauma, infection or inflammation of facial nerve and tumour of head and

neck (1, 7). Congenital hereditary paralysis of facial nerve was described in the literature (8, 9). Idiopathic paralysis of facial nerve known as Bell paralysis is very rare in the newly-born (3, 10). It was named after Scottish anatomist and surgeon Sir Charles Bell who first described it (11). The sign of Bell paralysis may vary from mild weakness to complete paralysis of mimic muscles of one side of the face (12). Prognostically, Bell paralysis has complete recovery in 80% of cases, in 15% permanent mild damages can be found, while severe damages are present in 5% of cases (4).

## CASE REPORT

A female newly-born was delivered by caesarean section due to pelvic position in the 40$^{th}$ gestational week, with Apgar score 9, and asymmetric facial muscles, diagnosed by clinical examination. (Figure 1.) The pregnancy was normal, without any data of intrauterine infections; the mother did not receive any medication during pregnancy. At the first examination of the pediatrician the findings were normal except the weakness of the right side of facial muscles. Laboratory analyzes excluded infections (leukocytes 8.6; CRP 0.1 mg/l; findings blood count were normal). Neurologist diagnosed with paralysis facial nerve, the other neuronal findings were normal. Ultrasound CNS were normal. The finding of otorhinolaryngologist were normal. Thirteen days after the birth the newly-born was examined by the physiatrist for the first time due to asymmetric mimic muscles. During the examination the physiatrist found weakness of the right side of the face, maual muscle test the right side of face the values 0, and administered stimulation treatment for the face muscles. The stimulation treatment included electric stimulation of the damaged muscles and application of thermotherapy in 15 therapeutic procedures, after which the 15-day-break in application of those agents was made. During the application of stimulation treatment, kinesiotherapy was conducted twice per day by making passive movements; kinesiotherapy was not interrupted except when it was necessary due to general condition of the infant (febricity, respiratory and urinary infections and vaccinations).

When the infant was four months old, EMNG examination was done; the finding pointed to lesion of facial nerve of peripheral type and serious degree. (Figure 5.) In order to detect the reason of this facial nerve lesion, MR examination of endocranium was carried out, which pointed to hypotrophy of cerebral parenchyma and dilatation of subarachnoid space, laterally and front-temporally. The finding of MR angiography was normal. After the ad-

**Figure 1**. Image after birth showing facial muscle asymmetry

**Figure 2**. Image at the age of seven months at which face symmetric facial muscles whit a peaceful expression.

**Figure 3**. Image at the age of seven months at which face asymmetric facial muscles during crying

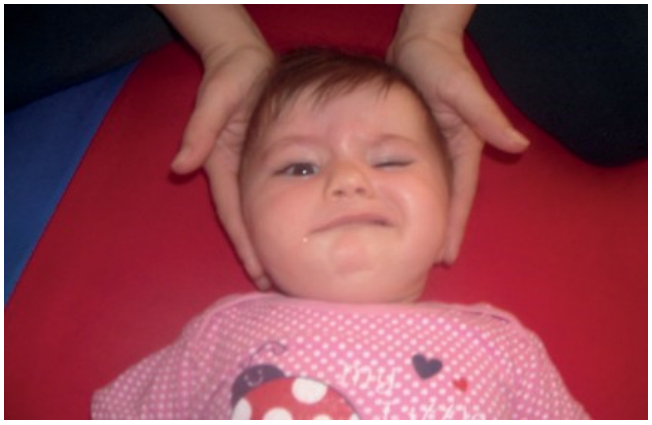

**Figure 4.** Image at the age of one year in crying at which face asymmetric facial muscles, is olso observed with partial clinical improvement

ministration of physical therapy and stimulation treatment in the duration of seven months, the facial asymmetry was still present together with the paralysis of the right side of the face. Manual muscle test the values of 1. In this period, physical treatment was primarily based on the application of kinesiothrapy which included the exercises of facial muscles, and later electro stimulation. At the age of twelve months the baby's development followed her calendar age, while the functional status of lesion of facial nerve revealed only partial improvement. The eye closed during the sleep and peaceful expression (Figure 2.), but during crying the facial asymmetry was still present. (Figure 3.) Intensive kinesiotherapy was applied further together with the thermotherapy as an introductory procedure. Further application of kinesiotherapy did lead to visible improvement in clinical presentation, manual muscle test the right side of face the values of 3. (Figure 4.)

## DISCUSSION

The frequency of congenital facial nerve paralysis is 2.1 per 1000 of live births (1). Congenital facial nerve paralysis may be involved in severe disease of neoplasm, a trauma, a congenital anomaly, but it is more frequently idiopathic (5, 6, 13). Due to its relatively superficial course and long pathway through bony structures of the skull, facial nerve is subject to damage at birth (1, 6, 14); specifically, in our case the risk factors for development of paralysis was caesarean section and to pelvic position. The factors that may lead to facial nerve paralysis are the newly-born weight higher than 3.5 kg at birth, caesarean section, and the first or premature delivery (3). Facial nerve paralysis inthe newly-born is clinically characterised by immobility offrontal muscles with loss of nasolabial fold and facial asymmetry in the region of cheeks without movements at cry-

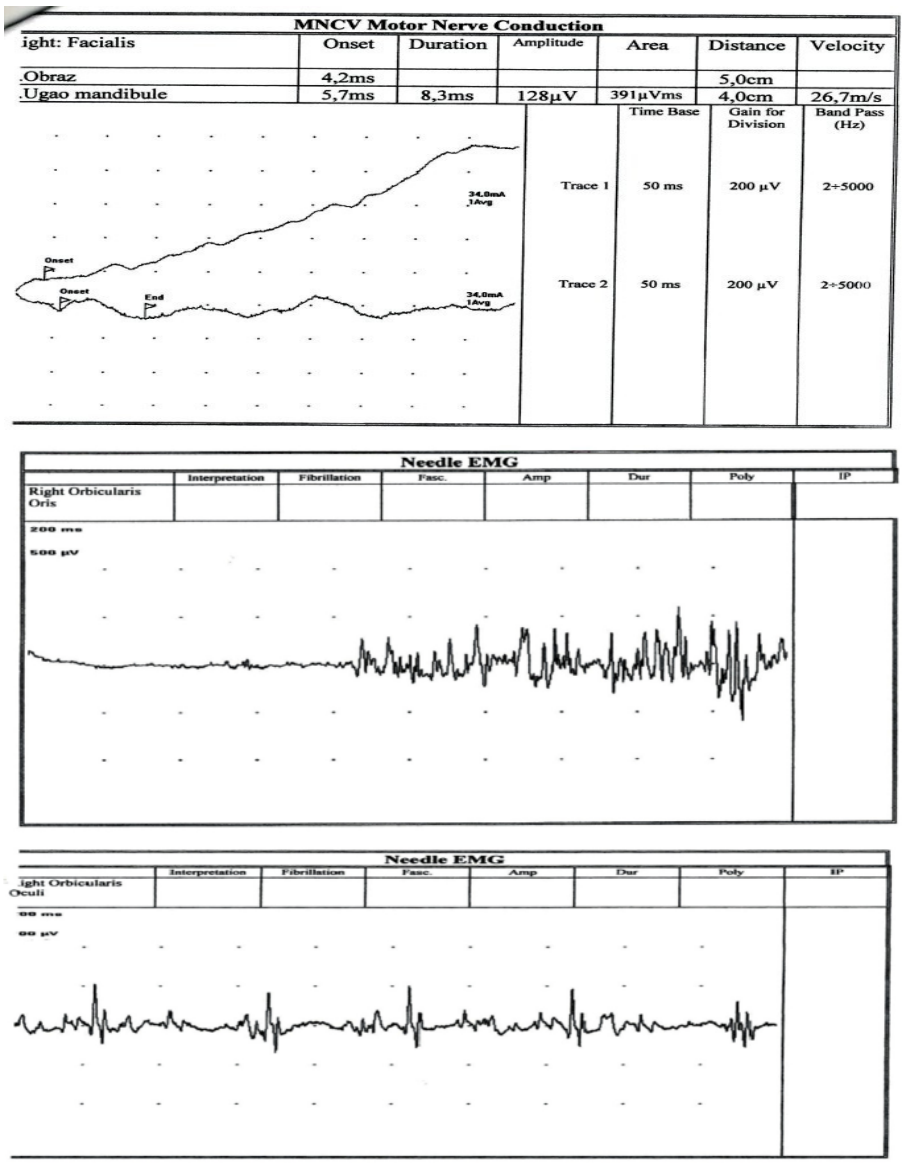


**Figure 5.** EMNG / the right cheek, mandibular angle, Orbicularis Oris, Orbicularis Oculi

ing, which was the clinical presentation in our case. (Figure 1.) In the cases of serious damage a child cannot close the eye due to complete paralysis of eye muscles (3).

A group of authors showed that the greatest number of facial nerve paralyses were caused by herpes simplex virus. In most of those patients conservative treatment was initiated and complete recovery occurred in 85% of children (14). The seriousness of paralysis influence the degree of recovery; the severe paralysis, like in our case, could hardly achieve complete recovery (3). In order to conduct adequate therapy of facial nerve paralysis, it is necessary to perform detailed diagnostics, since only the identification of authentic diagnosis can provide proper treatment (3). The application of physical therapy in the treatment of Bell paralysis is aimed at facilitation of recovery and decreasing the risk of complications (12). The administration of kinesiotherapy include the plan of correction which involves exercises for mimic muscles that will provide normal functioning of muscles, normal facial expression in peace, and facial symmetry in both voluntary and forceful emotional movements (15). If the administration of persistent physical therapy does not provide results, or the results are slight, it is necessary to perform surgery. The significance of physical therapy before the surgery itself is extremely great, since passive movements maintain trophic and elastic function of muscles and prevent contractions that may influence the result of operation. The greatest number of peripheral facial nerve lesions recover until the second month of life; after this period the possibility of surgery should be considered in cooperation with the specialist of plastic and reconstruction surgery (transfer of gracilis muscle, transplantation of masseteric nerve, stretching of temporalis muscle) (5, 16-18). The aim of this intervention is a restitution of smile and better social communication, since in addition to functional disorders (difficulties in feeding), these children may develop psychological problems caused by the reactions of their environment to their physical appearance. It is necessary to perform surgical treatment and rehabilitation until the seventh year of age, due to psychological status and social adaptation of patients (19). After the surgery, rehabilitation has also very important role in recovery, since it should be followed during kinesiotherapy programme (5). Kinesiotherapy will provide faster recovery and prevent the occurrence of possible complications. The paralysis of one side of the face in a newly-born caused by trauma has much better prognosis in comparison to congenital facial paralysis (1).

## CONCLUSION

The severity of facial nerve damage influences the degree of recovery; in slight damages complete recovery is possible, while in more serious damages the application of conservative methods of treatment is important for the process of recovery. It is of vital importance to identify exact type of damage, because only in this way, prompt and proper therapy can be conducted. The administration of physical therapy in the early period may influence the degree of recovery and length of treatment, thus preventing the occurrence of complications.

## ACKNOWLEDGEMENTS

For this review we received consent of the parent.

## REFERENCES

1. Mahale RR, Mehta A, John AA, Buddaraju K, Shankar AK, Rangasetty S. Newborn with congenital facial palsy and bilateral anotia/atresia of external auditory canal: Rare occurrence. J Pediatr Neurosci 2016;11(3):271-273.
2. Berania I, Awad M, Saliba I, Dufour JJ, Nader ME. Delayed facial nerve decompression for severe refractory cases of Bell's palsy: a 25-year experience. J Otolaryngol Head Neck Surg 2018;47(1):1.
3. Ciorba A, Corazzi V, Conz V, Bianchini C, Aimoni C. Facial nerve paralysis in children. World J Clin Cases 2015;3(12):973-9.
4. Alanazi WL, El-Fetoh NMA, Alanazi SL, Alkhidhr MA, Alanazi MA, Alonazi DS, et al. Profile of facial palsy in Arar, northern Saudi Arabia. Electron Physician 2017;9(10):5596-5602.
5. Guerreschi P, Gabert PE, Labbé D, Martinot-Duquennoy V. Facial palsy in children. Ann Chir Plast Esthet 2016;61(5):513-518.
6. Butler DP, Henry FP, Leckenby JI, Grobbelaar AO. The incidence of facial vessel agenesis in patients with syndromic congenital facial palsy. Plast Reconstr Surg 2014;134(6):955e-958e.
7. Ishii LE. Facial Nerve Rehabilitation. Facial Plast Surg Clin North Am 2016;24(4):573-575.
8. Hölmich LR, Medgyesi S. Congenital hereditary paresis of ramus marginalis nervus facialis in five generations. Ann Plast Surg 1994;33(1):96-9.
9. Vahidi Mehrjardi MY, Maroofian R, Kalantar SM, Jaafarinia M, Chilton J, Dehghani M. A Novel Loss-of-Function Mutation in HOXB1 Associated with Autosomal Recessive Hereditary Congenital Facial Palsy in a Large Iranian Family. Mol Syndromol 2017;8(5):261-265.
10. Babl FE, Mackay MT, Borland ML, Herd DW, Kochar A, Hort J. Bell's Palsy in Children (BellPIC): protocol for a multicentre, placebo-controlled randomized trial. BMC Pediatr 2017;17(1):53.
11. Terzi S, Dursun E, Yılmaz A, Özergin Coşkun Z, Özgür A, Çeliker M, et al. Oxidative Stress and Antioxidant Status in Patients with Bell's Palsy. J Med Biochem 2017;36(1):18-22.
12. Somasundara D, Sullivan F. Management of Bell's palsy. Aust Prescr 2017;40(3):94-97.

13. Yılmaz U, Cubukçu D, Yılmaz TS, Akıncı G, Ozcan M, Güzel O. Peripheral facial palsy in children. J Child Neurol 2014;29(11):1473-1478.
14. Das AK, Sabarigirish K, Kashyap RC. Facial nerve paralysis: A three year retrospective study. Indian J Otolaryngol Head Neck Surg 2006;58(3):225-228.
15. Jovanovic M, Roncevic R, Colic M, Stojicic M, Rasulic L. Treatment of facial nerve paralysis using static suspension methods. Acta Chir Iugosl. 2003; 50(1):69-72.
16. Sharma PR, Zuker RM, Borschel GH. Gracilis Free Muscle Transfer in the Treatment of Pediatric Facial Paralysis. Facial Plast Surg 2016;32(2):199-208.
17. Lindsay RW, Bhama P, Weinberg J, Hadlock TA. The success of free gracilis muscle transfer to restore smile in patients with nonflaccid facial paralysis. Ann Plast Surg 2014;73(2):177-82.
18. Bianchi B, Ferri A, Ferrari S, Copelli C, Salvagni L, Sesenna E. The masseteric nerve: a versatile power source in facial animation techniques. Br J Oral Maxillofac Surg 2014;52(3):264-269.
19. Harrison DH. Surgical correction of unilateral and bilateral facial palsy. Postgrad Med J 2005;81(959):562-567.

# INFORMATION FOR AUTHORS

## AIMS AND SCOPE

*Serbian Journal of Experimental and Clinical Research* (*Ser J Exp Clin Res*) is a peer-reviewed, open access journal which publishes original research articles, reviews, case reports and letters to the editor in all areas of the biomedical sciences that have not been published previously. *Ser J Exp Clin Res* was founded in 2000. under the name *Medicus* and over more than two decades has grown into one of the leading national journals in the field of biomedical sciences. *Ser J Exp Clin Res* is owned and published by Faculty of Medical Sciences University of Kragujevac. The journal adheres to the policies of the International Committee of Medical Journal Editors (ICMJE) and publishing ethics guidelines provided by the Committee on Publication Ethics (COPE).

## TYPES OF MANUSCRIPTS

- *Original research articles*: *Ser J Exp Clin Res* considers all original research manuscripts which present the results of an original research study (experimental or clinical). These manuscripts must contain sufficient information on all relevant research methods, as well as a detailed analysis of the results obtained.

- *Reviews*: *Ser J Exp Clin Res* considers literature reviews, systematic reviews and meta analyses addressed to a particular subject area, with special reference to new knowledge and facts. Manuscripts in this category must not be shorter than 6000 words, the text must cite more than 70 references of which 50% have been published in the previous 5 years. Systematic reviews should follow the PRISMA guidelines.

- *Case reports*: *Ser J Exp Clin Res* considers case reports presenting detailed information on the symptoms, signs, diagnosis, treatment (including all types of interventions), and outcomes of an individual patient. Case reports should usually describe new or uncommon conditions that serve to enhance medical care or highlight diagnostic approaches. Case reports should follow the CARE guidelines.

- *Letters to the editor: Ser J Exp Clin Res* considers letters to the editor related to different clinical and laboratory observations. They should be titled, not exceed 500 words, and have a maximum of 5 references. Up to 1 table or figure may be submitted, but will be published at the discretion of the Editor. No more than 3 authors should appear.

## MANUSCRIPT SUBMISSION

Manuscripts submitted to *Ser J Exp Clin Res* must neither be published previously nor be under consideration for publication in another journal. Manuscripts are accompanied with a suitable *cover letter* stating that: the manuscript is not submitted for publication elsewhere; all authors have agreed to submission; the study is carried out in accordance with relevant ethical international guidelines.

*Ser J Exp Clin Res* considers only manuscripts written in English using *Microsoft Office Word* format and uploaded online at https://www.editorialmanager.com/sjecr/.

Plagiarism, data fabrication and image manipulation are not tolerated. Plagiarism includes copying text, ideas, images, or data from another source, even from authors own publications, without providing any reference to the original source. If a study's design or the manuscript's structure or language has been inspired by previous works, these papers must be explicitly cited. All manuscripts submitted to *Ser J Exp Clin Res* are checked for plagiarism using the academic standard software prior to the first step of the editorial process.

## MANUSCRIPT PREPARATION AND ORGANISATION

### *Title Page*

The Title Page should contain the following information:

- Manuscript title
- Full author(s) names
- The affiliation(s) of the author(s)
- A clear indication and an active e-mail address of the corresponding author

Manuscript title should be concise and informative.

It is necessary to state the full names and surnames (middle letter or name is optional) of all authors and the exact affiliations of all authors - institution, (department), city, (state), country. *Ser J Exp Clin Res* remains neutral with regard to jurisdictional claims in institutional affiliations. Responsibility for affiliations ultimately rests with the author.

### *Abstract*

Provide an abstract of 150 to 250 words. Abstract should be structured (Background, Methods, Results, Conclusion), citation-free, without abbreviations if possible.

### *Keywords*

Three to five relevant keywords need to be added after the abstract. Keywords should be specific to the manuscript, yet reasonably common within the subject discipline.

### *Text Formatting*

Manuscripts should be submitted in *Microsoft Office Word*. The authors should use normal, plain *Times New Roman* font (12pt) for text. Pages should be numbered automatically. Italics may be used for emphasis. Abbreviations should be defined at the first mentioning in the text and used consistently thereafter (do not use a separate subtitle for abbreviations only). Please use no more than three levels of displayed headings. International System (SI) of Units should be used (imperial, US customary and other units should be converted to SI units).

*Original research articles* should contain following sections: Introduction, Materials and Methods, Results, Discussion, Conclusions, Acknowledgments, Conflict of Interest, and References. *Reviews* may require different formats, while *Case reports* manuscripts should follow the CARE guidelines.

*Introduction.* This section should contain context or background for the study, rationale, clear aim of research or tested hypothesis.

*Materials and Methods*. This section should provide sufficient detail for replication of the study. If more than one method is used in the research, use subsections with appropriate subheadings. The Materials and Methods section should also contain following statements:

a) Informed Consent Statement. In cases where the identification of personal information is necessary for scientific reasons, authors should obtain informed consent from all individuals included in the study.
b) Human Right Statement. Manuscripts containing information related to human should clearly state that the research has complied with all relevant international and national regulations and institutional policies and has been approved by the authors' institutional Ethics committee.
c) Animal Right Statement. Manuscripts containing information related to animals should clearly state that the research has complied with all relevant international and national regulations and institutional policies and has been approved by the authors' institutional Ethics committee.

For details and examples of statements please see part ‘Research and publication ethics’.

*Results.* The results should be presented in logical sequence in the manuscript. Do not repeat all the data in the tables or figures in the text.

*Discussion.* This section should explain obtained results, and not repeat them and interpret their significance and draw conclusions. It should discuss the study results in the light of previously published papers.

*Conclusions*. Within the Conclusions section the authors should clearly explain the main conclusions of the article, highlighting its importance and relevance.

*Acknowledgments*. Acknowledgments of people, grants, funds, etc. should be placed in a separate section after the Conclusions section. The names of funding organizations should be written in full. This may include administrative and technical support, or donations in kind (e.g., materials used for experiments).

*Conflict of Interest.* Authors must declare all relevant interests that could be perceived as conflicting. If there are no conflicts, the authors should state this. Submitting authors are responsible for coauthors declaring their interests.

*References*. References must be numbered in order of appearance in the text (including table captions and figure legends) and listed individually at the end of the manuscript. In the text, reference numbers should be placed in round brackets ( ), and placed before the punctuation – e.g. (1), (1–3) or (1, 3). The list of references should only include works that are cited in the text and that have been published or accepted for publication. Personal communications and unpublished works should only be mentioned in the text.

The reference list should include contain surnames and the first letter of the author's name, full title, abbreviated title of the journal, year of publication, volume, number and pagination (Vancouver style guide). In case where the list of authors are more than six, please use et al. after the sixth author.

The examples of correct referencing:

*For journal papers:*
Shoji F, Haro A, Yoshida T, Ito K, Morodomi Y, Yano T, et al. Prognostic significance of intratumoral blood vessel invasion in pathologic stage IA non-small cell lung cancer. Ann Thorac Surg. 2010; 89(3): 864-9.

*For journal papers by DOI*:
Ewy MW, Patel A, Abdelmagid MG, Mohamed Elfadil O, Bonnes SL, Salonen BR, et al. Plant-Based Diet: Is It as Good as an Animal-Based Diet When It Comes to Protein? Curr Nutr Rep. 2022. doi: 10.1007/s13668-022-00401-8.

*For books:*
Kleiner FS, Mamiya CJ, Tansey RG. 2001. Gardner’s art through the ages (11th ed.). Fort Worth, USA: Harcourt College Publishers.

*For chapter in an edited book:*
Mettam GR, Adams LB. How to prepare an electronic version of your article. In: Jones BS, Smith RZ, editors. Introduction to the electronic age, New York: E-Publishing Inc; 2009, p. 281-304.

**Tables, figures and images**

*Tables*

Tables should always be cited in text in consecutive numerical order. For each table, please supply a table caption (title) explaining the components of the table. Identify any previously published material by giving the original source in the form of a reference at the end of the table caption. Footnotes to tables should be indicated by superscript lower-case letters (or asterisks for significance values and other statistical data) and included beneath the table body.

*Figures*

Please submit each figure as an individual file separate from the manuscript text. All figures are to be numbered using Arabic numerals. Figures should always be cited in text in consecutive numerical order. Each figure should have a concise caption describing accurately what the figure depicts. Include the captions in the text file of the manuscript, not in the figure file.

For vector graphics, the preferred format is EPS, for halftones, please use TIFF format. *Microsoft Office* files are also acceptable. Vector graphics containing fonts must have the fonts embedded in the files.

*Line art*:

- Definition: Black and white graphic with no shading.
- Do not use faint lines and/or lettering and check that all lines and lettering within the figures are legible at final size.
- All lines should be at least 0.1 mm (0.3 pt) wide.
- Scanned line drawings and line drawings in bitmap format should have a minimum resolution of 1200 dpi.
- Vector graphics containing fonts must have the fonts embedded in the files.

*Halftone art*:

- Definition: Photographs, drawings, or paintings with fine shading, etc.
- If any magnification is used in the photographs, indicate this by using scale bars within the figures themselves.
- Halftones should have a minimum resolution of 300 dpi.

*Images*

Supply vector-based files such as those produced by *CorelDraw*, *Adobe Illustrator* or similar software. Vector files give us maximum flexibility for sizing your figures properly. Do not rasterize line art or text. Photographic images should have a minimum resolution of 300 dpi at final print size. Embedded images within a vector file should also have a minimum resolution of 300 dpi. Up sampling artwork (artificially increasing file size or resolution) will not improve quality and causes production problems. At final print size, line weights can be no thinner than 0.28 pt.

**PEER REVIEW PROCESS**

All submitted manuscripts received by the Editorial Office will be evaluated by a professional *Editorial board* to determine whether they are of sufficient quality; properly prepared and follow the ethical policies of *Ser J Exp Clin Res*. Manuscripts that do not fit with the quality and ethical standards of *Ser J Exp Clin Res* will be rejected before peer-review. Manuscripts that are not properly prepared according to the Instruction for authors will be returned to the authors for revision and resubmission.

Once a manuscript passes the initial evaluation, it will be assigned to at least two independent experts for single-blind peer-review process. If the outcomes of the performed reviews are opposite, the third review is required. The peer-review outcomes are one of following:

- *Accept (without any changes)* - the journal will publish the paper in its original form. This type of decision outcome is rare.
- *Minor revision* - the manuscript has high chance to be accepted after fulfillment of minor corrections. Authors will be asked to resubmit the revised manuscript within a suitable time frame, and the revised version will be returned to the reviewer for further comments.
- *Reconsider after Major Revision* - the acceptance of the manuscript would depend on the revisions. The authors are required to perform extensive and significant improvements in their manuscript. Authors will be asked to resubmit the revised manuscript within a suitable time frame, and the revised version will be returned to the reviewer for further comments.
- *Reject* - the manuscript is rejected for two reasons: 1. it has serious flaws, and/or makes no original significant contribution; 2. corrections and improvements during the (major) revision were not sufficient and satisfactory. No offer of resubmission to the journal is provided.

All reviewer comments should be responded point-by-point in a separate document entitled ‘Answers to reviewers comments’. Corrections should be marked within the text in a red colour or as a track changes. During the submission process, author should suggest two potential reviewers with the appropriate expertise to review the manuscript. Proposed reviewers should be from different institutions than the authors.

Upon editor's approval, after received positive manuscript reviews, the manuscript is accepted in the system, and the corresponding author receives information about the manuscript accepted for publication to the email address. Once accepted, the manuscript will undergo professional copy-editing, English editing, proofreading by the authors, pagination and publication. The Editorial board reserves the right to correct the English language after proofreading by the authors.

DOI number is assigned to the paper and, after proofreading and text break according to the Journal instructions, the paper is published as *Ahead of Print* first on *Sciendo* platform (https://sciendo.com/journal/sjecr) and then in one of the next issues of the Journal.

## RESEARCH AND PUBLICATION ETHICS

### Research Involving Human Subjects

When reporting on research that involves human subjects, human material, human tissues, or human data, authors must declare that the investigation was carried out following the rules of the Declaration of Helsinki of 1975 (https://www.wma.net/what-we-do/medical-ethics/declaration-of-helsinki/), revised in 2013. As a minimum, a statement including number of approval and name of the ethics committee must be stated in Section 'Statement of Human Rights' of the article. In addition, the protection of privacy is a legal right that must not be breached without individual informed consent. In cases where the identification of personal information is necessary for scientific reasons, authors should obtain full documentation of informed consent, including written permission from the patient prior to inclusion in the study.

*Example of Statement of Human Rights*: "The study was conducted in accordance with the Declaration of Helsinki, and the protocol was approved by the Ethics Committee of *Name of the Institution* (No. *number of approval*)."

*Example of Statement of Informed Consent*: "All subjects gave their informed consent for inclusion before they participated in the study".

For non-interventional studies (e.g. surveys, questionnaires, social media research), all participants must be fully informed if the anonymity is assured, why the research is being conducted, how their data will be used and if there are any risks associated. As with all research involving humans, ethical approval from an appropriate ethics committee must be obtained prior to conducting the study.

### Research involving Animals

When reporting on research that involves animal subjects, animal material or animal tissues, authors must declare that the investigation was carried out following the rules of the European Directive for the welfare of laboratory animals (No. 2010/63/EU) and national and institutional regulations. As a minimum, a statement including number of approval and name of the ethics committee must be stated in Section 'Statement of Animal Rights' of the article. Statements on animal welfare should confirm that the study complied with all relevant legislation. Also, authors must include details on housing, husbandry and pain management in their manuscript (section Materials and methods).

*Example of Statement of Animal Rights*: "All research procedures were carried out in strict accordance with the European Union Directive for the welfare of laboratory animals (No. 2010/63/EU) and approved by the Ethics Committee of *Name of the Institution* (No. *number of approval*)."

sciendo

Serbian Journal of Experimental and Clinical Research

2000

**FACULTY OF MEDICAL SCIENCES**
**Svetozara Markovica 69, 34000 Kragujevac, SERBIA**
**P.O. Box 124**
**Tel. +381 (0)34 30 68 00 • Tfx. +381 (0)34 30 68 00 ext. 112**
**e-mail: sjecr@medf.kg.ac.rs**

**https://medf.kg.ac.rs/sjecr**